Anti-Inflammation and Antiphagocytosis of Viral Vector Functionalized with Biomimetic Proteins

A Dissertation
Presented in Partial Fulfillment of the Requirements for the
Degree of Doctor of Philosophy
with a
Major in Biological Engineering
in the
College of Graduate Studies
University of Idaho
by

Esmael Mana Alyami

Approved by:
Major Professor: Ching-An Peng, Ph.D.
Committee Members: Tanya Miura, Ph.D.; Matthew Bernards, Ph.D.; Nathan Schiele, Ph.D.
Department Administrator: Dev Shrestha, Ph.D.

December 2021

Abstract

Gene therapy is a clinical technique that involves transferring specific genes to treat or prevent diseases. This process requires a vector to deliver the gene of interest to the target cells. While there are several carriers that can deliver the gene, modified viral vectors represent an efficient approach. However, the immune system's recognition of viral vectors as foreign bodies remains an obstacle. In this study, we used lentiviruses as the model viral vectors and masqueraded them with biomimetic proteins CD47 and CD200 to escape immunosurveillance. CD47 is a protein that reduces phagocytic activity by interacting with its receptor SIRPα (signal-regulatory protein α) on the macrophage surface. Lentiviral vectors tethered with the CD47 protein could have the ability to prolong their circulation in the blood by diminishing macrophage-mediated phagocytic clearance via CD47-SIRPα interactions, thereby facilitating gene delivery to the target sites. CD200, known as an anti-inflammatory transmembrane glycoprotein in the immunoglobin superfamily, interacts with its receptor CD200R, which is highly expressed on myeloid cells such as macrophages and neutrophils. Lentiviral vectors capped with CD200 protein are expected to reduce macrophage activation and chronic inflammation via the CD200-CD200R interaction. To achieve the goal of using these proteins in conjunction with the viral vector as a means of escaping immunosurveillance, the core-streptavidin (coreSA) gene was first cloned and engineered into a pET-30a(+) plasmid to obtain pET-30a(+)-coreSA plasmid. Then, the extracellular domain of CD47, CD200, or CD200-CD47 genes were cloned and constructed separately into the constructed pET30a-coreSA. The CD47ED-coreSA, CD200ED-coreSA and CD200ED-CD47ED-coreSA fusion proteins were expressed by IPTG induction and purified by immobilized metal affinity chromatography. The expression and purification of all fusion proteins were visualized with a clear band in the target region by SDS-PAGE and Western blot analysis. Biotinylated lentivirus was bound to the fusion proteins through coreSA-biotin interaction, which were functionalized with CD47ED, CD200ED and CD47ED-CD200ED-coreSA fusion proteins and then loaded onto macrophages to explore the potential use of these biomimetic nanocarriers for gene delivery. Unmodified and nonbiotinylated lentivirus vectors were evaluated as controls. Our results showed that our

modified viral vectors decreased phagocytosis activities of macrophages, with effectiveness increasing with viral vectors decorated with CD200ED, CD47ED, or CD47ED-CD200ED proteins in ascending order. In conclusion, surface modification of lentivirus vectors, especially with the CD47ED-CD200ED fusion protein, can potentially be used in therapeutic particle delivery in order to evade immune surveillance and enhance gene delivery efficiency.

Acknowledgements

First of all, I would like to thank my supervisor Prof. Ching-An Peng for his consistent support, guidance and encouragement throughout my research project. Prof. Peng was always willing and enthusiastic to help in any way he could during research. Prof. Peng, thank you for introducing me to the field of immunoengineering and biomaterials. I am sure this would brighten my future career and research work.

Furthermore, I would also like to show gratitude to all committee members, including Prof. Tanya Miura, Prof. Matthew Bernards, and Prof. Nathan Schiele. Thank you so much for your immerse feedback and insightful ideas that brought this dissertation to look better. I must appreciate Prof. Schiele for the classes he taught me in the past few years. Thank you so much for being such a great instructor. Your teaching style and research discussion was unique, which improves my comprehensive reading and understanding of scientific reports.

I am also thankful to Ammar Tarar for being a great co-worker. I appreciate your collaboration in my research as well as other projects that we have accomplished. Together, we created such a great memory that would last for long and we turned the hard work to go easy. I also would like to thank my research group Soha Alkhaldi and Sharjeel Jokhio, who have been unwavering in their professional and personal support during the last few years I spent at the university. I must also thank my previous co-worker Dr. Jun Zhang for helping me with experiment design and showing me an example of wonderful colleagues. Finally, I need to thank our wonderful department staff, Judy Vandegrift. Thank you for your timely helpful and being so friendly. Thank you so much all!

Dedication

This work is completely dedicated to my respectful father who has been constantly supporting and encouraging me through my Ph.D. study. Without his encouragement, I may not achieve this accomplishment.

This work is also dedicated to my family: my wife, my mother, my siblings, and little son for providing me with unfailing support thought the years of study.

Table of Contents

List of Figures

Chapter 1: Introduction and Background

General Introduction

The mononuclear phagocyte system (MPS) is involved with identifying foreign particles that will be eliminated from the body[1]. Markers such as cell membrane proteins CD47 and CD200 allow cells to be recognized by the immune system as self and therefore safe. Red blood cells can have their markers for four months before they are destroyed by the immune system[2]. The MPS is a barrier that all intravenous drug carriers must overcome to reach targeted sites[3]. For a therapeutic carrier to be effective it is required to have prolonged longevity in the circulatory system, as well as the ability to target its specific site of entry[4], and their size, shape, and surface characteristics must fall between ideal parameters. When such delivery particles are non-biocompatible, they are easily recognized by the MPS, rendering them ineffective as drug delivery carriers. Ideal carriers are between 10 and 200 nm, however, carriers larger than 200 nm can be modified to improve drug delivery efficiency[5]. Means of enhancing delivery include tethering targeting molecules enables the therapeutic carriers to aim at disease site[6]. Altering the surface characteristics of a carrier can also reduce the rate of opsonization (the mechanism of identifying invading particles (antigens) through specific components called opsonin) and avoid complement activation[7]. To overcome the biochemical and immunological obstacles that therapeutic carriers face, the ability to attach polyethylene glycol (PEG) chains to a molecule or carrier was developed; a process called PEGylation. PEG chains offer stealth-like properties when attached and consequently several conjugation strategies have been developed for therapeutic use[8]. PEGylated dendrimers, liposomes, and micelles have shown to be viable therapeutic agents in cancer therapy[9]. PEGylation of other compounds such as protein molecules and monoclonal antibodies has demonstrated to exhibit increased circulation times and a reduction of immunogenicity without a decrease in effectiveness[10]. PEGylation has indeed improved the pharmacokinetics of therapeutic carriers, but there are still immunological obstacles that need to be overcome. These include issues such as hypersensitivity and non-biodegradability[11,12]. These drawbacks indicate that research into biochemical processes that can reduce opsonization is required. One such example are

erythrocytes (red blood cells), as these can last in the circulation for up to four months while performing complex biological tasks without being recognized as a foreign particle[13].

Typically, nanoparticles (NPs) are solid, colloidal particles in the range of 10 to 1000 nm; for drug delivery systems the preferred size is < 200 nm[14]. The small size of particles enhances their solubility, increases their bioavailability, and permits better absorption in the various organ systems. It is postulated that size and shape influence cellular internalization and consequently the size and shape of the particles are extensively studied with respect to their biodistribution *in vivo*[15]. NPs also allow targeted delivery of macromolecules as therapeutics, which is a challenge with traditional drug delivery systems[16]. Despite these advantages, the utility and success of the delivery system can only be measured on its ability to deliver cargo intracellularly. This includes overcoming systemic-, organ specific-, and cellular barriers- to enter the host[17]. More so, for systemically delivered engineered NPs, overcoming the protective mechanisms of multiple level organ responses such as those operative in the spleen, liver, and mononuclear phagocyte system (MPS) pose a grave challenge. Design challenges include overcoming host defense mechanisms, whilst modifying vectors to achieve tailored release of the drug. Sensor-based drug release and degradation of drug carriers post-release are also desirable traits[17]. The quest to achieve these desirable properties has led to biomimicry wherein delivery systems mimic biological systems, allowing them to overcome the natural biological barriers of the host under consideration and accentuate drug delivery[18]. The current chapter discusses the use of synthetic and bioinspired strategies in the development of drug delivery carriers that allow them to overcome the natural host defense mechanisms and the application of these carriers under different disease settings.

The Host Defense Mechanism

Before covering means of prolonging circulation of NPs in the human host, it is first important to understand how the innate host immune mechanism targets and clears the NPs from circulation. The mammalian immune system is a multi-tiered security platform that has a checkpoint at every level. The MPS in systemically fixed tissues, along with the help of their heterogeneous population of phagocytic cells, plays a significant role in the

identification and clearance of perceived antigenic threats (immune complexes, and exogenous and endogenous antigens)[19]. The composition of the MPS includes the Kupffer cells of the liver, the microglia of the brain, the alveolar macrophages of the lung, and macrophages of the bone marrow and the lymph nodes[20]. The antigens may be internalized (phagocytosed) either through non-immune receptor mediated phagocytosis or by immunocytophagic effects mediated by binding to Fc receptors or complement receptors[21]. Macrophage phenotype also has been found to have a role in NP uptake. Namely, the M1 polarized phenotype was shown to have a higher uptake in an isolated culture system in comparison to the M2 phenotype[22]. The MPS does not encounter bare NPs. The contact of NPs with blood or other tissues allows its conditioning to the host MPS and produces protein adsorption to the NPs' surface[23]. This protein adsorption, also known as corona, serves as opsonins that prime the NPs for enhanced uptake and clearance[23]. These opsonized particles enter the phagocytes through several receptors such as the Toll-like receptors, Fc receptors, scavenger receptors, and MARCO receptors. Upon internalization, the particles are processed and presented for clearance[23].

Stealth Functionalization of Chemical Synthesis

Having realized the challenges faced by the NPs in the human host by the innate immune responses, one proposed strategy to overcome this is to sequester these particles and prolong their circulation in the host to ensure targeted drug delivery. One of the means of achieving this stealth functionality is through polymer grafting. It was preliminarily observed that hydrophobic and charged particles have a higher propensity to opsonization compared with hydrophilic or uncharged particles[23]. Some of the polymers used to confer stealth properties on NPs include PEG. These molecules are hydrophilic and flexible, and their presence on the NP sterically impedes the interaction of the NPs with the opsonin proteins, thus resulting in their increased circulation in the blood, and therefore, directing most of attention on PEGs[22]. The process of PEGylation involves the attachment of repeat units of PEG to the NPs or the drug. PEGylation prevents the binding of opsonin proteins to the NPs in part due to their molecular weight, surface chain density, and conformation of the polymer[22].

Currently close to 20 PEGylated products are under review or approved by the FDA. These include various classes of drug molecules from recombinant proteins (cytokines, growth factors, coagulation factors, antibodies, hormones, peptides). While PEGylation of biological products is the primary focus to date, there is development for expanding their use into non-biologic products (e.g. small organic molecules, aptamers, and synthetic peptides)[24]. PEGylated drugs find application in the treatment of cancers, Hepatitis C, acromegaly, neutropenia, and wound healing, among other disorder[25]. While PEG has been a natural choice for surface coating of several NPs, reports indicate the presence of anti-PEG immunity in a significant proportion of PEG naïve and exposed individuals[26]. These include anti-PEG antibodies of type IgG and IgM[27,28]. It is believed that the presence of these antibodies contributes to the phenomenon of accelerated blood clearance. This in turn may result in complications such as rapid clearance of drugs or deliveries of non-effective therapeutic doses, and side effects, such as anaphylaxis[27,29].

Viral Vectors

Virus-based drug delivery

Virus can be used in therapeutics, broadly categorized for their application in different disease settings either as carriers of genes or as cell lytic agents (these two uses may not always be mutually exclusive). Virus families commonly used for gene delivery include adenoviruses, adeno associated viruses, retroviruses, and herpes simplex virus[30]. Viral vectors are mostly used for somatic cell gene delivery, especially given that clinical use of germ line gene editing is ethically limited[31,32]. Depending on the mode of delivery, the targeting is categorized as *in-vivo*, *ex-vivo*, and *in-situ*[33,34]. Classification is also based on the kind of genetic material *viz*, DNA or RNA, that the virus carries. The utility of viral drug delivery systems is seen in infectious diseases, cancers, neurological diseases, and cardiovascular diseases[35]. The potential of plant- and bacteria-based viral drug delivery systems is also being explored[36].

Lentivirus, herpes simplex virus, adenovirus, and adeno-associated virus (AAV) vectors have been used for gene transfection in the brain. However, the use of viral vectors has met with limited success in the systemic treatment of brain disorders, because of the

inability of viral particles to cross the blood-brain barrier and issues of toxicity in human patients[37]. Viral particles can specifically target host cells, and the size of the particle makes them a desirable drug delivery vehicle and thus they have been exploited as therapeutic molecules, in particular with *in-situ* delivery of therapeutics. However, the inability of viral carriers to replicate autonomously, and the associated safety risks with respect to genome recombination, limit their potential use as gene delivery agents. Potent anti-cancer vaccines that stimulate dendritic cells have been devised using lentiviruses – a genus of RNA viruses in the family Retroviridae - to initiate the immune reaction[38]. These viruses are presently the focus of further research into the mechanisms by which they could alter the behavior of cancer cells[39]. Using lentiviral vectors for gene therapy is of particular interest, because lentiviruses are efficient transducers of both dividing and non-dividing cells; furthermore, lentiviruses are incorporated into host chromatin, which enables the transgene to be expressed in a stable and enduring manner[40,41]. Nevertheless, a significant drawback to using viruses as gene transfer vectors is that the viruses are targets for the body's adaptive and innate immune responses, thus they may be destroyed before successful incorporation[40]. Therefore, the current focus of research is directed less at the fundamental concept of viruses being immunogene transfer molecules, and instead the focus is on developing mechanisms that could enable the viruses to evade the host's immune response.

Virus-like particles

Virus-like particles (VLPs) are non-infectious particles of viral origin assembled from the coat protein of the native virus. VLPs are genome-free and thus are essentially an empty viral coat that can carry material (either biological in origin *viz*, proteins and nucleic acids or synthetic *viz*, synthetic chemotherapeutics) within or on the viral surface for targeted delivery[42]. One recent study assessed the role of three different types of VLPs - namely, MS2 spheres, tobacco mosaic virus (TMV) disks, and nanophage filamentous rods - for delivering doxorubicin *in-vivo* for treatment of glioblastoma. It was found that all three particles displayed adequate drug delivery, cellular uptake, and increased survival rate and only in diseased animals, with the most promising being the TMV treated mice[43]. Further studies have also demonstrated the efficiency of these VLPs as carriers of genetic

material. VLPs were reassembled from capsid proteins from RNA bacteriophage MS2, which carried a si-RNA targeted to the bcl-2 oncogene transcript[44]. The VLPs were also conjugated with a human protein to mediate better targeting. In another independent study, VLPs composed of hepatitis B virus capsid shell, conjugated with P19 RNA binding protein and RGD peptide, carried siRNA to melanoma tumor cells *in vivo*[45]. VLPs offer all the advantages of using conventional viruses as drug delivery systems yet without the threat of its inherent genetic material. This offers added safety and more flexibility over the size and content of the cargo. Additionally, VLPs are inherently immunogenic, and easily phagocytosed; while this property makes them non-stealth in function, it does mean they are effective tools as delivery agents to innate immune cells, and to sites with low immune responses (such as tumor microenvironments) among others[46].

Carrier Cells for Therapeutic Delivery

Successful delivery of therapeutic agents to target sites in the presence of a hostile environment can be achieved by hiding them inside endogenous circulating cells. For example, erythrocyte-infused therapeutic delivery since these cells can travel through narrow capillaries networks escaping the spleen clearance[47]. T-lymphocytes use the circulatory system to move between lymphatic agents and sites of foreign antigen expressions and this tumor-targeting T cell can act as cell carriers for systematic delivery[48]. An attractive candidate as a cell carrier is the mesenchymal stem cell (MSC) which has the ability to differentiate into several lineages and also has the highest degree of plasticity[49]. These cells are isolated from a variety of human tissues and organs such as the brain, liver, kidneys, and lungs. MSC's ability to migrate to sites of injury and tumor microenvironments further supports their candidacy to be ideal cell carriers. Furthermore, MSCs can be modified by gene vectors to release therapeutic agents[50]. For a cell carrier to be effective in releasing targeted therapeutics, it is necessary for these cells to travel across small spaces such as capillaries and the endothelium. MSCs migrate across the endothelium to targeted tissues by the physicochemical pairing of the respective cytokines and receptors (Figure 1.1).

Erythrocyte

Erythrocytes exhibit all the properties of an ideal drug carrier. They have a flexible structure, possess a unique shape, and are small in size. Erythrocytes' ability to pass through narrow capillary networks and avoid elimination makes them uniquely able to be employed as therapeutic carriers. To investigate their effective therapeutic carrier, researchers use the natural semi-permeable membrane to load with therapeutic agents (Figure 1.1). This offers a sustained release of small-molecule therapeutics and retention of larger proteins within the membrane. Advances in molecular biology and bioengineering have provided scientists with a greater understanding of the physicochemical and biological function of red blood cells. One major advancement was the discovery of CD47, the marker of self. Oldenburg et al. reported that CD47 functions as a marker of self and demonstrated the inverse relationship with increased phagocytosis and reduced marker levels[51]. This supports the role of CD47 expression in long-term erythrocytes in the bloodstream. CD47 regulates phagocytosis by its interaction with SIRP-alpha on macrophages. Through this ligation, tyrosine phosphatase is activated and myosin accumulation at the phagocytic synapse is suppressed. This leads to inhibition of Fcγ which mediates phagocytic signals[51]. Furthermore, by inhibiting Fcγ a reduction or inhibition of phagocytosis occurs.

T-lymphocytes

An advantage of using T-cells is the ability to exploit their tumor-homing capabilities. These cells can be used to deliver oncolytic viruses to the targeted tumor. The addition of therapeutic agents does not affect the integrity of these cells. Cytokine-induced killer cells have demonstrated the ability to localize into leukemia tissue and cause toxicity to the tissue[52]. These cells have been effective in the treatment of solid malignancies in ovaries. The success of this treatment *in vivo* has led to clinical studies with encouraging results. T-cell based immunotherapies have been successful in tumor immunotherapy by increasing the numbers of endogenous NK and CD8 T-cells which are potent mediators of antitumor immunity. T-cells co-transcribed with prostate tumor antigens to target tumor cells were successfully used for tumor treatment by Kloss et al[53]. T-cells were rendered to be tumor-specific and demonstrated a result of tumor remission without sacrificing the reactivity of the cell. T-lymphocytes are attractive drug delivery systems as T-cells are

specific and in response to an antigenic stimulus can mediate lysis of the target (antigen-presenting) cell. Further, their ability to cross the blood-brain barrier, makes them a potential agent of drug delivery for disorders of the nervous systems[54] (Figure 1.1).

Mesenchymal stem cells

Mesenchymal stem cells (MSCs) are also attractive for targeted delivery of genes and viruses, which migrate to and incorporate within the connective tissue of tumors but actively seek out metastases far removed from the tumor site (Figure 1.1). MSCs have been utilized as delivery vehicles of interactions to improve anti-cancer immune surveillance by activating cytotoxic lymphocytes and NK cells. Nakamua et al. delivered gene-modified MSCs by the infection with an adenoviral vector encoding human IL-2 that enhanced antitumor effect and prolonged survival of tumor-bearing rats[55]. MSCs are also delivery agents for gene-directed enzyme drug therapy. Results have shown that delivery of MSC transfected with cytosine deaminase (CD) resulted in a significant prolongation of survival of rats with glioma cells[55]. Transfected MSCs with antiviral vectors with CD demonstrated deceased tumor visibly.

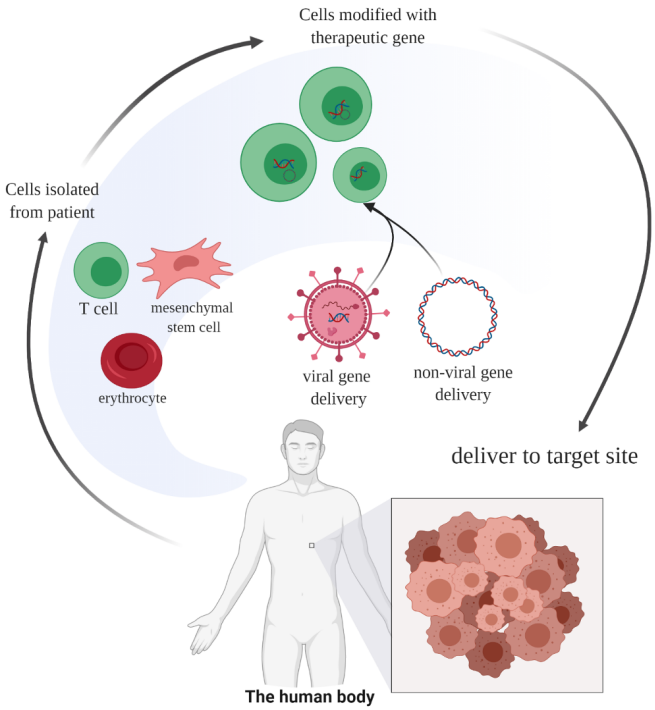

Figure 1.1. Native human cells such as T cells, MSCs, and erythrocyte can be used as carrier for the drug delivery. Therapeutic genes are delivered through viral or non-viral method to modify the cells which then home to target site while escaping the immunity.

Membranes from Ghost Cells

The cell membrane is a lipid bilayer. Retrospectively, the cell does serve as a vehicle for intracellular components. Some of these vehicles are mobile whereas some are stationary. The use of lipids as NPs is discussed in the larger context of cell membrane-based NP. We will explore the use of four cell populations *viz*, erythrocytes, MSCs, leukocytes, and platelets which have been explored as NPs for drug delivery (Figure 1.2).

Ghost erythrocytes

The long half-life, availability, and motile nature make erythrocytes as the most desirable drug delivery agents. The absence of a nucleus and genetic material makes it easy to manipulate. Additionally, their abundant numbers ease purification. The presence of a self-cell marker (CD47) on the RBC membrane shields them from phagocytosis. Two variants of erythrocytes *viz*, erythrosomes and nanosponges find application in drug delivery systems. While erythrosomes[56] are RBC membrane-derived liposomes, nanosponges[57] are erythrocyte membrane conjugated to polymers. To develop an RBC carrier, a multitude of techniques have been developed to load erythrocytes with therapeutic agents. Hypotonic treatment is the standard preparation that retains the physicochemical characteristics of the RBC membrane[58]. Erythrocytes are placed in a hypotonic solution where osmotic pressure releases the intracellular contents within the RBC membrane. The therapeutic agent passively diffuses into RBC's and is retained via isotonic buffer resealing[59]. This technique has been done in using RBC's to deliver b-glucosidase and b-galactosidase for the treatment of Gaucher's disease[47]. These specialized cells are called erythrocyte ghosts and have been harnessed for the delivery of oligonucleotide and plasma DNA. RBC carriers are also used to entrap small dry molecules which increases the biodistribution of therapeutics (Figure 1.2).

Erythrocyte ghosts have been engineered to contain hemagglutinin fusion protein on lipid membranes which is the therapeutic design of the anti-cancer drug Decitabine[60]. Nano-erythrosomes were first reported and are RBC membrane-derived liposomes. Daunorubicin-conjugated nano-erythrosomes had a greater antineoplastic index than the free drug. Using plasma membrane of erythrocyte ghosts to cloak biodegradable polymeric nanoparticles via membrane extension and demonstrates extended blood circulation half-

time of RBC membrane camouflaged polymeric nanoparticles. PEG-coated nanoparticles had an elimination half-life of 15.8 hours, while the RBC coated nanoparticles had an elimination half-life of 39.6 hours. While this is a significant improvement in half-life circulation, risks include rejection of immunogenic species that are not removed and surface antigens of specific blood groups interfering with drug optimization of the RBC carrier. Further research has used the properties of RBC cells by coupling therapeutic agents on the outer surface by covalent conjugation. Ligands on the RBC surface such as complement receptor, drugs can be conjugated and their circulation time increased. A hitchhiking strategy was employed to attach therapeutic polymeric nanoparticles to the surface to increase circulation time. Doshi et al. synthesized RBC-like particles that mimic the capabilities of RBCs such as the ability to carry oxygen and flow through smaller spaces than their diameter[61]. Merkel et al. synthesized hydrogel microparticles with turnable elasticity that resembled RBCs[62]. Both studies demonstrated that mechanobiological mimicry of RBCs was capable and has the capability of extended circulation times and increased particle deformability. One of the earliest such reported NP was a polymer of poly(lactic-*co*-glycolic acid) (PLGA) coated with erythrocyte membrane. Some of the other polymers that are coated with erythrocyte membranes include polycaprolactone, polypyrrole, poly(lactic acid), Fe_3O_4, magnetic nanoclusters, mesoporous silica, gold, and gelatin. Erythrocyte membrane coated nanoparticles have been used to deliver chemotherapeutic agents (doxorubicin, paclitaxel), proteins (b-glucosidase, b-galactosidase), and small molecules (folic acid, gambogic acid)[63].

Ghost MSC

The unique function and non-immunogenicity of MSC makes it very popular in field of medicine and drug/gene delivery. One study developed a natural gene delivery platform using nanoghosts derived from MSC (NG-MSC) with pDNA encoding cancer-toxic gene to target multiple cancers. Their results showed a significant suppression of prostate (80%) and metastatic orthotopic lung cancer growth as well as prolong animal survival[64,65]. The same group also investigated the effect of NG-MSC obtained from MSC pretreated with cancer cells conditioned-media (CM-NGs) or proinflammatory cytokines (Cyto-NGs). Outcomes enhanced the targeting of cancer cells and immune cells; where

Cyto-NGs revealed the more tumor-targeted ones while MC-NGs is more targeting immune cells[66] (Figure 1.2).

Ghost leukocyte

Like erythrocytes, the utilization of white blood cells (leukocyte) membranes were explored for coating nanoparticles to achieve stability, ability to cross immune barriers, targeting, and localization. Leukocytes comprise lymphocytes, monocytes, macrophages, and neutrophils (Figure 1.2). Leukocyte membrane-based NPs are either ghost leukocytes or leukocyte membranes coated onto other nanoparticles-termed as leukolike NP. A study assessing the efficacy of leukolike NPs found that leukolike NP ligands could communicate with receptors on endothelial cells, were able to deliver payloads across an inflamed reconstructed endothelium, and could retain functionalization *in vivo*[67]. In addition, human cytotoxic T-lymphocytes serve as another leukocyte membrane-based that camouflaged PLGA nanoparticles to target gastric cancer cells. As a result, T-lymphocytes ghost-membrane inhibit phagocytic activity by macrophages and therefore revealed more than 88% of the tumor growth suppression[68]. Monocyte/macrophages are among the most reviewed choice of leukocytes for developing leukolike particles. Drugs loaded in macrophages have a prolonged lifespan and are shielded from MPS elimination. The efficacy of macrophage biomimetic NPs has been assessed in artheroscelorsis[69], cancers of varied origin[70,71], and anti-HIV therapy[70]. Neutrophil membranes are preferred for neutrophil abundance, their ability to transmigrate, and the swelling of their numbers in response to inflammation. Kang *et al* have shown that PLGA loaded with carfilzomib (a proteasome inhibitor) encapsulated in neutrophil membrane homed to premetastatic sites within the tumor[72]. An independent study assessing *in-vivo* models of pancreatic tumor, treated with celastrol loaded on naïve neutrophil membrane encapsulated PLGA or PEG were found to prolong survival and minimize liver metastases[73].

Ghost platelets

Platelet-derived nanoparticles (PNPs) are constructed by wrapping platelet membranes onto solid NP cores (Figure 1.2). PNPs target passively using natural markers on the cell surface or actively through engagement with specific markers such as CLEC-2,

P-selectin, integrin α6β1, and integrin αIIbβ3. PNPs have been used to deliver drugs for the rebuilding of injured vasculature, tumor, and inhibition of drug-resistant bacteria[74]. In addition to specific cell membrane particles being wrapped around solid nanoparticles core, cancer cell membranes are also used for biomimicry. Either independently or as hybrids with macrophage or platelet membranes, these NPs are finding wide use in theranostics[75–77].

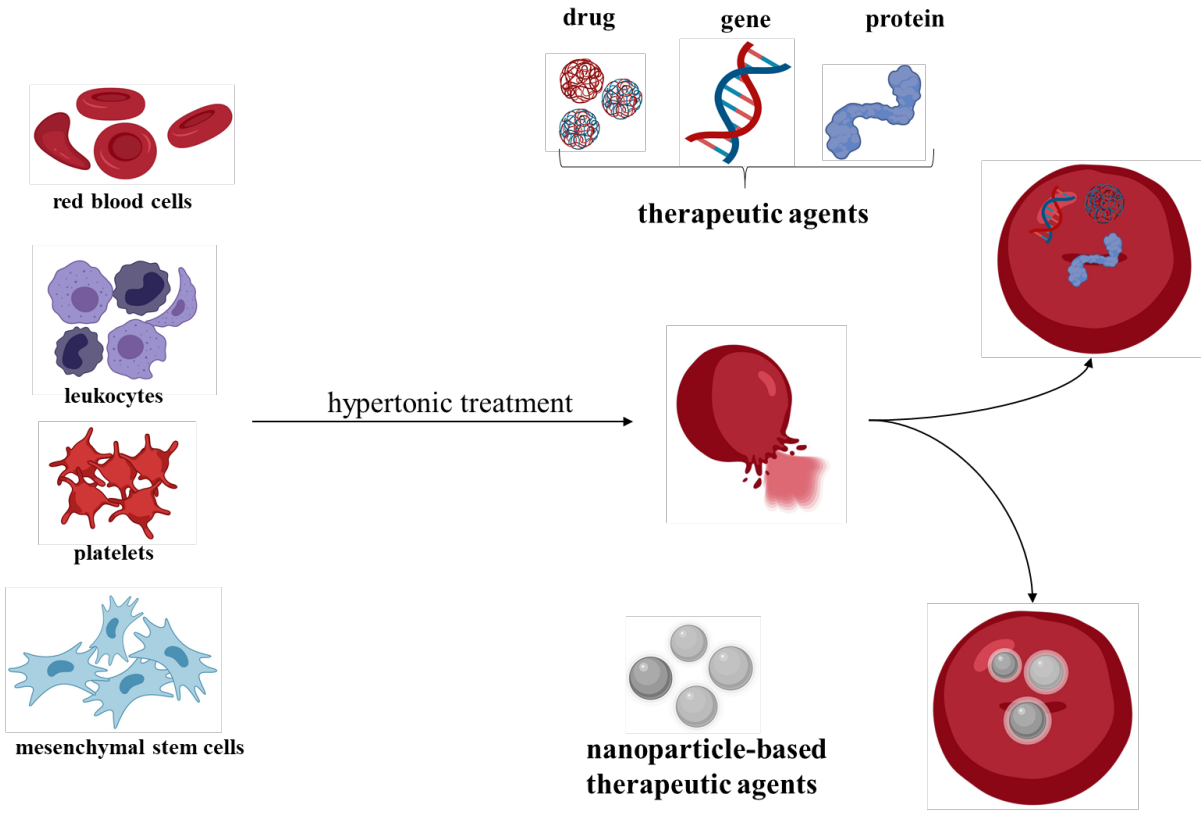

Figure 1.2. Ghost cells derived nanocarriers using RBCs, MSCs, T cells, leukocytes, and platelets. These ghost-mediated therapeutic carriers are prepared using hypertonic treatment of cells and harbor with various therapeutic agents.

Immunoglobulin Superfamily Proteins

Proteins serve a wide variety of functions in and for the cell such as recognition, transport, and metabolism. Proteins are also highly immunogenic and thus their use in stealth functionalization needs attention. When it comes to drug delivery, proteins are

coated onto the solid NP core. Some of the commonly employed protein molecules for biomimetic drug delivery are discussed below.

CD47 protein

CD47 is a self-cell marker that prevents phagocytosis of self-cells through the CD172a phagocytic pathway. It has been reported that PEG NP when coated with CD47, preferentially reduced phagocytic activity by the M1 phenotype[78]. Further higher accumulation of CD47 coated graphene oxide nanosheets were observed in tumor sites as compared to PEGylated graphene oxide nanosheets[22]. Another use of host protein for stealth functionalization includes serum albumin. Serum albumin is an abundant host protein. Studies with serum albumin coated tobacco mosaic virus were shown to exhibit reduced antibody recognition, longer circulation time[79].

CD47 has been established as a marker of self on RBC surfaces. It is suggested that CD47 could represent a viable solution in the design of macrophage evading therapeutics. CD47's N-terminal domain is a ligand for an immunoinhibitory receptor SIRPα that is abundant on macrophages and some nonphagocytic cells. Upon CD47 binding, SIRPα activates the phosphate SHP-1 which inhibits the cytoskeleton-intensive phagocytosis of cells and large particles that are opsonized by antibodies and complement factors[80]. By this pathway, it supports the discovery that CD47 acts as a marker of self. This was originally described when CD47 deficient red blood cells were infected into control mice and were rapidly cleared by splenic macrophages.

CD47 is less effective at inhibiting uptake for rigid targets and viruses are much stiffer than red blood cells. Soluble CD47 protein effect on phagocytosis activity was first demonstrated by Hsu et al. In the study, the extracellular domain of the CD47 gene was cloned into bacterial vector pre-constructed with streptavidin gene (SA), expressed in BL21 bacterial strain. After purifying the CD47-SA recombinant protein by biotinylated agarose column, antiphagocytic effect were evaluated by treated J774A.1 macrophages for 1 h, prior to adding perfluorocarbon-based oxygen carriers which successfully escape the immune clearance by macrophages (Figure 1.3). Another study hypothesized that overexpression of full-length human CD47 on a standard virus-producing cell line would generate lentivirus with sufficient CD47 to signal against macrophage uptake[80]. During the structural studies of

CD47-lentivirus, *in vitro* assessment of the uptake by phagocytic cells and nonphagocytic cells was investigated. NOD SCID gamma (NSG)mice are then used to assess *in vivo* whether CD47-lentivirus showed enhanced circulation and gene delivery to lung cancer xenografts. NSG mice express a unique mouse variant of SIRPα that binds human CD47. It should be noted that NSG mice lack functional lymphocytes but have functional macrophages. Thus, the NSG model allows the focused study of macrophages in lentiviral vector clearance. It is suggested that this can be systemically delivered across multiple sites of disease. Marker of self-inhibition of liver clearance is less clear from past studies than splenic clearance, thus the effects on Kupffer cells which is the dominant liver macrophage are sought to be understood. It was found that splenic macrophages, as well as bone marrow-derived macrophages, are clearly inhibited by CD47 on cells. Findings suggest that lentivirus which buds through cell membranes rich in CD47 have the ability to inhibit the uptake of liver macrophages. This is a desirable target that warrants future investigation of the expression of transgenes in therapeutic drug delivery.

CD200 protein

CD200 is known as an anti-inflammatory transmembrane glycoprotein in the immunoglobulin superfamily[88]. CD200 interacts with its receptor CD200R which is highly expressed on myeloid cells such as macrophages and neutrophils. This interaction has been known to reduce macrophage activation and chronic inflammation. To harness the immunomodulatory property of CD200 for surface modification, CD200-streptavidin fusion protein was expressed from bacteria transformed with PET20b plasmid-encoded with CD200 extracellular domain and core streptavidin[88]. The purified CD200-SA protein was bound to biotin-coated fluorescent polystyrene particles of various sizes ranging from 0.15 to 2 μm (Figure 1.3). In a culture with THP1 macrophages, these NPs showed reduced activation and phagocytic ability and significantly reduced amounts of pro-inflammatory cytokine TNF-alpha and Interleukin-6 (IL-6)[88].

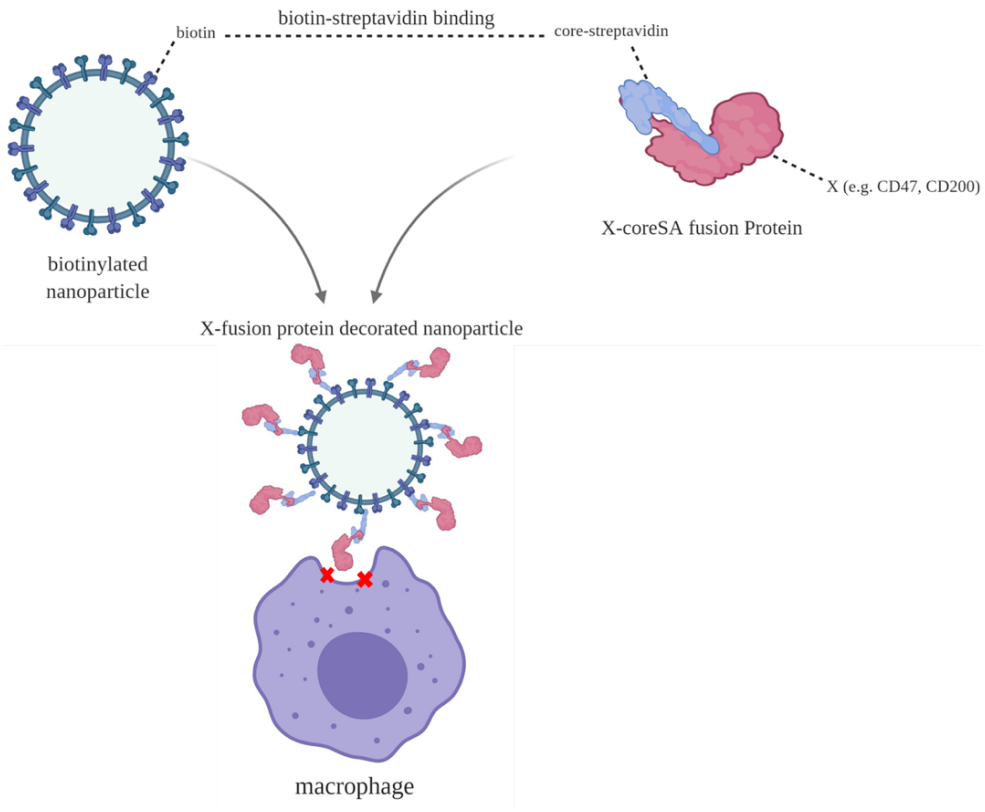

Figure 1.3. Biomimetic virus particles using fusion protein of streptavidin with immunoglobulin family proteins (e.g. CD47, CD200) which helps the nanoparticle to escape immunity.

Rationale and Specific Aims

Specific Aim 1: Produce and characterize biotinylated lentivirus

Lentiviral vectors will be produced by transfecting the plasmids that make up the genome of viral vectors into HEK 293T cells using polyethyleneimine (PEI). HEK 293T cells will be pre-fed with biotin-lipid to obtain the biotinylated virus. HEK 293T cells will be infected with biotinylated and non-biotinylated native lentivirus to evaluate the effect of biotin on virus infectivity. Successful biotin anchor on lentivirus surface will be confirmed by mixing biotinylated virus with streptavidin-conjugated gold nanoparticles and visualizing by transmission electronic microscopy. The time entry of viral particles into the cells will be assessed by labeling the biotinylated virus with streptavidin-FITC, prior to treating J774A.1 macrophages. The amount of biotin on the outer surface of the lentivirus will be determined using the HABA assay.

Specific Aim 2: Construct, express and characterize recombinant proteins

The extracellular domain of mouse CD200, CD47 and CD47/CD200 genes will be separately engineered into the previously constructed plasmid pET-30a(+)-coreSA. Each constructed plasmid will be transformed separately into Lemo21(DE3). Proteins will then be expressed and purified using immobilized metal affinity columns to obtain CD200ED-coreSA, CD47ED-coreSA and CD47ED/CD200ED-coreSA fusion proteins, respectively. The expression and purification of all fusion proteins will be characterized by SDS-PAGE and Western blot.

Specific Aim 3: Determine antiphagocytic activity of functionalized viruses

The surface of biotinylated virus will be coated with the ectodomain of CD200, CD47 or CD47/CD200 protein through biotin-coreSA binding. The immobilization of the recombinant proteins on the virus surface will be examined using dot blot analysis. The antiphagocytic effects of CD200ED, CD47ED or CD47ED/CD200ED fusion proteins on J774A.1 macrophages will be evaluated along with the control of un-decorated viral vectors. Further assessment of phagocytosis suppression from each fusion protein will be examined by the inhibition assay using antibodies to block 1) proteins on viral surface, and 2) the receptors on macrophages surface. J774A.1 macrophages will be treated with unblocking sample of CD200ED-, CD47ED- or CD47ED/CD200ED-functionalized lentivirus, respectively, as a control.

Specific Aim 4: Evaluate pro-inflammatory cytokine secretion of functionalized viruses

Interaction of CD200-CD200R associate with chronic inflammation reduction on macrophage. The anti-inflammatory secretion of interleukin-6 (IL-6) and tumor necrosis factor-α (TNF-α) from J774A.1 macrophages treated with CD200ED-, CD47ED- or CD47ED/CD200ED-modifed virus will be analyzed by enzyme-linked immunosorbent assay (ELISA). Untreated J774A.1 macrophages and unmodified biotinylated lentivirus will be tested as negative and positive controls, respectively.

Chapter 2: Less Phagocytosis of Viral Vectors by Tethering with CD47 Ectodomain

Abstract

Many viral vectors, which are effective when administrated *in situ*, lack efficacy when delivered intravenously. The key reason for this is the rapid clearance of the viruses from the blood circulation via the immune system before they reach target sites. Therefore, avoiding their clearance by the immune system is essential. In this study, lentiviral vectors were tethered with the ectodomain of self-marker protein CD47 to suppress phagocytosis via interacting with SIRPα on the outer membrane of macrophage cells. CD47 ectodomain and core-streptavidin fusion gene (CD47ED-coreSA) was constructed into pET-30a(+) plasmid and transformed into Lemo21 (DE3) competent *E. coli* cells. The expressed CD47ED-coreSA chimeric protein was purified by cobalt-nitrilotriacetate affinity column and characterized by SDS-PAGE and Western blot. The purified chimeric protein was anchored on biotinylated lentivirus via biotin-streptavidin binding. The CD47ED-capped lentiviruses encoding *GFP* were used to infect J774A.1 macrophage cells to assess the impact on phagocytosis. Our results showed that the overexpressed CD47ED-coreSA chimeric protein was purified and bound on the surface of biotinylated lentivirus which was confirmed via immunoblotting assay. The process to produce biotinylated lentivirus did not affect native viral infectivity. It was shown that the level of *GFP* expression in J774A.1 macrophages transduced with CD47ED-lentiviruses was threefold lower in comparison to control lentiviruses, indicating antiphagocytic effect triggered by the interaction of CD47ED and SIRPα. Through the test of blocking antibodies against CD47ED and/or SIRPα, it was confirmed that the phagocytosis inhibition was mediated through the CD47ED-SIRPα axis signaling. In conclusion, surface immobilization of CD47ED on lentiviral vectors inhibits their phagocytosis by macrophages. The chimeric protein of CD47 ectodomain and core-streptavidin is effective in mediating the surface binding and endowing the lentiviral nanoparticles with antiphagocytic property.

Introduction

Viral vectors are at the forefront of gene delivery vector technology with a large usage in clinical trials[81]. Despite their potential, many viral vectors are highly vulnerable to the immune system of the host when administrated intravenously[33,82,83]. Studies of viral therapeutics in murine models have revealed that liver and spleen uptake is a major impediment to systemic delivery, where the vast majority of the virus is immediately taken up from the circulation by resident macrophages of the mononuclear phagocyte system following intravenous infusion[84,85]. To overcome the obstacles that will allow us to move toward efficacious viral gene therapy, several attempts have been made to improve the circulatory persistence and efficacy of viral vectors. An intriguing strategy to overcome the host immune response is to hide the virus from immune scrutiny. This approach relies upon the use of an immunologically inert cell carrier (e.g., mesenchymal stem cells, tumor-infiltrating lymphocytes)[86,87] that is infected *ex vivo* followed by the administration to mice. Another immune evasive approach is to chemically shield viruses with polymers. Chemical modification of viral coat proteins by conjugation of biocompatible hydrophilic polymers, such as *N*-(2-hydroxypropyl)methacrylamide and polyethylene glycol masks viral surface epitopes, and therefore provides viruses the ability to evade the humoral and cellular immune response and extend the circulation times to facilitate targeting[88–95].

An alternative strategy is to disguise foreign viral particles as self-using a transmembrane protein CD47. This molecule has been suggested to function as a marker of self on red blood cells since in the absence of CD47 such cells are cleared rapidly from the bloodstream by splenic red pulp macrophages[2]. This self-marker protein protects red cells from elimination by binding to a cognate receptor, signal regulatory protein α (SIRPα) on macrophage cell outer membranes[96,97]. It was also shown that evasion of phagocytosis through up-regulation of the antiphagocytic antigen CD47 is the mechanism by which tumor cells escape immune surveillance[98–100]. In fact, CD47 analogues have also been encoded by myxoma virus[101] to escape this type of immune surveillance. Therefore, CD47-SIRPα interaction may represent a viable approach for the design of immune-evading viral vectors. Sosale et al.[102] used HEK 293T cells transduced with a lentivector encoding CD47-*GFP* and puromycin resistance transgenes as a CD47-overexpressing producer cell line to generate CD47-lentivectors. It was found that CD47-lentivectors showed prolonged circulation in lung

cancer xenografts and the macrophages transduced with CD47-lentiviruses were threefold lower comparing to the ones done with lentiviruses without CD47 functionalization. Another published study by Milani et al.[103] using a multiple-plasmid co-transfection method to generate CD47-shielded lentiviral vectors from transfected HEK 293T cells. It showed that CD47-shielded lentiviral vectors improved gene therapy in non-human primates with diminished phagocytosis by liver macrophages and consequent immune sensing. The enhanced transduction contributed by the prolonged circulation of the lentiviral particles augmented hepatocyte gene transfer efficiency. Both of the aforementioned "inside-out" approaches generate CD47-expressing lentiviral particles involving overexpressing the full length of CD47 on the lentiviral producer cell line (i.e., HEK 293T). Thus, when viral particles bud out of producer cells, they pinch off the cell membrane already expressing CD47 protein.

Since the diminution of macrophage phagocytosis via CD47-SIRPα interaction mainly relies on the ectodomain of CD47 rather than the full-length protein, the "outside-in" approach was attempted in the present study by tethering VSV-G pseudotyped lentiviral vectors with CD47 ectodomain via biotin-streptavidin affinity. Ectodomain of mouse CD47 fused with core streptavidin protein (CD47ED-coreSA) was constructed, expressed, and purified with some modifications of a previously reported paper[104]. The CD47ED-coreSA chimeric protein was further tethered on the biotinylated lentivirus obtained from HEK 293T cells pre-treated with biotin-lipid. The immunoblotting assay demonstrated the presence of CD47ED on the surface of the biotinylated virus through biotin-streptavidin binding. Our results showed that the infectivity of CD47ED-tagged lentivirus to murine J774A.1 macrophage was much less in comparison with mock lentivirus, indicating the signal created via the interaction of CD47ED tethered on the surface of lentivirus and SIRPα on macrophage cell outer membrane led to the suppression of phagocytosis. Moreover, the levels of secreted proinflammatory cytokines (IL-6 and TNF-α) were decreased if the lentiviral particles were anchored with CD47ED.

Materials

High Fidelity Phusion polymerase, Quick-Load Purple 2-log DNA ladder, Fast digest restriction enzymes (XhoI, EcoRI, and BamHI), T4 DNA ligase, T7 Express Lemo21(DE3)

competent *E. coli*, L-rhamnose, and NEB 5-alpha competent *E. coli* were all purchased from New England Biolabs (Ipswich, MA, USA). Plasmid Maxi Kit was purchased from QIAGEN (Valencia, CA, USA). Dulbecco's modified Eagles' medium (DMEM) culture media, penicillin-streptomycin, 0.25% trypsin-EDTA, B-PER bacterial protein extraction reagent, Halt™ protease inhibitor EDTA-free, streptavidin-fluorescein isothiocyanate (SA-FITC), fetal bovine serum (FBS), HisPur™ cobalt resin, Coomassie brilliant blue R 250, ECL western blotting substrate, Tween-20, bicinchoninic acid (BCA) protein assay kit including bovine serum albumin (BSA) standard, mouse TNF-α ELISA kit and IL-6 ELISA kit, streptavidin monoclonal antibody, protein concentrator PES MWCO = 10 kDa, and methanol were all purchased from Thermo Fisher Scientific (Waltham, MA, USA). Biotin-Cap-PE was purchased from Avanti Polar Lipids (Alabaster, AL, USA). Mouse IgG HRP (horseradish peroxidase)-conjugated antibody was bought from R&D Systems (Minneapolis, MN, USA). Anti-mouse CD47 monoclonal antibody was purchased from BioLegend (San Diego, CA, USA). Phosphate buffer saline (PBS) was purchased from Boston BioProducts (Ashland, MA, USA). Maxi columns were purchased from G-Biosciences (St. Louis, MO, USA). Ethanol, 2-(4-hydroxyazobenzene) benzoic acid (HABA), hexadimethrine bromide (Polybrene), isopropyl β-D-1-thiogalactopyranoside (IPTG), lysogeny broth (LB) media, imidazole, sodium hydroxide, polyethyleneimine (PEI), and potassium phosphate were purchased from Sigma-Aldrich (St. Louis, MO, USA). 2-(N-morpholino) ethanesulfonic acid (MES) was purchased from TCI (Portland, OR, USA). Kanamycin sulfate and dimethyl sulfoxide (DMSO) were purchased from Santa Cruz Biotech (Dallas, TX, USA). Tris/glycine/SDS buffer, Laemmli sample buffer, Tris-buffer saline (TBS), TGX FastCast acrylamide solutions, and polyvinylidene difluoride (PVDF) membrane (0.2 μm) were purchased from Bio-Rad (Hercules, CA, USA). 2-mercaptoethanol was purchased from Gibco (Grand Island, NY, USA). Tris-hydrochloride (Tris-HCl) was bought from Promega (Madison, WI, USA). Acetic acid was bought from J.T. Baker (Philipsburg, NJ, USA). Trypan blue was purchased from BTC Beantown chemical (Hudson, NH, USA). J774A.1 macrophage cell line was obtained from ATCC (Manassas, VA, USA).

Methods

Construction of mouse CD47ED-coreSA encoding plasmid

Core-streptavidin (coreSA) was amplified from pSTE2-215 (yol)[105] by polymerase chain reaction (PCR) using forward 5'-AGATCCGAATTCGGTGCTGCTGAAGCAGGT-3' and reverse primers 5'-ATTATACTCGAGGGAGGCGGCGGACGGCTT-3'. A commercially available clone of mouse CD47 in pCMV-SPORT6 vector was procured from Harvard Medical School (Boston, MA, USA). The ectodomain of mouse CD47 (CD47ED) was PCR amplified using forward primer 5'-GCGATGGCCATGGATATCATGCTACTGTTTAGTAACGTCA-3' and reverse primer 5'-GCTCGAATTCGGATCCTCCTTTCTCCTCCTCGTAAGAACAG-3'. A 50 µL PCR was set up for each DNA by mixing the following components: 1X Phusion HF buffer, 200 mM dNTPs, 0.5 µM forward primer, 0.5 µM reverse primer, 1 µg DNA, 1.0 unit of Phusion DNA polymerase, and reaction volume was made up with nuclease-free water (New England Biolabs). The PCR for both genes were carried out using a T-100 thermocycler (Bio-Rad) with an initial denaturation temperature of 98°C for 30 s, followed by 30 cycles of denaturation at 98°C for 10 s, annealing at 60°C for 15 s, and extension at 72°C for 15 s. The final extension was set for 5 min at 72°C and PCR products were purified using a Monarch PCR & DNA cleanup kit (New England Biolab). Finally, PCR products were confirmed by 1% agarose gel electrophoresis. CoreSA was digested and cloned into pET-30a(+) between XhoI and EcoRI sites to yield plasmid pME005. Further, mouse CD47 ectodomain was inserted into pME005 between the EcoRI and BamHI sites yielding plasmid pME006.

Expression of CD47ED-coreSA chimeric protein

The expression of CD47ED-coreSA fusion gene encoded in pET30a(+) plasmid transformed into Lemo21(DE3) was performed using previously reported procedures[104]. Briefly, Lemo21 (DE3) competent *E. coli* cells carrying pME006 plasmid were grown in 1 liter of LB media containing 50 µg/mL kanamycin and 0.5 mM of L-rhamnose at 37°C with shaking at 225 rpm. When OD_{600} reached to 0.6-0.8, culture was induced with 0.4 mM IPTG and kept shaking overnight at 18°C. Then, cells were harvested by centrifugation at 4,500 ×g

for 15 min and cell pellets were resuspended in a lysis buffer containing proprietary non-ionic detergent B-PER supplemented with 50 mM Tris-HCl, and 1× EDTA-free protease inhibitor (pH 7.5). The lysate was incubated at room temperature (RT) for 20 min and sonicated under cold conditions for 30 min with power output set at 5 of tip sonicator (Misonix, Farmingdale, NY, USA). The bacterial lysate was centrifuged for 20 min at 18,000 ×g, and the supernatant was collected and purified (i.e., soluble crude protein).

Purification of CD47ED-coreSA chimeric protein

The purification of CD47ED-coreSA chimeric protein was carried out by immobilized metal affinity chromatography (IMAC) using HisPur™ cobalt nitrilotriacetic acid (Co-NTA) resin according to the manufacturer's instructions and protocol. In brief, the cobalt-NTA resin was equilibrated with two resin-bed volumes of equilibrium buffer (10 mM imidazole, 50 mM Na_2HPO_4, 300 mM NaCl, pH 7.4) in affinity column. Mixtures of crude protein and equilibrium buffer (1:1 ratio) were prepared and then added to the equilibrated cobalt-NTA resin. Polyhistidine tagged CD47ED-coreSA chimeric protein in the crude protein was bound to the resin by gentle shaking at 4°C for 2 hours. After collecting the non-binding protein flow-through, the resin was washed with five resin-bed volumes of wash buffer (10 mM imidazole, 50 mM Na_2HPO_4, 300 mM NaCl, pH 7.4) or until the absorbance of wash-fraction at OD_{280} nm approached the minimum baseline. The target protein was eluted out from the resin with five resin-bed volume of the elution buffer (250 mM imidazole, 50 mM Na_2HPO_4, 300 mM NaCl, pH 7.4) or until the absorbance of elution-fraction at OD_{280} nm approached the minimum baseline. The eluted protein fractions were concentrated using polyethersulfone (PES) membrane with a 10 kDa molecular weight cut off (MWCO = 10 kDa). The protein solution was aliquoted and stored at -80°C until further use. The coreSA protein used for the control group was expressed and purified from plasmid pME005 (pET-30a(+)-coreSA) with the same procedures mentioned above.

Characterization of CD47ED-coreSA chimeric protein

Sodium dodecyl sulfate-polyacrylamide gel electrophoresis (SDS-PAGE) of the expressed recombinant histag-chimeric protein was carried out on a vertical slab assembly

using polyacrylamide gels run under denaturing conditions. The 12% polyacrylamide gels prepared by Mini-PROTEAN Tetra handcast systems as guided by Bio-Rad were used. 15 μL of each sample was diluted to 1:1 ratio with 2X Laemmli sample loading buffer supplemented with 5% (v/v) of 2-mercaptoethanol and heated to 95°C for 5 min prior to loading. Electrophoresis was performed with Tris-glycine electrode buffer (1X), pH 8.3 at 200 V for 40 min; the gels were stained for three hours with Coomassie brilliant blue R-250. For Western blot analysis, three electrophoresed samples were transferred to separate nitrocellulose membranes 0.2 µm (Bio-Rad) by Trans-Blot® semi-dry system (Bio-Rad) conducted at 20 V for 1 hour. Next, membranes were immersed in blocking buffer (5% BSA in TBST) for 1 hour at RT. The blots were washed with TBST buffer thrice for 5 min each and then incubated separately with primary antibody solutions of anti-histag monoclonal antibody, anti-streptavidin monoclonal antibody, and anti-mouse CD47 monoclonal antibody at 4°C overnight. After incubation, the blots were washed thrice again and incubated separately with secondary antibody solutions (1:1000 dilution of HRP-labeled mouse IgG in blocking buffer) at RT for 2 hours. Finally, after gentle washing, the blots were developed using ECL substrate and imaged using a chemiluminescence imager (PXi Syngene, Frederick, MD, USA). BCA protein assay was performed to determine the concentration of CD47ED-coreSA chimeric protein. According to the manufacturer's instructions, serial dilution of BSA solution (2 mg/mL) was initially prepared as protein standards. Next, working reagent was prepared by mixing BCA reagents A and B at 50:1 ratio, respectively. 30 µL of BSA proteins standards and chimeric protein were mixed with 200 µL of working reagent and maintained at 37°C for 30 min. Finally, the absorbance of all samples was measured at 562 nm by a microplate reader (Spectramax M2e, Molecular Devices, Sunnyvale, CA, USA) and concentration was calculated using a calibration curve of the BSA standard curve.

Cell culture

Cultures of HEK 293T and J774A.1 cells were seeded in T75 culture flasks in Dulbecco's Modified Eagle Medium (DMEM) supplemented with 10% fetal bovine serum (FBS) and 1% penicillin/streptomycin (complete culture medium, CM) and maintained at

37°C in 5% CO_2 humidified incubator. Cells were harvested using 25% trypsin and centrifugated at 300 xg for 5 min.

Preparation of PEI/ DNA complexes

A pH neutralized solution of PEI (200 µg/mL) was prepared, and filter sterilized. Next, 6 µg of each DNA plasmid [all purchased from Addgene (Watertown, Massachusetts, USA)]: the packaging plasmid (pCMV delta R8.2, ID#12263), the virus envelope plasmid (pMD2.G, cat#12259), and the tracker EGFP-encoding plasmid (pLJM1-EGFP, cat#19319) were mixed with the PEI solution at N/P ratio of 5:1 (PEI:DNA). The complex was then incubated at RT for 30 min before being added to cultured cells.

Native lentivirus and biotinylated lentivirus production

HEK 293T cells were cultured in two T-75 flasks containing Dulbecco's modified eagle's medium (DMEM) supplemented with 10% fetal bovine serum (FBS) and 1% penicillin-streptomycin at 37°C in a 5% CO_2 and humidified incubator. One of the flasks was additionally supplemented with 0.02 mg/mL biotin-lipid (Biotin-Cap-PE). Upon 80 % confluency, cells in both flasks were transfected with the PEI/DNA complexes. Lentiviruses from both flasks were collected every 24 hours and replaced with fresh culture media supplemented with and without biotin-lipid. Native lentivirus (non-biotinylated) and biotinylated lentivirus were separately filtered through a 0.45 µm syringe filter and stored at -80°C for later use. Culture supernatant containing lentivirus collected on the third day post-transfection was concentrated using a previously reported method [106]. Briefly, the supernatant was mixed with an equal volume of 320 µg mL^{-1} of a polybrene solution and incubated for 30 min at 37°C. After incubation, the lentivirus was pelleted by centrifugation at 10,000 ×g for 10 min at 4°C. The pellet was resuspended in 1 mL PBS and stored at -80°C till further use.

Transmission electronic microscopy preparation and analysis

To differentiate the features of biotinylated and native lentiviruses, concentrated by polybrene polymer, streptavidin-conjugated gold nanoparticles (SA-AuNPs) was separately mixed with each sample and prepared for TEM analysis. Briefly, 10 µL of biotinylated and

native lentiviruses were diluted in 1 mL of PBS supplemented with 0.05 mg/mL of SA-AuNPs (with size of 10 nm) and incubated at 4°C for 1 hour under gently shaking condition. The non-binding gold nanoparticles were removed by washing and centrifugation with 1x PBS twice at 10,000 ×g for 10 min. The samples were prepared by adding 4 µL of the collected lentivirus-gold nanoparticles on Formvar grid and incubated under the fume hood for 2 min. The samples were negatively stained with 4 µL of 2% Phosphotungstic Acid (PTA) aqueous solution for 2 min and dried under a heat lamp for 30 min prior to analyze the lentiviral vectors and gold nanoparticle attached to their surface with TEM.

Quantification of biotin on the lentivirus surface

Biotin amount on lentivirus surface was estimated with HABA assay according to a previously published report [107]. Lentivirus culture was diluted 10-fold using the HABA/Avidin solution (6 µmol of HABA and 5 mg of avidin). To do so, a cuvette containing 0.9 mL of the HABA/Avidin solution was set to measure optical density at 500 nm (OD_{500}) using a microplate reader. The biotinylated virus (0.1 mL) was added to the cuvette and then measured spectrophotometrically at OD_{500}. The decrease in absorbance compared to the HABA/Avidin was recorded and the amount of biotin per lentivirus was calculated.

Infectivity of biotinylated and native lentivirus

HEK 293T cells were seeded in 6-well tissue culture plates. Upon reaching confluency of 50%, cells were infected with biotinylated and native lentivirus, respectively at a multiplicity of infection (MOI) of 12. After incubating for 3 hours, the media were replaced and the cells were imaged at 24-, 48- and 72-hours post-infection, using fluorescence microscopy (DMi8 equipped with Leica EC3 camera, Leica Microsystems, Wetzlar, Germany). Post-completion, cells were harvested to measure *GFP* expression using a flow cytometer (Accuri C6, BD Biosciences, San Jose, CA, USA). For flow cytometry, cells were trypsinized and centrifuged. The cell pellets were washed with PBS, harvested by centrifugation, resuspended again in PBS, and incubated in ice. Fluorescence was determined for at least 100,000 events. To define the timing of viral entrance, biotinylated lentivirus was

concentrated and mixed with 0.02 mg/mL of streptavidin-FITC with gentle shaking at 4°C for an hour. Unbound streptavidin-FITC was removed by centrifugation and washing of pellet with PBS. The streptavidin-FITC labeled virus particles were used to infect the J774A.1 macrophages, which were cultured in a 6-well tissue culture plate. Phagocytosis was monitored at an hourly interval up until 4 hours post-infection using fluorescence microscopy.

Biotinylated lentivirus immobilized with CD47ED-coreSA chimeric protein

The biotinylated viral suspension (500 µL) was mixed with 1 mL of CD47ED-coreSA chimeric protein and rotated gently for 1 hour at 4°C to allow streptavidin-biotin binding. Unbound protein was removed by washing twice with PBS through centrifugation. The pellet was finally resuspended in PBS. Attachment of CD47ED-coreSA on the surface of biotinylated lentivirus was characterized using the dot blot assay. Five µL of the sample (CD47ED-capped virus) was spotted on the nitrocellulose membrane. After the sample was air-dried, the membrane was immersed in a blocking buffer for 1 hour at RT. The membrane was washed thrice for 5 min each using TBST buffer and allowed to react with primary antibody solution (1:1000 dilution of anti-mouse CD47 antibody in blocking buffer) for 1 hour at RT. The membrane was again washed thrice followed by incubation with secondary antibody solution (1:1000 dilution of HRP-conjugated mouse IgG antibody in blocking buffer) for 1 hour at RT. The image was detected using ECL substrate. Uncoated biotinylated lentivirus and CD47ED-coreSA protein were used as the negative and positive control, respectively.

Phagocytosis of biotinylated lentivirus immobilized with CD47ED-coreSA

J774A.1 macrophage cells were seeded on a 6-well tissue culture plate according to protocols reported previously. Upon 60% confluency, cells were infected with biotinylated lentivirus, coreSA-tagged lentivirus, and CD47ED-tagged lentivirus. Three hours post-infection, the cells were washed and replenished with culture media. Cells were imaged and analyzed for the percentage of phagocytosis (i.e., rate of infectivity) using fluorescence

microscopy. HEK 293T cells were used as the non-phagocytic cell control and infected with biotinylated lentivirus tagged and non-tagged with CD47ED.

Blocking CD47ED/ SIRPα interaction

The impact of blocking CD47ED and/or SIRPα on the uptake of lentivirus by J774A.1 cells was assessed by an inhibition assay. Before the infection, CD47ED-modified lentivirus was treated with anti-mouse CD47 antibodies under gentle shaking conditions at 4°C for an hour. Similarly, macrophages were treated with anti-SIRPα antibody for an hour before being infected with CD47ED-modified lentivirus. CD47ED-modified lentivirus and J774A.1 macrophages were both blocked with anti-mouse CD47 and anti-SIRPα antibodies, respectively, before incubating together. Unblocked CD47ED-modified lentivirus and macrophages were used as controls.

Effect of CD47ED on proinflammatory cytokine secretion

J774A.1 macrophages were seeded at a density of 5×10^4 cells/cm^2 in 6-well plates, before treating with either CD47ED-modified lentivirus or native lentivirus for a period of 18 hours. The secretion of IL-6 and TNF-α in the culture media was determined by commercial ELISA assays. In short, the 96 well ELISA plate was coated overnight at 4°C with 100 µL coating buffer containing either IL-6 or TNF-α capture antibody. The coating solution was then removed, and the wells were washed three times with a wash buffer (PBS + 0.05% Tween 20), followed by blocking with 200 µL 1× ELISPOT diluent per well for 1 hour at RT. The wells were washed three times and 100 µL of culture media or appropriate standards and controls were added to the test plate for 2 hours at RT. Following removal of samples, the plate was again washed three times, and the IL-6 and TNF-α detection antibodies prepared in ELISPOT diluent were added in 100 µL per well for 1 hour at RT. The detection antibodies were removed, and the wells were washed three times. 100 µL per streptavidin-HRP in ELISPOT diluent was added and incubated at room temperature for 30 min. Following removal of the conjugate, the wells were washed five times, and 100 µL of 1× tetramethyl benzidine solution was added to each well for 15 min at RT. Addition of 50 µL per well of 1 M phosphoric acid stopped the reaction. The resultant absorbance at 450 nm

was determined on a microplate reader. The concentrations of IL-6 and TNF-α in the culture media were determined using the standard curves.

Statistical analysis

All data are presented as the mean ± standard deviation from at least three independent experiments and analyzed using one-way analysis of variance (ANOVA), followed by Tukey multiple comparisons post hoc tests in between experimental groups. *P* value less than 0.05 is considered statistically significant.

Results

Construction of plasmid encoding CD47ED-coreSA chimeric gene

PCR products of CD47ED ~400 bp and coreSA ~387 bp were obtained by PCR. The pME006 was constructed by cloning PCR product of CD47ED and coreSA in between EcoRI/BamHI and XhoI/EcoRI respectively of pET-30a(+) as shown in Figure 2.1A. The gene coding sequence of CD47ED (~400 bp) and coreSA (~387 bp) in pME006 were verified by PCR and running on 1% agarose gel shown in Figure 2.1B. Given the sequence of CD47ED 400 bp (~14.6 kDa) and coreSA 387 bp (~14.2 kDa), the molecular weight of CD47ED-coreSA chimeric protein was estimated around 29 kDa which is consistent with the SDS-PAGE analysis shown in Figure 2.2B.

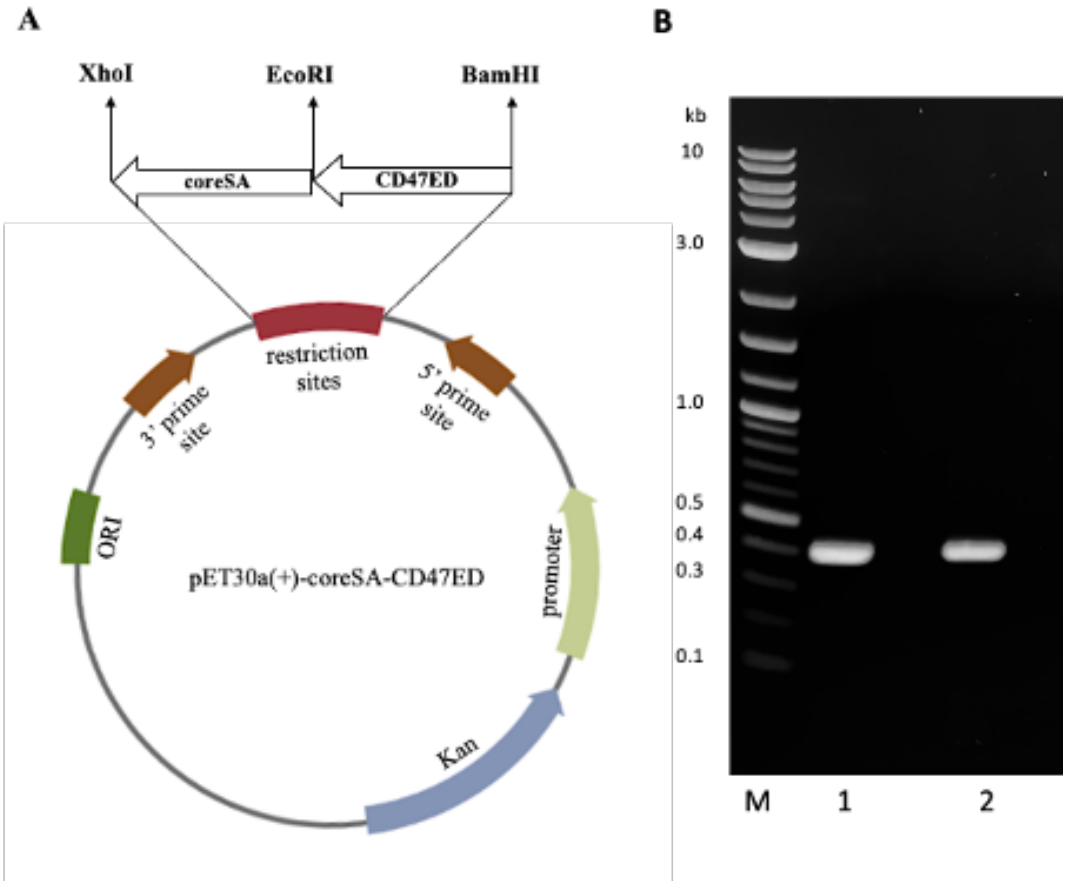

Figure 2.1. Plasmid map and PCR amplification of genes of interest. (A) vector map of plasmid pET-30a(+) showing cloning site of both genes of interest; ectodomain of mouse CD47 (CD47ED) and core streptavidin (coreSA) in between respective restriction sites; (B) DNA gel electrophoresis of PCR products of CD47ED in lane 1, coreSA in lane 2; M reflects the DNA ladder.

Expression and purification of CD47ED-coreSA chimeric protein

The constructed pME006 vector was transformed into Lemo21(DE3) competent *E. coli* cells and screened using a kanamycin agar plate. A single colony was picked and cultured in LB media supplemented with 500 µM L-rhamnose and induced expression with inoculation of 400 µM IPTG. The target chimeric protein was purified from lysates using IMAC columns packed with Co-NTA resin, and the elution profile was plotted by measuring absorbance at OD_{280} of each wash and elution fraction (Figure 2.2A). The soluble crude fraction along with purified chimeric protein was run on 12% SDS-PAGE followed by Coomassie staining, showing 29 kDa predominant band as predicted for the CD47ED-coreSA chimeric protein in the soluble crude extracts of the *E. coli* cells (Figure 2.2B lane 2).

The purified chimeric protein appeared as a monomeric band of 29 kDa (Figure 2.2B lane 3). The elution fractions were concentrated using a protein concentrator (MWCO = 10 kDa) and the concentration was measured by BCA to be 383 ± 23 µg/mL. The purified protein was further characterized by Western blot analysis against three commercially procured antibodies: anti-histag antibody, anti-streptavidin antibody, and anti-mouse CD47 antibody, which bind the purified chimeric protein. Each antibody exhibits a single band at the target protein size of MW ~29 kDa (Figure 2.2C).

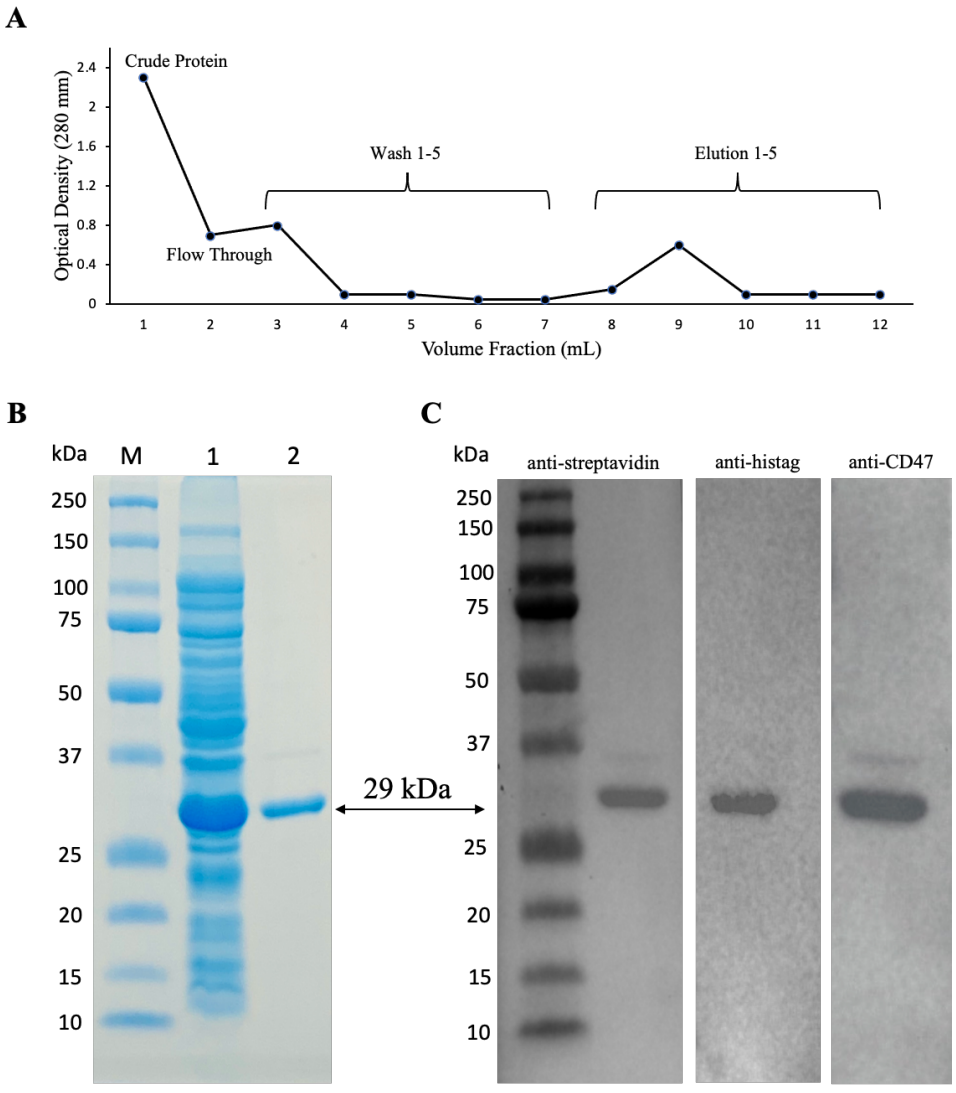

Figure 2.2. Characterization of CD47ED-coreSA chimeric protein. (A) elution profile of the protein purification process showing that most of the target protein eluted at the fraction 9; (B) SDS-PAGE image showing the protein marker (lane M), soluble crude protein with overexpressed

chimeric protein around 29 kDa (lane 1), and purified concentrated chimeric protein ~ 29 kDa (lane 2); (C) Western blot analysis revealing reactivity of anti-streptavidin antibody, anti-histag antibody and anti-CD47 antibody against the purified chimeric protein.

Infectivity of biotinylated lentivirus

The amount of biotin bound on the lentivirus surface was quantitated using the HABA/Avidin assay. It was estimated about 1.27×10^{-7} μmoles of biotin per virion particle (equivalent to 7.65×10^{10} molecules). The effect of biotinylation on infectivity of lentiviral vectors was qualitatively or quantitatively assessed against HEK 293T cells using fluorescence microscopy and flow cytometry. Figure 2.3A illustrates the levels of *GFP* expression in HEK 293T cells infected with native and biotinylated lentivirus are similar. The flow cytometry histograms further quantitatively confirmed that with mean fluorescent intensity (MFI) = 7,087 for biotinylated lentivirus and MFI = 6,935 for native lentivirus (Figure 2.3B). As a result, the infectivity of biotinylated lentivirus remains intact after biotinylation.

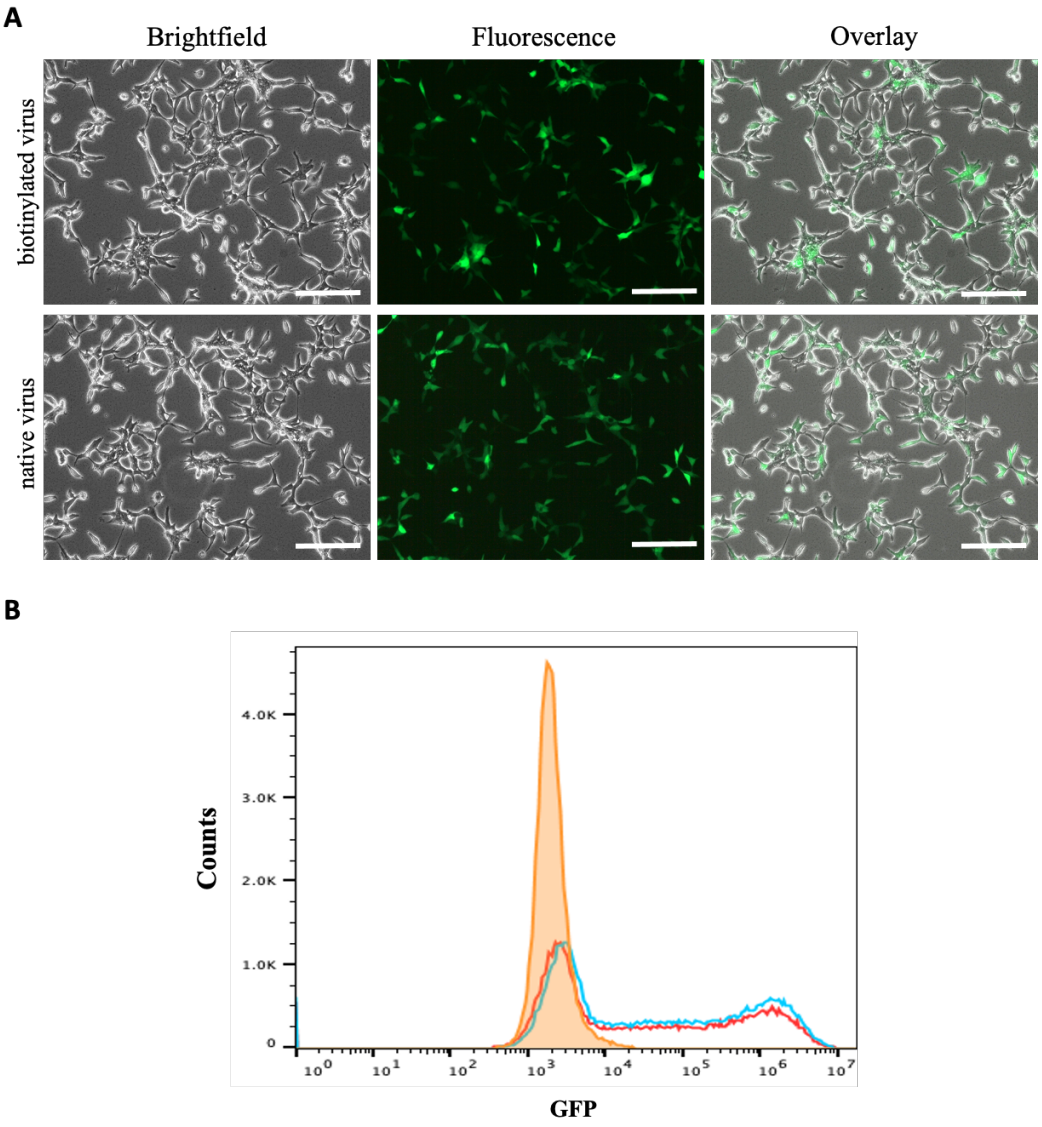

Figure 2.3. Characterization of biotinylated and native lentivirus. (A) showing phase contrast, fluorescence, and overlay images of HEK 293T cells treated with biotinylated and native lentivirus for 72 hours (scale bar denotes 100 µm); (B) representing the histograms of GFP intensity in HEK 293T cells treated with biotinylated (red, MFI = 7,087.25) and native lentivirus (blue, MFI = 6,934.71), respectively. Orange curve represents untreated HEK 293T cells negative control.

The biotin lipid labeling lentivirus was analyzed using SA-AuNPs by TEM. Biotinylated lentivirus was successfully capped with AuNPs, which bound all over the viral surface (Figure 2.4A). However, the native lentivirus exhibited no attachment of SA-AuNPs due to the lack of biotin (Figure 2.4B).

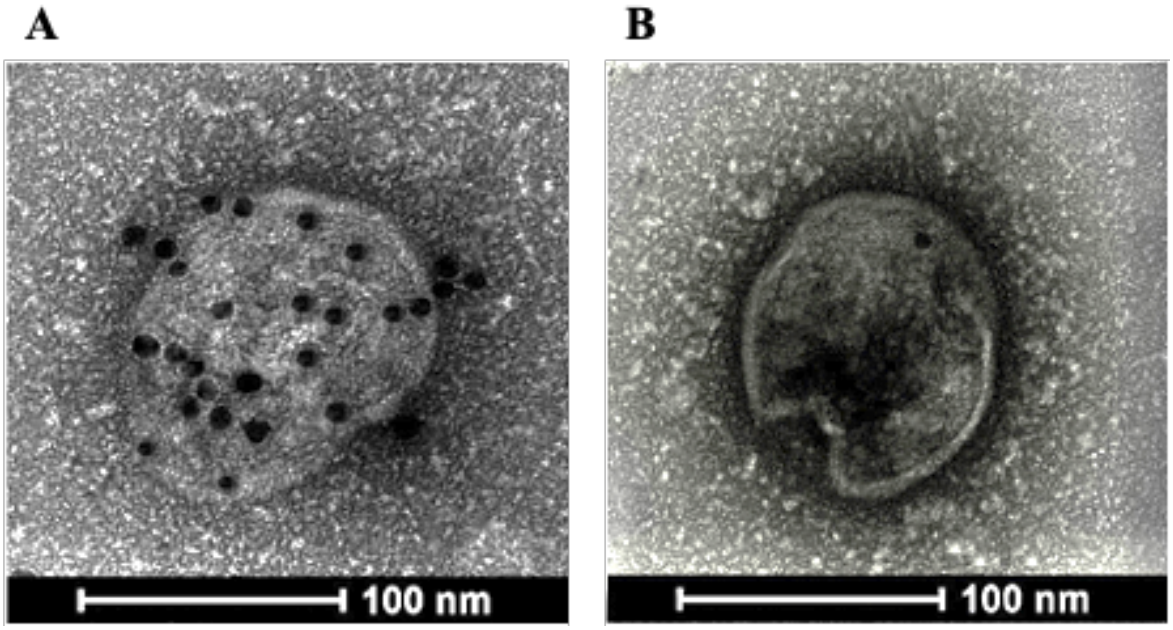

Figure 2.4. Transmission electronic microscopy of lentivirus. (A) biotinylated lentivirus capped with streptavidin gold nanoparticles; (B) native lentivirus mixed with gold nanoparticles.

In addition, biotinylated lentiviruses were tagged with streptavidin-FITC before infecting J774A.1 macrophage cells to visualize cell entry of dye-labeled viruses. The fluorescence intensity of FITC confirmed the early time entry of the virus into macrophages within 1 hour. The fluorescence intensity was found to increase with the passage of time, which was observed on an hourly basis for up to 4 hours. Figure 2.5A demonstrated the virus entering the macrophages within 4 hours post-infection was much higher comparing to the 1 hour, which indicates the rate of virus engulfment by macrophage is increasing. Therefore, the viral treatment for three hours was chosen as the time period for macrophage phagocytosis of lentiviruses in this study.

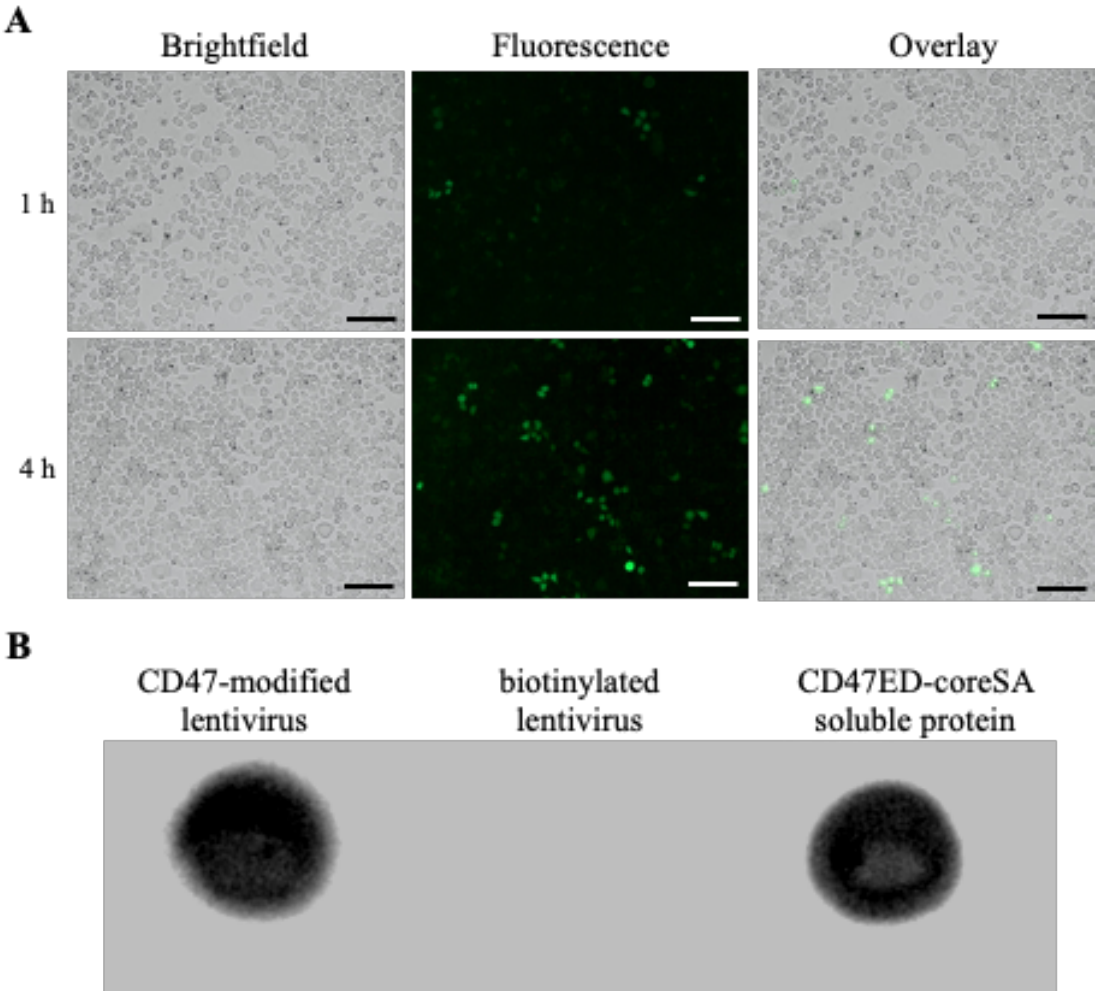

Figure 2.5. Cell entrance of biotinylated lentivirus. (A) biotinylated lentivirus conjugated to streptavidin-FITC was loaded onto J774A.1 macrophages. According to the level of green FITC fluorescence, lentiviruses entered macrophages 1-hour post-infection and continued the process at the end of 4-hours observation (scale bar denotes 100 µm); (B) dot blot assay showing biotinylated lentiviral particles can bind CD47ED-coreSA via biotin-streptavidin. CD47ED-modified virus, unmodified biotinylated lentivirus (negative control) and CD47ED-coreSA soluble protein (positive control) were blotted on the membrane and evaluated against anti-CD47 monoclonal antibody. The outcomes confirmed the presence of CD47ED protein in two groups: CD47ED-modified virus and CD47ED-coreSA soluble protein, while unmodified biotinylated lentivirus (negative control) revealed no CD47ED signal.

Characterization of biotinylated lentivirus tagged with CD47ED-coreSA

Five µL of biotinylated lentivirus tagged with CD47ED-coreSA was added to the PVDF membrane along with controls. Anti-mouse CD47 antibodies bound to biotinylated lentiviruses tagged with CD47ED-coreSA (shown in Figure 2.5B) and soluble CD47ED-coreSA protein (positive control, shown in Figure 2.5B), whereas the antibodies were not

able to bind to biotinylated lentiviruses (shown in Figure 2.5B). The presence of the CD47ED-coreSA protein and the CD47ED-modified virus were clearly expressed, while there was no expression of CD47ED-coreSA protein on the biotinylated lentivirus surface. Judging by the dot blot assay, the binding of CD47ED-coreSA with biotinylated lentivirus was successful.

Antiphagocytic effect of CD47ED-coreSA immobilized on biotinylated lentivirus

In vitro study was performed using two cell lines, phagocytic J774A.1 and non-phagocytic HEK 293T cells, to study the effect of CD47ED protein on macrophage activation. Phagocytic J774A.1 cells were treated with biotinylated lentivirus, coreSA-modified lentivirus, and CD47ED-modified lentivirus. After 72 hours of infection, the level of *GFP* expression in phagocytic J774A.1 macrophages treated with biotinylated lentivirus (Figure 2.6A (i)) and coreSA-modified lentivirus (Figure 2.6A (ii)) was way much higher than the macrophages treated with CD47ED-modified lentivirus (Figure 2.6A (iii)). According to density plot analysis of *GFP* expression, the percentages of GFP expression are 0.18% (Figure 2.6B), 62.2% (Figure 2.6C), 55.9% (Figure 2.6D), and 34.3% (Figure 2.6E) for J77A.1 cells untreated with biotinylated lentivirus, treated with the biotinylated virus, coreSA-modified lentivirus, and CD47ED-modified lentivirus, respectively. The flow cytometer histogram showed MFI = $1.40\times10^6 \pm 5{,}191$ for unmodified biotinylated virus, MFI = $1.26\times10^6 \pm 6{,}842$ for coreSA-capped virus and MFI = $8.06\times10^5 \pm 3{,}977$ for CD47ED-capped virus (data not shown). The decrease of *GFP* expression level for the CD47ED-capped virus group was about 40-45% compared to the biotinylated virus and coreSA-tethered virus. The finding was furthered confirmed by fluorescence plate reading, the macrophage cells expressed 3-fold less *GFP* in the group treated with CD47ED-modified lentivirus in comparison with biotinylated lentivirus and coreSA-modified lentivirus (Figure 2.6F). The decreasing of the phagocytosis activity illustrates that CD47ED-modified virus could interact with SIRPα receptor located on the surface of macrophages and inhibit their activation to prevent the virus entry, therefore *GFP* expression (i.e., virus infectivity) decreased.

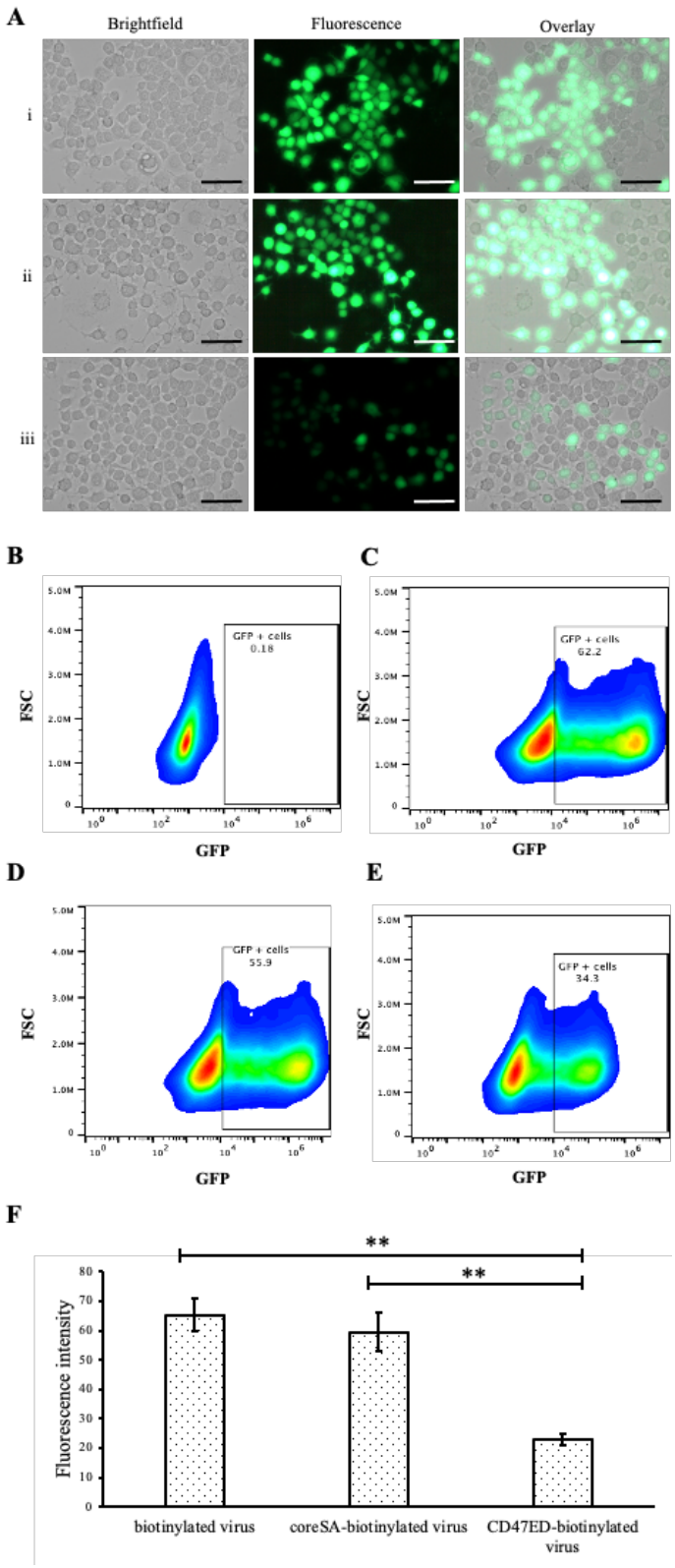

Figure 2.6. Reduced macrophage phagocytosis of lentivirus tethered with CD47ED. (A) showing brightfield, fluorescence, and overlay images of J774A.1 macrophage cells ingested (i) biotinylated

lentivirus, (ii) coreSA-biotinylated lentivirus, and (iii) CD47ED-biotinylated lentivirus, respectively. Scale bar denotes 100 μm; (B-E) density plot of macrophages expressing *GFP* using flow cytometer – (B) untreated J774A.1 macrophages (negative control), (C) J774A.1 macrophages treated with unmodified biotinylated lentivirus (positive control), (D) 774A.1 macrophages treated with coreSA-modified biotinylated lentivirus, and (E) J774A.1 macrophages treated with CD47ED-modified biotinylated lentivirus; (F) measurement of fluorescence intensity per cell using ImageJ of J774A.1 macrophages treated with biotinylated lentivirus, coreSA-biotinylated lentivirus, and CD47ED-biotinylated lentivirus at 72 hours post-treatment. Statistical analysis was performed using one-way ANOVA followed by Tukey post hoc multiple comparisons test and data were presented as mean ± standard deviation (n = 5); ** denotes $P<0.01$.

Unlike macrophages, HEK 293T cells treated with CD47ED-modified lentivirus could not inhibit phagocytosis due to the very low expression of SIRPα[102] on their surfaces (Figure 2.7A). Therefore, the percentage of *GFP* expression for HEK 293T cells treated with the biotinylated virus (75.8%, Figure 2.7C) was similar to the ones infected with CD47ED-capped virus (74.1%, Figure 2.7D). This finding was further confirmed by the flow cytometer histogram, which showed MFI = $1.94\times10^6 \pm 9{,}851$ for unmodified biotinylated virus, and MFI = $1.85\times10^6 \pm 13{,}217$ for CD47ED-capped virus (data not shown).

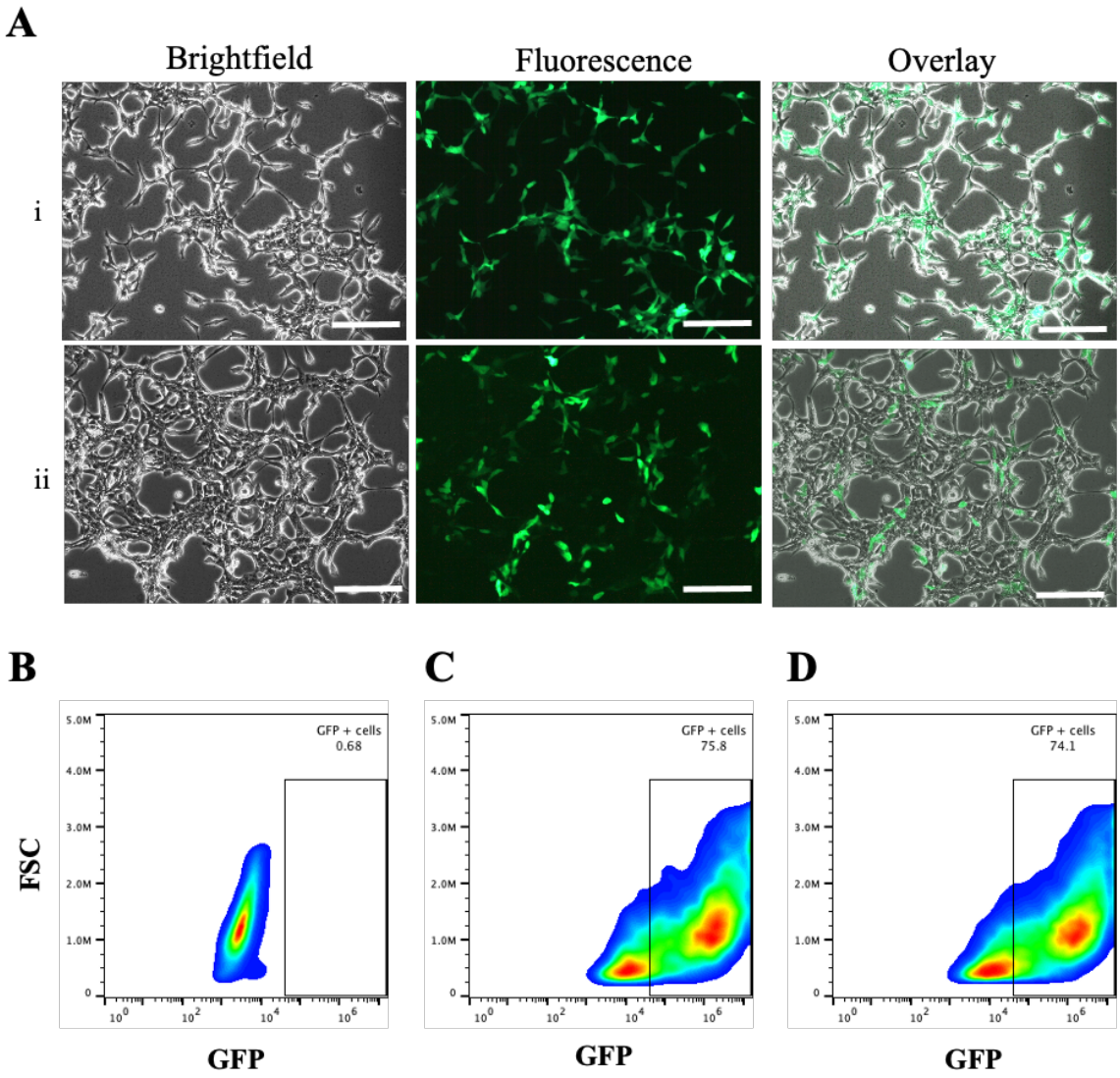

Figure 2.7. Non-phagocytic cells treated with CD47ED-capped virus. (A) (i) HEK 293T cells treated with CD47ED-modified and (ii) unmodified biotinylated lentivirus for a period of 72 hours culture; (B-D) density plot of HEK 293T cells expressing *GFP* using flow cytometer – (B) untreated HEK 293T cells (negative control), (C) HEK 293T cells treated with unmodified biotinylated lentivirus (positive control), and (D) HEK 293T cells treated with CD47ED-modified biotinylated lentivirus. Scale bar denotes 100 µm.

Inhibition of phagocytosis by blocking of CD47-SIRPα interaction

It has been previously reported that CD47 activates the SIRPα receptor on the macrophage surface suppressing phagocytic engulfment[108]. To confirm the findings, anti-

CD47 and anti-SIRPα monoclonal antibodies were used separately to block CD47ED on lentivirus and SIRPα on the macrophage cell membrane. Infection of macrophages was mediated with blocked CD47 but unblocked SIRPα, blocked SIRPα but unblocked CD47ED and blocked both CD47ED and SIRPα. Figure 2.8A showed the blocking of CD47ED protein or the SIRPα receptor on the macrophage surface increased phagocytosis of virus engulfment by macrophages due to the disruption of CD47-SIRPα axis signaling, therefore increasing *GFP* expression. The change in fluorescence intensity was measured using a microplate reader, with respect to unblocked CD47ED-modified virus control, demonstrated a statistically significant increase in the phagocytosis of viral particles upon the blockage of either CD47ED, SIRPα, or both (Figure 2.8B).

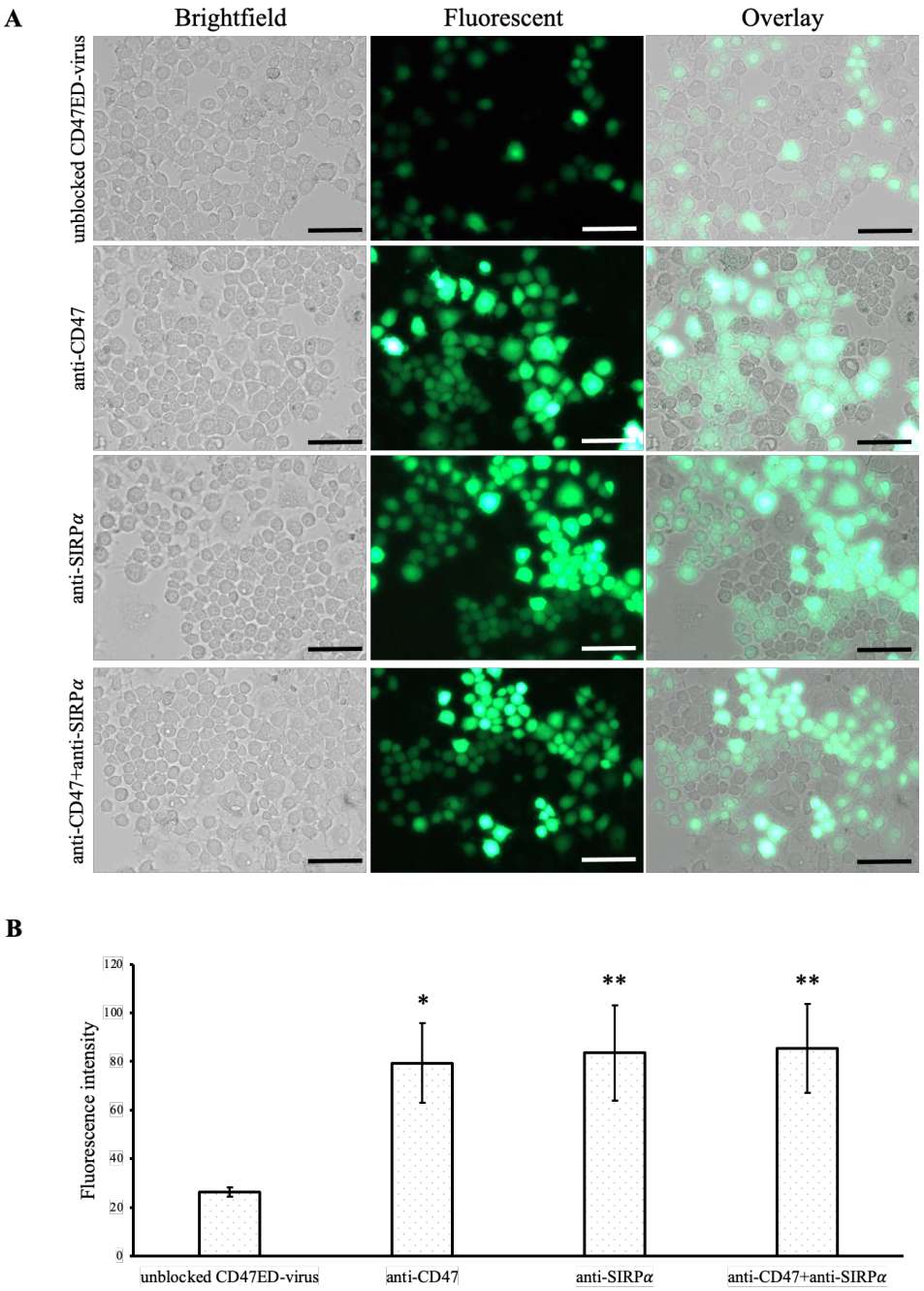

Figure 2.8. Inhibition of macrophage phagocytosis via CD47ED-SIRPα axis. (A) showing brightfield, fluorescence, and overlay images of J774A.1 macrophages infected with mouse CD47ED-modified lentivirus with unblocked, blocking CD47ED protein, blocking SIRPα receptor, and blocking CD47ED protein and SIRPα receptor together; (B) presenting the fluorescence intensity of J774A.1 macrophages incubated with and without antibodies blocking either CD47ED, SIRPα, or both, then treated with CD47ED-tethered lentivirus. The fluorescence intensity per cell was calculated using ImageJ, and statical analysis was performed using one-way ANOVA with Tukey post hoc multiple comparisons test. Scale bar denotes 100 µm and data were presented as mean ± standard deviation (n = 5). *P<0.05 and **P<0.01 comparing to the unblocked CD47ED-modified virus.

Effect of CD47ED on proinflammatory cytokine secretion

The secretion of proinflammatory cytokines (IL-6 and TNFα) from macrophages in response to the treatment of CD47ED-modified lentivirus, biotinylated lentivirus, or untreated control was evaluated using ELISA. The amount of cytokine's secretion from untreated J774A.1 macrophages was 414 ± 30 pg/mL for TNFα and 19 ± 4 pg/mL for IL-6. Figure 2.9A showed the amount of IL-6 secreted from macrophages treated with CD47ED-modified lentivirus (33 ± 4 pg/mL) was 40% less than macrophages were treated with biotinylated lentivirus (55 ± 6 pg/mL). Similarly, J774A.1 macrophages treated with biotinylated lentivirus secreted about 1,359 ± 143 pg/mL for TNFα. However, the level of TNFα secretion from macrophages treated with CD47ED-coated lentivirus was dropped to 874 ± 78 pg/mL, which is about 35% less than the one treated with biotinylated lentivirus (Figure 2.9B).

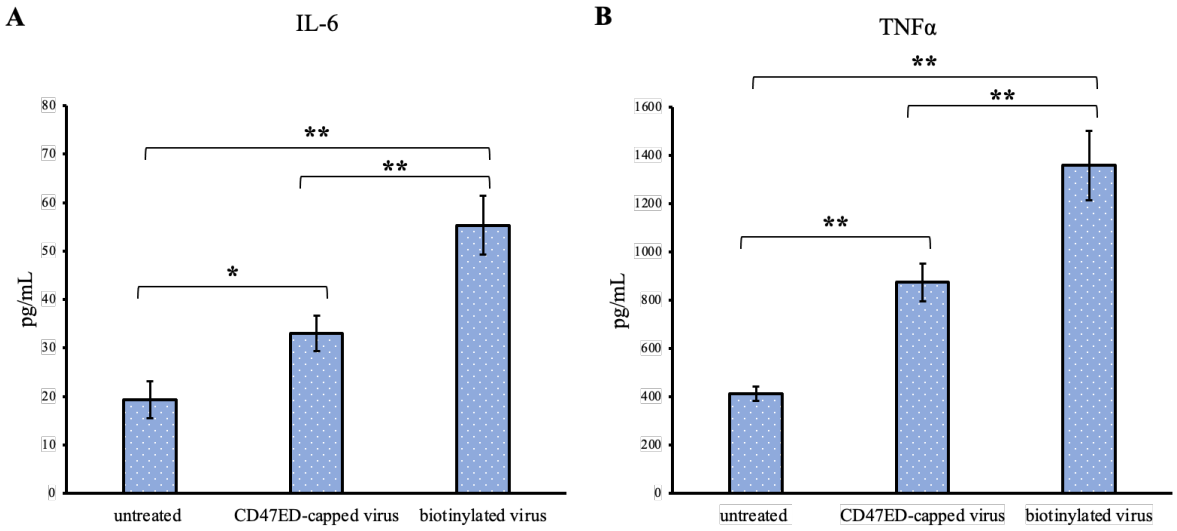

Figure 2.9. IL-6 and TNF-α secreted by J774A.1 macrophages. Proinflammatory cytokines secretion of TNF-α (A) and IL-6 (B) from macrophages challenged with untreated, CD47ED-capped lentivirus, and biotinylated lentivirus for 18 hours. Statistical analysis was performed using one-way ANOVA followed with Tukey post-tests comparing all conditions. Data were presented as mean ± standard deviation; * and ** denoting $P<0.05$ and $P<0.01$, respectively.

Discussion

The soluble and immobilized CD47 ectodomain have been previously reported in our studies and found there was inhibition of the phagocytosis activity due to the CD47-SIRPα interaction, resulting in fewer particles taken up by macrophages[109,110]. However, the

structure of virus and the components that make up the viral genome are much more complicated comparing to nonviral particles. Virus immunogenicity has become a huge challenge for gene therapy[41]. The immune system within a body is able to recognize foreign bodies including vectors carrying transgenes and will generate antibodies to fight them, therefore, transgenes will be cleared by the mononuclear phagocyte system before arriving at their target and expressing the genes of interest[40]. The present study investigated the efficacy of surface immobilization of CD47ED on lentiviral nanoparticles for overcoming macrophage-mediated phagocytosis. CD47-mediated stealth functionalization is an important biomimetic strategy used for the treatment of cancer and coating of implant surfaces[111,112]. While its importance in therapeutic drug delivery has been discussed, its utility in preparing viral nanoparticles for gene delivery is less explored. In this study, we used an *in vitro* set up with J774A.1 macrophages and infected them with biotinylated lentiviral vectors immobilized with the CD47ED-coreSA chimeric protein and found a reduced uptake of particles in comparison to the mock group. It has been reported previously, the presence of CD47 on lentiviral vectors, inhibits phagocytosis of the virus[102,103]. However, while some studies had the full length of CD47 expressed through the viral membrane[102,103], we have demonstrated that the viral particles can escape phagocytosis through surface immobilization of CD47ED. This also indicates that the ectodomain of CD47 is functionally capable and immobilization has not resulted in structural vis-à-vis functional changes in the chimeric protein. To further confirm that the inhibition of phagocytosis is mediated through the CD47-SIRPα pathway[113,114], we simultaneously blocked the CD47ED protein on the lentivirus, the SIRPα protein on the macrophage membrane, and both to assess the impact on phagocytosis. Expectedly, inhibition of either or both protein moieties resulted in more virus engulfment by macrophages. Hence, the lentiviral vectors capped with CD47ED-coreSA showed less entry to macrophages due to the presence of VSV-G in virus particles which enhance the cellular interaction with the ubiquitous receptor[115]. Furthermore, macrophages are known to secrete proinflammatory cytokines in response to pathogens including viruses[116–118]. When J774A.1 macrophages were treated with biotinylated lentivirus, the amounts of secreted TNFα and IL-6 were increased; while macrophages that were not exposed to inflammatory stimuli showed low levels of TNF-α and IL-6. In this study, cytokines secretion from J774A.1 macrophages treated with CD47ED-capped lentivirus was significantly less than uncoated lentivirus,

indicating phagocytic resistance attributed to CD47ED/SIRPα interaction which could downregulate proinflammatory cytokine secretion.

We have genetically engineered a chimera that combines the ectodomain of mouse CD47 with the affinity domain of core-streptavidin. It has been previously reported that full-length streptavidin (SA) forms an aggregate of higher-order and thus displays poor solubility. Contrastingly, core-streptavidin is found to be more soluble than full-length SA[119]. Further, the combination of L-rhamnose and IPTG to induce protein overexpression along with native conditions, permitted threefold overexpression of the soluble CD47ED-coreSA chimeric protein. The method permitted overcoming the formation of insoluble proteins in inclusion bodies, which needs a higher recovery time and reduces protein yield[110,120]. The use of the ectodomain is justified by the functional significance of the domain in regulating several immune responses through multiple cellular processes[121,122]**.** Ultracentrifugation is a commonly used method for the collection of viral particles. However, it is a time-consuming process and the envelope proteins are not robust under high shear stress[123]. For the separation of biotinylated viruses, conventionally used techniques involve the use of avidin-based affinity columns[106] or avidin-coated paramagnetic particles[124]. These methods necessitate the recovery of viral particles from the column thereby increasing the time of viral recovery. Here, we constructed biotinylated lentiviral vectors, concentrated and purified them using a simple flocculation method described previously by Landazuri et al[106]. It is a simple, cost-effective, and efficient method including flocculation and disaggregation.

While existing chemical biotinylation technologies have been reported to increase viral transduction of target cells[125–128], they are limited by the fact that the chemical biotin labeling methods involve random covalent attachment to virion amino acids and require prior purification of the labeled substrate. Moreover, one must play a balancing act of adding sufficient numbers of biotin for the expected functionality, while avoiding over-alkylation with biotin derivatives that may lead to inactivation of the biotinylated virus[129,130]. In this study, an alternative approach – producing biotinylated viruses directly from living cells pre-fed with biotinylated lipid[131]. Due to membrane fluidity, biotin-lipids are distributed in various viral budding sites. Subsequently, viruses are spontaneously labeled with biotin during viral natural assembly and budding processes. Since the whole viral biotinylation

performed spontaneously in the viral replication cycle, operations such as incubation with conjugate chemicals (e.g., Sulfo-NHS-LC-Biotin) and additional purification before and/or after conjugation can be avoided. Thus, biotinylated viral bioactivity can be kept to the greatest extent compared with traditional chemical biotinylation of viruses. It should be noted that for free biotin, one coreSA binds four biotins. However, since one coreSA probably can only bind up to two biotins immobilized on the viral surface, the number of CD47ED molecules tagged on a virus via biotin-SA affinity should be no more than half of the number of biotin molecules per virion. Based on the biotin molecules calculated from the HABA/Avidin assay (i.e., 7.65×10^{10} molecules) and lentivirus diameter of ~100 nm, the surface density of CD47ED tethered on the virion is estimated to be 1.22×10^{12} molecules/μm^2. This value probably is overestimated due to the inaccuracy of HABA/Avidin assay[132]. Nonetheless, the surface density of CD47ED capped on the viral surface is way above the minimum level of CD47 density on red blood cells (~1,000 molecules/μm^2)[133] and cancer cells (~600 molecules/μm^2)[108]. Hence, the amount of CD47ED coated on viruses should be more over the threshold value to engage with SIRPα receptors on J774A.1 macrophages and lead to reduced phagocytosis. Our dot blotting assay confirmed the active binding of the chimeric protein on the biotinylated lentiviral surface. Moreover, their infectivity was not reduced as demonstrated by similar infectivity of both biotinylated and native lentivirus to HEK 293T cells. Independently, the ability of the lentiviral vectors tagged with CD47ED protein was also assessed and no significant difference was observed in the ability of the CD47ED-tagged virus to infect the cells. It is believed that the immobilization via biotin-streptavidin affinity has not introduced any surface changes on the virus thus enabling their uptake by the HEK 293T cells. This also indicates that despite the presence of the chimeric protein, the virus can infect the cells, thus mediating gene transfer, which is the preliminary function of lentivirus-based vectors.

Chapter 3: Viral Vectors Tethered with Immunoregulatory CD200 Protein Enhance Anti-inflammatory and Antiphagocytic Capability

Abstract

CD200, known as an immunoglobulin superfamily glycoprotein, is expressed on a wide range of cell types and mediates anti-inflammatory responses by interaction through its cognate receptor CD200R, which is expressed on the surface of myeloid and lymphoid cells. The aim of this study was to investigate the potential of CD200 anchored on lentiviral vectors for anti-inflammation and antiphagocytosis. Mouse CD200 ectodomain and core-streptavidin fusion gene (CD200ED-coreSA) was constructed into pET-30a(+) plasmid and transformed into Lemo21(DE3) competent *E. coli*. The expressed CD200ED-coreSA fusion protein was purified by cobalt-nitrilotriacetate affinity column and characterized by SDS-PAGE and Western blot. The purified fusion protein was immobilized on the outer surface of biotinylated lentiviruses. J774A.1 mouse macrophage cells were infected with the modified lentiviral particles. Our results showed that macrophages treated with the CD200ED-modified lentiviral particles led to a significant reduction in the induction of proinflammatory cytokines (i.e., TNFα and IL-6). Moreover, lentiviral particles tethered with CD200ED-coreSA fusion protein were phagocytosed significantly lesser than the non-modified lentiviral particles.

Introduction

It has been reported that virus-mediated innate immune responses, such as production of inflammatory cytokines, complement proteins, and neutralizing antibodies compromise the systemic antitumor efficacy of viruses[134–139]. Studies of viral therapeutics have also revealed that liver uptake is a major roadblock to systemic delivery, where most of viruses were immediately removed from the blood circulation by resident macrophages of the reticuloendothelial system (RES) following intravenous administration[84,85]. One strategy to overcome the host immune response is to hide the virus from immune scrutiny. For instance, associating the virus with mesenchymal stem cells would allow the immunologically inert carrier cells to chaperone the therapeutic virus to the tumor sites[86,140]. An alternative immune evasive approach is to chemically modify viral coat proteins by conjugation of biocompatible hydrophilic polymers (e.g., polyethylene glycol) to mask viral surface epitopes and therefore provide viruses the ability to evade immunosurveillance. Oldenborg et al. reported another potentially interesting system for disguising foreign particles as self, namely the use of a immunoglobulin superfamily (IgSF) glycoprotein CD47[2]. This marker protects red cells from elimination by binding to a cognate receptor, signal regulatory protein α (SIRPα) on macrophage membranes[96,97]. Recently, CD47-SIRPα antiphagocytic axis has been harnessed to construct immune-evading CD47-shielded lentiviral vectors[102,103].

CD200, known as an anti-inflammatory transmembrane glycoprotein in the IgSF, is expressed in a myriad of cells such as myeloid cells (macrophages, dendritic cells), lymphoid cells (T, B cells), neurons, cardiomyocytes, keratinocytes, and endothelial cells[141–143]. Its extracellular domain containing two regions - Ig-variable (IgV) and Ig-constant (IgC)[141,144]. CD200R known as CD200 cognate receptor is expressed on the surface myeloid cells such as macrophages, neutrophils, and microglia[145,146]. Hoek et al. found that CD200-CD200R interaction elicits an inhibitory signal that downregulates macrophage activity[145]. In cancer stem cell (CSC) immunology, the expression of CD200 on CSCs allows the CSCs to evade or suppress the immune system[147]. Several other studies also supported the inhibitory role of CD200-CD200R signal in the activation of macrophages and dendritic cells[148–150]. Activation of immune cells following recognition of non-self molecules such as pathogens is regulated by CD200 signaling[151]. Due to this role, CD200-CD200R signaling has been recognized as a target for therapeutic treatment of disease[152]. The CD200-CD200R inhibitory signaling

pathway also is involved in limiting inflammation in a variety of inflammatory diseases by inhibits the expression of pro-inflammatory cytokines (e.g., IL-1β, IL-6 and TNF-α)[153].

Most functional findings of CD200-CD200R interaction have focused on dampening pro-inflammatory cytokine secretion of myeloid cells. The involvement of CD200-CD200R interaction with decreased myeloid cell phagocytosis has been reported recently. For example, *in vivo* CD200-Fc administration facilitated white matter recovery by suppressing phagocytosis of susceptible oligodendrocyte precursors[154]. The absence of CD200-CD200R interaction led to increased engulfment of FITC-labelled amyloid-β or fluorescently labelled 1-μm latex beads in microglial cells isolated from $CD200^{-/-}$ mice. Very Recently, it was reported that both nano- and micro-sized particles decorated with the ectodomain of CD200 (containing both IgV and IgC region) decreased phagocytosis activities of THP-1 macrophages. Such diminution of phagocytosis was examined to be associated with downregulation of Toll-like receptor 4 (TLR4) expression on the surface of macrophages. These results can be explained through the interaction of CD200R with its ligand CD200, which leads to phosphorylation of tyrosine residues of the intracellular domain of CD200R by kinases of the Src family. This phosphorylation in turn results in the recruitment of adaptor protein Dok2, which initiates the cascade of inhibitory signaling. Recruitment of Dok2 results in inhibition of both mitogen associated protein kinase (MAPK) and Janus kinase/signal transducer activator of transcription (JAK/STAT) signaling pathways[152,155]. Moreover, enhancement or suppression of phagocytosis is related to adaptor protein Dok2, which plays an important role in the regulation of TLR4 by CD200 protein[156,157]. Moreover, the secretion of pro-inflammatory cytokine tumor necrosis factor-α (TNF-α) from THP-1 macrophages treated with CD200-coated particles was diminished[158]. In fact, CD200 homologs have also been encoded by herpesviruses[159] and poxviruses[160] to undermine host immune defenses. Therefore, CD200-CD200R interaction may represent a viable approach for the design of immune-evading viruses. In this study, we intend to functionalize lentiviruses with CD200-IgV ectodomain to avoid viruses ingested by phagocytes, as well as decrease the secretion of pro-inflammatory cytokines. Our results showed that the virus masqueraded under CD200-IgV could limit its exposure to the immune system and prolong its persistence in the blood, hence allowing for therapeutic targeting.

Methods

Construction of mCD200ED-coreSA encoding plasmid

Core streptavidin (coreSA) was amplified by polymerase chain reaction (PCR) from pSTE2-215 (yol)[105] using forward 5'-AGATCCGAATTCGGTGCTGCTGAAGCAGGT-3' and reverse primers 5'-ATTATACTCGAGGGAGGCGGCGGACGGCTT-3'. A commercially available clone of mouse CD200 (mCD200) in pCMV-SPORT6 was procured from Harvard Medical School (Boston, MA). The IgV ectodomain of mouse CD200 (CD200ED) was PCR amplified using forward primer 5'-AGATCCGAATTCGGTGCTGCTGAAGCAGGT-3' and reverse primer 5'-ATTATACTCGAGGGAGGCGGCGGACGGCTT-3'. A 50 µL PCR was set up for each DNA by mixing the following components: 1X Phusion HF buffer, 200 mM dNTPs, 0.5 µM forward primer, 0.5 µM reverse primer, 1 µg DNA, 1.0 unit of Phusion DNA polymerase, and reaction volume was made up with nuclease-free water (New England Biolab, MA). The PCR cycling conditions for both genes included an initial denaturation temperature of 98°C for 30 s, followed by 30 cycles of denaturation at 98°C for 10 s, annealing at 60°C for 15 s, and extension at 72°C for 15 s. The final extension was set for 5 min at 72°C. The PCR products were purified using a Monarch PCR DNA cleanup kit (New England Biolab, MA) and analyzed on a 1% agarose gel by electrophoresis. The purified coreSA was digested and cloned into the plasmid pET-30a(+) between two restriction enzyme sites, XhoI and EcoRI, to produce the plasmid pME005. Similarly, CD200ED was inserted into the plasmid pME005, between the restriction sites BamHI and EcoRV to produce the pME007 plasmid.

Expression and purification of the CD200ED-coreSA fusion protein

The pME007 plasmid encoding CD200ED-coreSA fusion gene was expressed, extracted and purified following our previous method study[104]. In short, the pME007 was transformed into T7 Lemo21(DE3) competent *E. coli* cells, which were grown on an agar plate supplemented with 50 µg/mL kanamycin and incubated overnight at 37°C. A single colony was picked up and grown in 5 mL of lysogeny broth (LB) media supplemented with 50 µg/mL kanamycin and shaken overnight at 230 rpm at 37°C. Next day, 1 ml of the suspension was added to a large flask containing 1 liter of LB medium supplemented with 500 µM of L-rhamnose and 50 µg/mL of kanamycin and incubated at 37°C with shaking at

225 rpm. When the optical density (OD_{600nm}) of the culture reached 0.6 – 0.8, culture was induced with 400 μM IPTG and kept shaking overnight at 18°C to induce expression. Thereafter, the cells were harvested by centrifugation at 4500g for 20 min. The cell pellet was resuspended in B-PER bacterial protein extraction reagent (5 mL of reagent per gram of cell pellet) supplemented with 50 mM Tris-HCl and 1× EDTA-free protease inhibitor (pH 7.5). According to the manufacturer's instructions, the resuspended cell pellet was incubated at room temperature (RT) for 20 min. The cells were further maintained in the ice bath and dispersed by sonication for 30 min with power output set at 5 (Misonix, NY, USA). The lysates were centrifuged at 18,000 xg for 20 min and supernatant (soluble crude protein) was collected for purification process.

The purification of CD200ED-coreSA fusion protein was performed by immobilized metal affinity chromatography (IMAC) using HisPur™ Co-NTA resin. According to the manufacturer's protocols, the resin was equilibrated with two bed-volumes of equilibrium buffer (10 mM imidazole in 1x PBS, pH 7.4). Then, the crude protein sample was mixed with an equal volume of equilibration buffer (1:1 ratio) before loading onto the equilibrated cobalt resin. The binding was enhanced by gentle shaking of the resin under cold conditions for 2 hours. The flow-through of unbound proteins was collected, and the resin was washed with two resin-bed volumes of equilibration buffer for a minimum of five washes or until the 280 nm absorbance reached the baseline value. The target protein (CD200ED-coreSA) was collected by five resin-bed volume of elution buffer (250 mM imidazole in 1x PBS, pH 7.4) or until the absorbance at 280 nm returned to baseline. The purified protein fractions were concentrated with protein concentrator PES (MWCO = 10 kDa). The concentration of CD200ED-coreSA recombinant protein was characterized by BCA assay. The soluble crude protein and purified fusion protein were analyzed by Sodium dodecyl sulfate-polyacrylamide gel electrophoresis (SDS-PAGE) and western blotting. The pME005 plasmid encoding coreSA only was similarly expressed and purified as stated above and used as an experimental control.

SDS-PAGE and Western blot

SDS-PAGE was performed using 12% polyacrylamide Mini-PROTEAN Tetra handcast systems gels to analyze the soluble crude protein and the purified CD200ED-coreSA recombinant protein. Samples were mixed with equal volumes of 2x Laemmli sample buffer containing 5% (v/v) of 2-mercaptoethanol before heating at 95°C for 5 min. Electrophoresis was performed with tris-glycine electrode buffer (1X), pH 8.3 at 200V for 40 min. The gel was stained with Coomassie brilliant blue R250 staining solution containing 40% (v/v) methanol and 10% (v/v) acetic acid for a minimum of 3 hours. The gel was fast destained with solution containing 40% (v/v) methanol and 10% (v/v) acetic acid for 1 hour at RT, and then the gel was incubated in a slow-destaining solution containing 10% (v/v) methanol and 10% (v/v) acetic acid for overnight.

For western blot, three electrophoresed samples from SDS-PAGE were transferred onto a PVDF membrane (0.45 µm) by Trans-Blot® semi-dry system (Bio-Rad) conducted at 20 V for 1 hour. Three blots were blocked with blocking buffer (5% bovine serum albumin (BSA) in tris buffered saline-Tween 20 (TBST)) for 1 hour at RT. The blots were washed with TBST buffer thrice and then incubated separately with anti-mouse CD200 monoclonal antibody, anti-streptavidin monoclonal antibody, and anti-histag monoclonal antibody under gentle shaking at 4°C overnight. Next, the blots were washed three times with TBST and separately incubated with a 1: 1000 dilution of HRP labeled mouse IgG (secondary antibody) at RT for 2 hours. After 3 times washing with TBST, the blots were developed using ECL substrate and imaged using a chemiluminescence imager (PXi Syngene, Frederick, MD).

Attachment of CD200ED-coreSA protein on the surface of biotinylated lentivirus

CD200ED-coreSA was immobilized on the surface of biotinylated viral vector through core streptavidin and biotin binding. In short, 500 µL of biotinylated virus was mixed with 1 mL of CD200ED-coreSA protein in a microcentrifuge tube, and the mixture was gently rotated for 1 hour at 4°C. Unbound CD200ED-coreSA protein was removed by centrifugation and washing twice, and the pellet was resuspended in PBS. Successful attachment of CD200ED-coreSA protein on the surface of biotinylated lentivirus was

confirmed using dot blot assay. In short, 5 μL of resuspended sample was added to a PVDF membrane, which was subsequently blocked with blocking buffer for 1 hour at RT. Thereafter, the membrane was probed with a 1:500 dilution of anti-mouse CD200 primary antibody (Santa Cruz, CA) in 1x TBST for 1 hour at RT. After washing three times with TBST for 5 min, the membrane was incubated at RT for one hour in a 1:1000 dilution of anti-mouse IgG HRP conjugate. After three washes with 1x TBST, the HPR activity was used to demonstrate the presence of CD200ED on the PVDF membrane. The assay was controlled by the addition of biotinylated virus and CD200ED-coreSA soluble protein as negative and positive controls, respectively.

Effect of CD200ED-coreSA on proinflammatory cytokine secretion by macrophages

The induction of pro-inflammatory cytokines, IL-6 and TNFα by J774A.1 cells treated with biotinylated lentiviral particles was measured. Cultured J774A.1 cells (5×10^4) were incubated with lentivirus, lentivirus tagged with CD200ED-coreSA and untreated macrophages for a period of 18 hours. The culture supernatant was collected to measure the cytokine levels using commercial enzyme-linked immunosorbent assays (ELISA). Briefly, 96-well microtiter plates were coated with anti-IL6 and anti-TNFα antibody and incubated overnight at 4°C. The plates were washed thrice to remove unbound antibodies using a wash buffer consisting of PBS with 0.05% tween-20. The plates were blocked using the ELISPOT diluent for 1 hour at RT. The wells were again washed thrice and incubated with controls i.e., standard IL-6, TNFα, and test samples (culture supernatant) for 2 hours at RT. The wells were washed thrice and re-incubated with anti-IL-6 or anti-TNFα detection antibodies respectively at recommended dilutions for 1 hour at RT. The detection antibodies were discarded, and wells were washed thrice and treated with streptavidin HRP at RT for 30 min. Substrate, tetramethyl benzidine (TMB) was added to the wells and the plate was incubated in dark at RT for 15 min. The reaction was stopped using 1 M phosphoric acid. The resultant absorbance at 450 nm was measured using a microplate reader (SpectraMax M2e). The concentrations of IL-6 and TNF-α in the culture media were interpolated using the standard curves.

Phagocytosis of biotinylated lentivirus tagged with CD200ED-coreSA

To evaluate the effect of CD200ED on macrophage activation, J774A.1 macrophages were separately infected with the biotinylated lentivirus tethered with and without CD200ED-coreSA protein for 3 hours, prior to replacing the culture media. The J774A.1 macrophage cells expressing *GFP* were evaluated at 72 hours post treatment by fluorescent microscopy and flow cytometry to determine the lentivirus rate of infection and the efficiency of phagocytosis. HEK 293T cells, applied as non-phagocytic cell line control, were treated and analyzed the same way as macrophages. More control experiments were performed using coreSA protein mixed with biotinylated virus and nonbiotinylated lentivirus mixed with CD200ED-coreSA to evaluate their phagocytic effect on J774A.1 macrophages in comparison to biotinylated virus coated with CD200ED-coreSA.

CD200/CD200R inhibition assay

To confirm the downregulation of macrophages is due to the interaction of CD200/CD200R axis, J774A.1 macrophages were treated with CD200ED-modified virus in the presence or absence of anti-CD200R or anti-mouse CD200. First, macrophages were cultured into 6-wells tissue culture plate. Three J774A.1 macrophages groups were separately treated with: CD200-decorated virus blocked with anti-mouse CD200 antibody, macrophages were pre-incubated with anti-CD200R antibody to block the CD200 receptor located on their surface, followed with CD200ED-modified virus treatment, and CD200-decorated viral vectors and macrophages were incubated with anti-mouse CD200 and anti-CD200R, respectively. Unblocked CD200-modified lentivirus treated J774A.1 macrophages was performed as control.

Statistical analysis

All data are presented as the mean ± standard deviation from at least three independent experiments and analyzed using one-way analysis of variance (ANOVA), followed by Tukey multiple comparisons post hoc tests in between experimental groups. *P* value less than 0.05 is considered statistically significant.

Results

Construction of plasmid encoding the recombinant CD200ED-coreSA fusion gene

The gene sequences for the CD200 ectodomain (291 bp) and the coreSA (384 bp) were cloned by PCR and confirmed by DNA gel electrophoresis. Figure 3.1 shows the PCR products for the CD200ED at ~ 0.3 kb and coreSA at ~0.4 kb. The plasmid construct pME007 produced the coreSA gene sequence (~14.2 kDa) cloned in between XhoI and EcoRI, and CD200ED (~10.77 kDa) cloned into BamHI and EcoRV and about 6 pb (~0.22 kDa) located in between the EcoRI and BamHI (Figure 3.1A). This produced the CD200ED-coreSA recombinant protein with an approximate molecular weight of ~25 kDa.

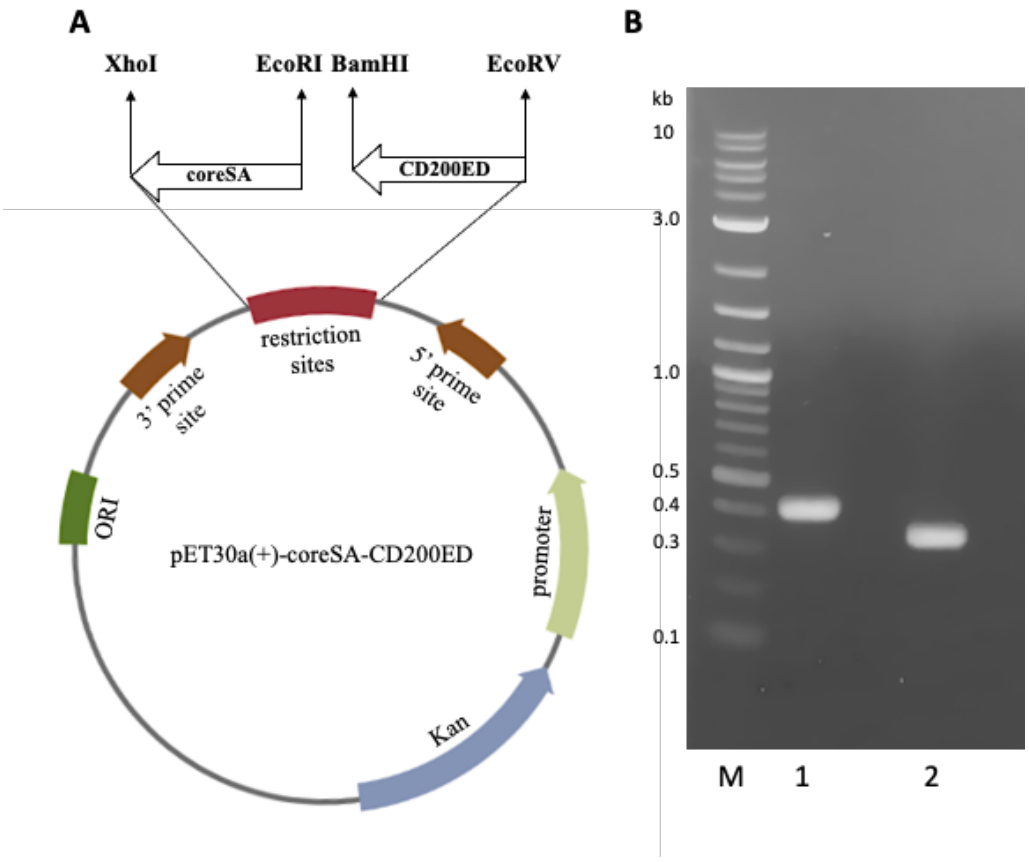

Figure 3.1. DNA gel electrophoresis of cloned fusion gene product (A) The circular map showing multiple cloning sites for CD200ED-coreSA fusion gene. CoreSA was inserted between XhoI and EcoRI; the ectodomain of mouse CD200 was inserted between BamHI and EcoRV. (b) DNA gel electrophoresis with DNA ladder (M), coreSA (~0.4 kb) (lane 2) and ectodomain of CD200 (~0.3 kb) (lane 3).

Characterization of CD200ED-coreSA recombinant protein

The plasmid vector encoding CD200ED-coreSA fusion gene (pME007) was successfully transformed into Lemo21(DE3) competent *E. coli* and screened by kanamycin agar plate. The elution fractions, monitored by measuring the absorbance at OD_{280} to obtain the elution profile curve, indicate most of the target recombinant protein was eluted in fraction 9 (Figure 3.2A). The crude lysate protein and purified CD200ED-coreSA were checked by 12% SDS-PAGE followed by Coomassie staining, showed an overexpressed protein band at 25 kDa in crude lysate (Figure 3.2B). The size of purified protein was identical to the estimated molecular weight of CD200ED-coreSA recombinant protein, 25 kDa. The elution fractions were concentrated using a protein concentrator (MWCO = 10 kDa) and the concentration was measured by BCA to be 461 ± 22 μg/mL. The purified CD200ED-coreSA protein was further characterized by Western blotting analysis, which was detected by anti-histag, anti-streptavidin, and anti-mouse CD200 antibodies. The three blots showed a single protein band at target protein size ~25 kDa (Figure 3.2C).

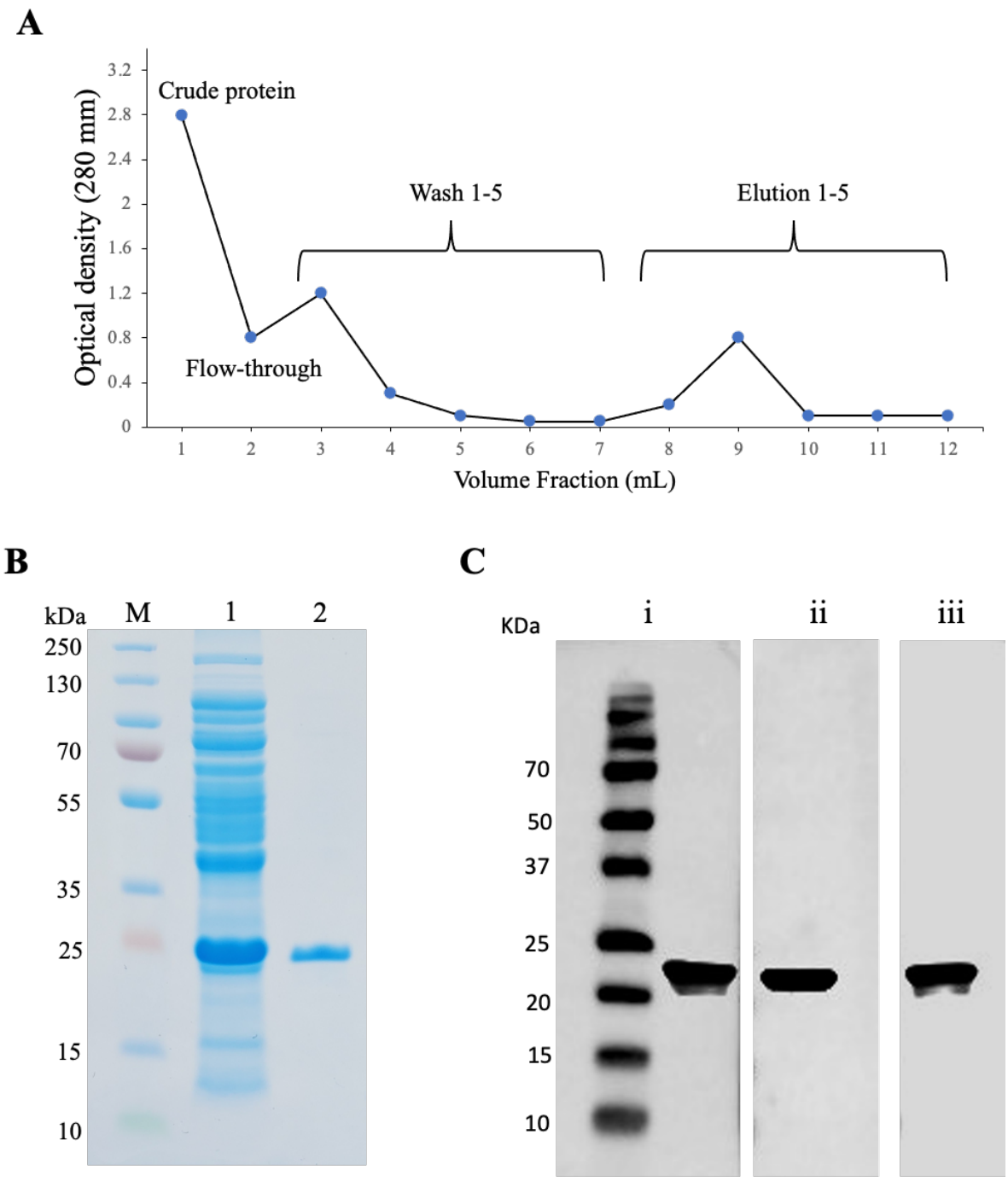

Figure 3.2. characterization of mouse CD200ED-coreSA fusion protein. (A) The elution profile of CD200ED-coreSA protein; (B) SDS PAGE analysis with protein ladder (M), crude lysate protein of *E. coli* (lane 2), and CD200ED-coreSA purified recombinant protein (lane 3); (C) Western blot developed using anti-mouse CD200 (i), anti-streptavidin (ii), and anti-histag (iii) as primary antibodies.

Characterization of biotinylated lentivirus tethered with CD200ED-coreSA recombinant protein

Dot blot analysis demonstrated the immobilization of CD200ED-coreSA on the biotinylated virus surface using anti-mouse CD200 antibody (Figure 3.3). Results therefore revealed successful antibody binding to soluble protein (positive control) and virus tethered with CD200ED-coreSA, whereas no antibody binding was detected for biotinylated virus (negative control), which confirms the attachment of CD200ED-coreSA on the surface of biotinylated viral vectors was successful.

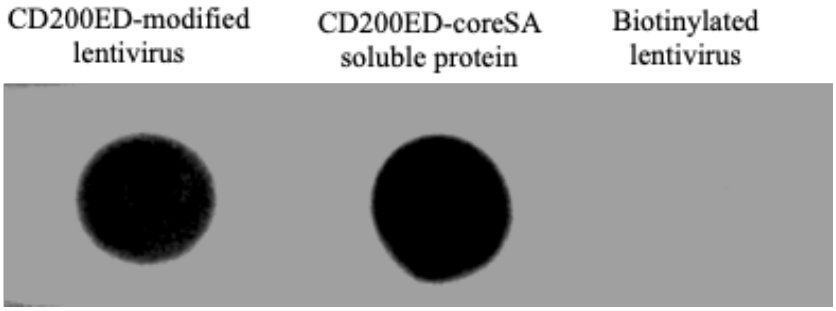

Figure 3.3. Dot blot characterization of CD200ED-modified virus. dot blot assay showing biotinylated lentiviral particles can bind CD200ED-coreSA via biotin-streptavidin. CD200ED-modified virus, CD200ED-coreSA soluble protein (positive control), and unmodified biotinylated lentivirus (negative control) were blotted on the membrane and evaluated against anti-mouse CD200 monoclonal antibody. The outcomes confirmed the presence of CD200ED protein on the modified lentivirus and CD200ED-coreSA soluble protein, while unmodified biotinylated lentivirus (negative control) detected no CD200ED signal.

The effect of CD200ED-coreSA on cytokines secretion from J774A.1 macrophage

Cytokine secretion from macrophages were assessed for two pro-inflammatory cytokines, IL-6 and TNF-α, using ELISA. The amount of TNF-α and IL-6 secreted from J774A.1 macrophages treated with uncoated biotinylated lentivirus was 1312 ± 169 pg mL^{-1} and 52 ± 8 pg mL^{-1}, respectively. However, untreated macrophages control secreted less TNF-α (67%) and IL-6 (65%) comparing to the macrophages infected with unmodified biotinylated lentivirus. The cytokines secretion was also reduced by 47.1% for TNF-α (701 ± 96 pg/mL) and ~55% for IL-6 (23 ± 3 pg/mL) for macrophages treated with CD200ED-coated lentivirus (Figure 3.4). This reduction secreted from macrophages treated with

CD200ED-coated virus indicates suppression of macrophage activation and antiphagocytic resistance (Figure 3.4 A-B).

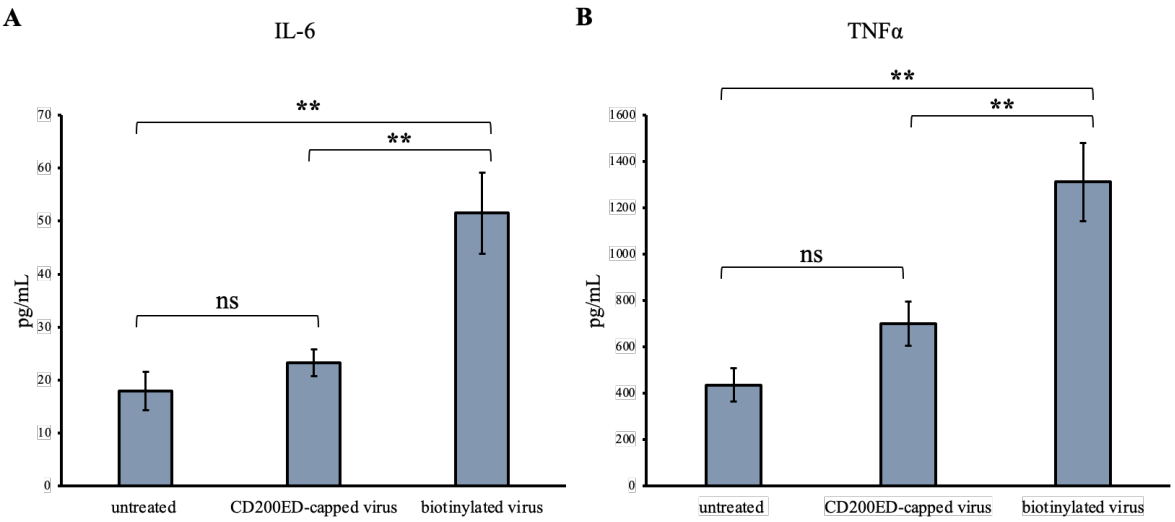

Figure 3.4. IL-6 and TNF-α secreted by J774A.1 macrophages. Proinflammatory cytokines secretion of IL-6 (A) and TNF-α (B) from macrophages challenged with untreated, CD200ED-capped lentivirus, and biotinylated lentivirus for 18 hours. Statistical analysis was performed using one-way ANOVA followed with Tukey post-tests comparing all conditions. Data were presented as mean ± standard deviation; ns denotes not significant and ** denotes $P<0.01$.

Antiphagocytic efficacy of CD200ED-coreSA tagged on biotinylated lentiviral surface

Qualitative results from experiments gauging the effect of biotinylated lentivirus tagged with CD200 ectodomain on macrophage activation, gauged by *GFP* expression to determine viral infectivity, demonstrated that the *GFP* expression was lower in J774A.1 macrophage cells compare to HEK 293T cells (Figure 3.5A and 3.6A). This finding was further emphasized by density plot analyzing the *GFP* expression, which demonstrated the difference of *GFP* expression in macrophages for untreated negative control (0.57%), treated with unmodified biotinylated virus (61.1%) and treated with the CD200ED-modified lentivirus group (46%) (Figure 3.5B-D). Based on this finding, CD200ED immobilized on virus surface decreased ~27% of engulfment by macrophages as comparing to unmodified biotinylated virus. These finding results were further confirmed using the flow cytometer histogram, which showed MFI = $1.37\times10^6 \pm 6{,}032$ for unmodified biotinylated virus, and MFI = $9.6\times10^5 \pm 4{,}102$ for CD200ED-modified virus.

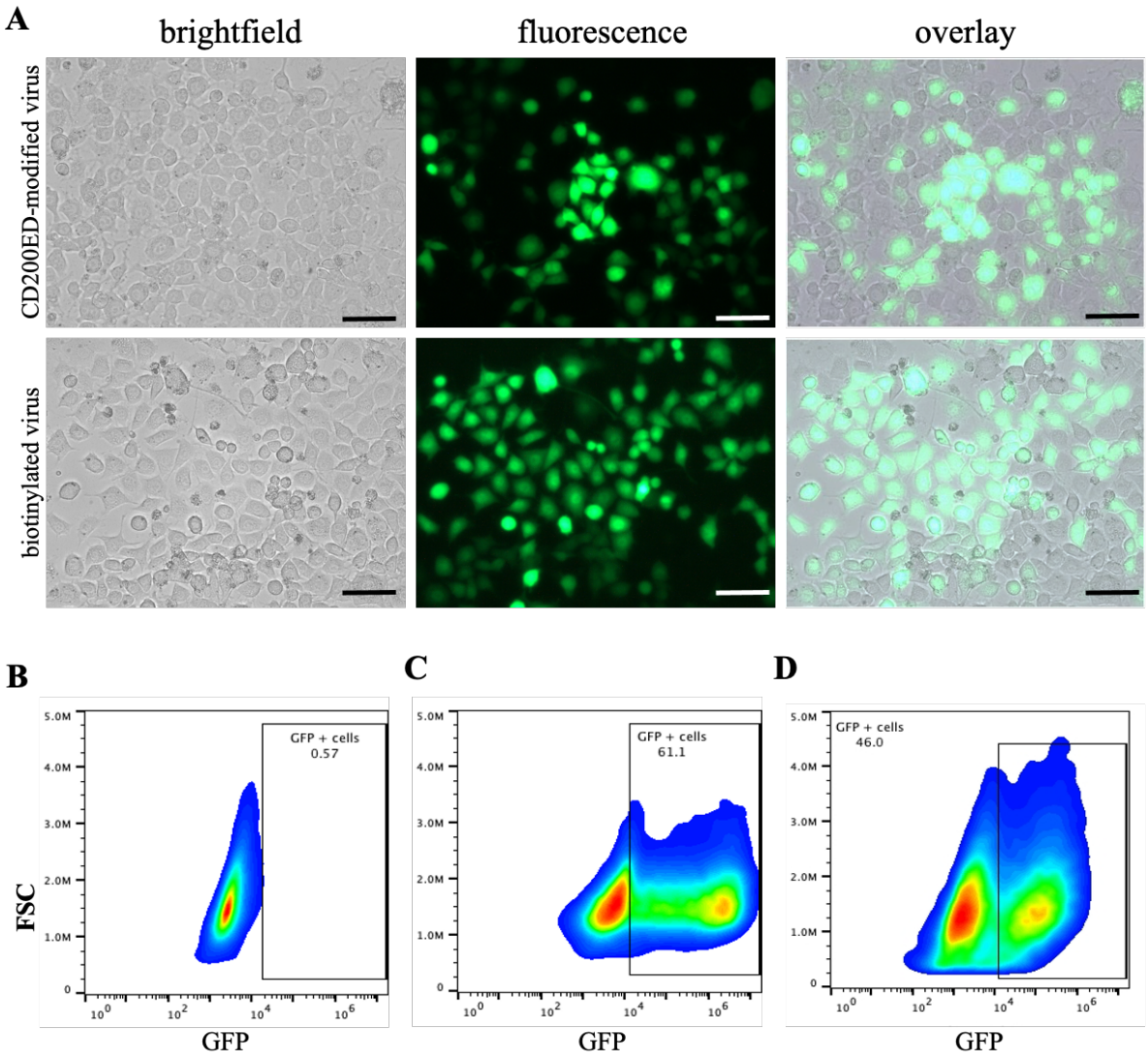

Figure 3.5. Reduced macrophage phagocytosis of lentivirus tethered with CD200ED. (A) showing brightfield, fluorescence, and overlay images of J774A.1 macrophage cells ingested CD200ED-biotinylated lentivirus and biotinylated lentivirus, respectively; (B-D) density plot of macrophages expressing *GFP* using flow cytometer – (B) untreated J774A.1 macrophages (negative control), (C) J774A.1 macrophages treated with unmodified biotinylated lentivirus (positive control), (D) J774A.1 macrophages treated with CD200ED-modified biotinylated lentivirus.

In contrast, HEK 293T cells infected with CD200ED-coreSA modified virus fail to respond to CD200 signaling and, therefore, had greater virus particles uptake, and exhibited similar level of *GFP* expression from biotinylated virus (Figure 3.6C-D). The MFI obtained by the flow cytometer histogram further confirmed this finding, which showed MFI = $1.94\times10^6 \pm 10{,}918$ for unmodified biotinylated virus, and MFI = $1.91\times10^6 \pm 12{,}106$ for

CD200ED-modified virus. However, the phagocytic reduction of CD200ED-modified virus clearance is due to the interaction of CD200ED with the CD200R located on J774A.1 macrophages surface, which downregulates macrophage activation and prevents viral entry.

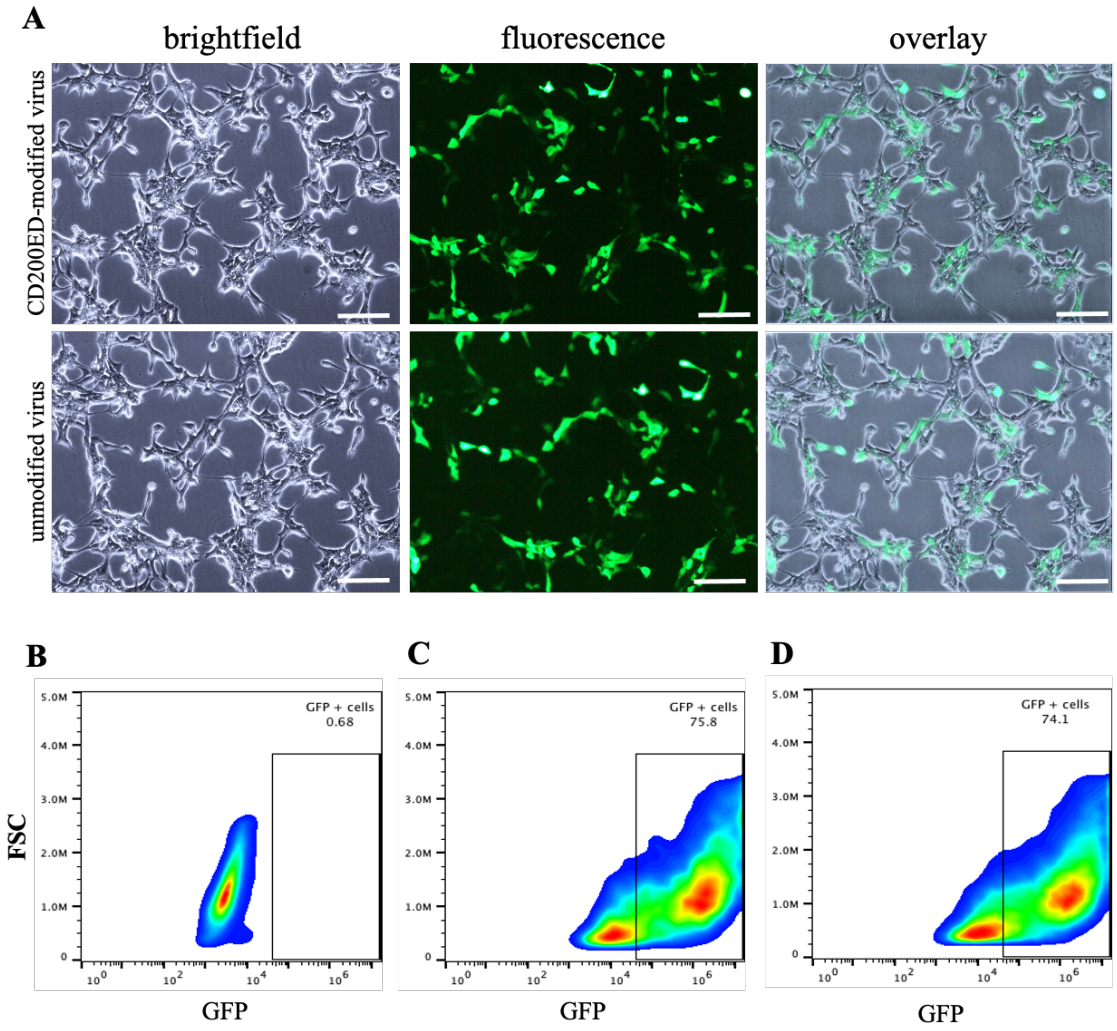

Figure 3.6. Non-phagocytic cells treated with CD200ED-capped virus. (A) HEK 293T cells treated with CD200ED-modified and unmodified biotinylated lentivirus, respectively, for a period of 72 hours culture; (B-D) density plot of HEK 293T cells expressing *GFP* using flow cytometer – (B) untreated HEK 293T cells (negative control), (C) HEK 293T cells treated with unmodified biotinylated lentivirus (positive control), and (D) HEK 293T cells treated with CD200ED-modified biotinylated lentivirus. Scale bar denotes 100 µm.

J774A.1 macrophages were separately infected with coreSA-modified virus and non-biotinylated lentiviral vectors mixed with CD200ED-coreSA protein to further evaluate the

of interaction of CD200ED-CD200R axis. It was found that these two groups could not mediate phagocytosis due to the lack of CD200ED protein or inability of CD200ED-coreSA protein to immobilize on non-biotinylated virus surface (Figure 3.7A). In addition, the fluorescence intensity of J774A.1 macrophages expressing *GFP* showed these two groups were 1-fold higher than the CD200ED-modified virus group (Figure 3.7B). Judging from these findings, CD200 ectodomain played an important role in the downregulation of macrophages and inhibition of phagocytosis.

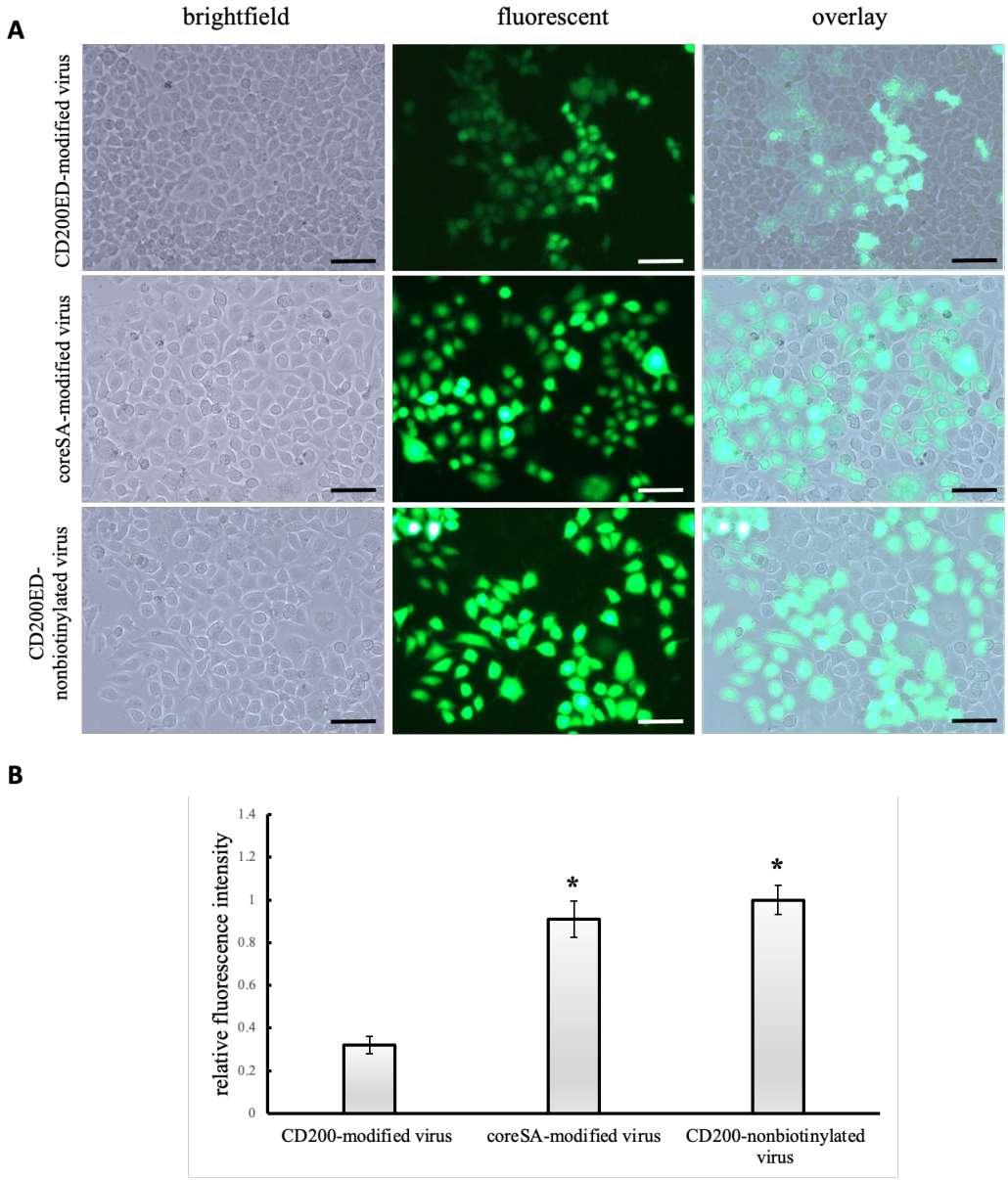

Figure 3.7. CD200 ectodomain is essential for inhibition of phagocytosis. (A) shows brightfield, fluorescence, and overlay images of lentivirus tagged with CD200ED-coreSA protein, coreSA-

modified lentivirus, and non-biotinylated lentivirus mixed with CD200ED-coreSA protein, respectively. Images were taken with 20x magnification, and the scale bar denotes 100 μm. B) image representing fluorescence intensity per cell measured using ImageJ for CD200ED-coreSA-modified lentivirus, coreSA-modified lentivirus, and non-biotinylated lentivirus mixed with CD200ED-coreSA protein. Statistical analysis was performed using one-way ANOVA followed by Tukey post hoc multiple comparisons test and data were presented as mean ± standard deviation (n = 5); * denotes $P<0.05$.

Inhibition of phagocytosis by blocking of CD200-CD200R interaction

Figure 3.8A shows the qualitative result of blocked CD200ED protein immobilized on lentivirus membrane (i), blocked CD200 receptor located on the macrophage surface (ii) or blocked of both CD200ED, and its receptor (CD200R) (iii) exhibit high level of *GFP* expression in comparison with unblocked CD200ED-modified virus (control) (iv). These findings demonstrate that the increase of lentivirus engulfment by macrophages and failure to resist phagocytosis and anti-inflammation is because of the disrupting of CD200-CD200R axis binding. This finding was further confirmed by measuring the amount of *GFP* intensity per cell, which demonstrated about ~1-fold increase of virus uptake by macrophages in all three groups due to the blocking of CD200 and/or CD200R comparing to unblocked CD200-modified lentivirus group (Figure 3.8B).

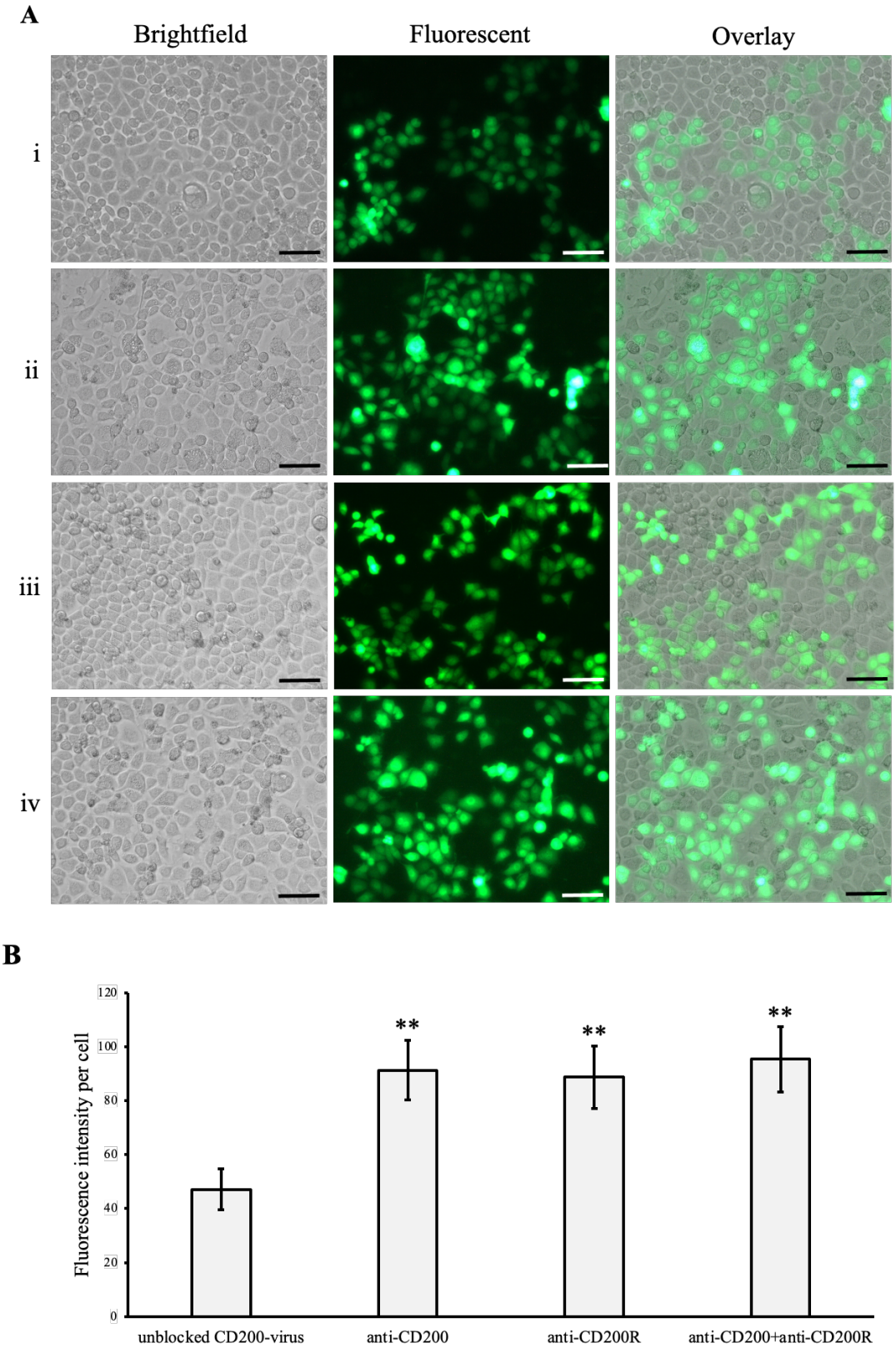

Figure 3.8. CD200 is essential for phagocytosis inhibition. (A) shows brightfield, fluorescence, and overlay images of (i) lentivirus tagged with CD200ED-coreSA protein (unblocked), (ii) lentiviral

particles treated with anti-CD200 antibody, (iii) macrophages treated with anti-CD200R antibody, and (iv) macrophages treated with anti-CD200R antibody and infected with lentiviral particles treated with anti-CD200 antibody. Images were taken with 20x magnification, and the scale bar denotes 100 μm. B) image representing fluorescence intensity per cell measured using ImageJ. Statistical analysis was performed using one-way ANOVA followed by Tukey post hoc multiple comparisons test and data were presented as mean ± standard deviation (n = 5); ** denotes $P<0.01$ comparing to unblocked CD200-virus group.

Discussion

The use of viral vectors for gene delivery has been of increased research attention due to their highly efficiency. However, the immunogenicity of virus-derived vectors composed of various biochemical components (e.g., capsid proteins, nucleocapsids, and membrane/envelope proteins) limit their usage in the field of gene therapy[41]. As unrecognized cargos that carry transgenes, they will be cleared by antibodies generated by the immune system before reaching to the target of abnormal genes[40]. This study investigated the macrophage response to lentivirus biomimicry functionalized with the IgV domain of anti-inflammatory transmembrane protein, CD200, to downregulate immunoregulatory and decrease the clearance of virus by macrophages. The CD200 immunomodulatory protein is known to interact with its inhibitory receptor, CD200R which is expressed on macrophages and other myeloid cells and reduce macrophage activation and chronic inflammation. It has previously been shown that CD200R is expressed only on myeloid cells and T cells and interaction of CD200 with CD200R results in immune suppression[161]. Hoek et al. reported that CD200-deficient mice had increased macrophage activation because of the lack of interaction between CD200 and CD200R[145]. Similarly, another study also showed microglial cells obtained form CD200-deficient mice enhanced phagocytosis[162]. In contrast, peritoneal macrophage treated with soluble CD200-Fc fusion protein suppressed phagocytosis of the oligodendrocyte precursor cells[154]. All these studies concluded that the CD200 protein plays an important role in downregulation of macrophages and phagocytosis inhibition through binding to CD200R expressed on macrophage surface. The present study adds to these findings, and furthermore found that the extracellualr domain of CD200 protein is cabable of suppressing macrophage activation by treating murin J744A.1 macrophages with biotinylated lentivirus tagged with CD200 IgV domain. Our results also align with those of Zhang *et al.,* where it was found that micro/nanoparticles decorated with the extracellualr domain of

CD200 were engulfed less by macrophages comparing to the uncoated micro/nanoparticles[158]. Moreover, the secretion of pro-inflammatory cytokine tumor necrosis factor-α (TNF-α) from THP-1 macrophages was diminished after interacting with CD200-coated particles.

Most functional findings of CD200-CD200R interaction have focused on dampening pro-inflammatory cytokine secretion of myeloid cells. Very Recently, it was reported that both nano- and micro-sized particles decorated with the ectodomain of CD200 (containing both IgV and IgC region) decreased phagocytosis activities of THP-1 macrophages. Such diminution of phagocytosis was examined to be associated with downregulation of Toll-like receptor 4 (TLR4) expression on the surface of macrophages. This can be explained through the interaction of CD200R with its ligand CD200, which leads to phosphorylation of tyrosine residues of the intracellular domain of CD200R by kinases of the Src family. This phosphorylation in turn results in the recruitment of adaptor protein Dok2, which initiates the cascade of inhibitory signaling. Recruitment of Dok2 results in inhibition of both mitogen associated protein kinase (MAPK) and Janus kinase/signal transducer activator of transcription (JAK/STAT) signaling pathways[152,155]. Moreover, enhancement or suppression of phagocytosis is related to adaptor protein Dok2, which plays an important role in the regulation of TLR4 by CD200 protein[156,157].

While most viruses encoding CD200 homolog contain the two Ig-like domains (IgV and IgC), some viruses like poxvirus express M141R protein which contains only the IgV domain[163]. The M141R protein is responsible for macrophage and T-cell downregulation through binding to CD200R[160,164,165]. In addition, Barclay et al. showed Kaposi's sarcoma-associated herpesvirus (KSHV) expresses the K14 protein (CD200 homolog) encoding about 44% amino acid similarity to the N-terminal Ig-domain of the human CD200 protein[166]. This same study also demonstrated that K14 can interact with human CD200 receptors on myeloid cells with almost the same kinetics and affinity to human CD200, and that binding of K14 to the CD200R is capable of downregulating macrophage activation, as well as of other immune cells[166]. In this study, the IgV domain of CD200 was used as biomimicry and attached on the surface of a lentivirus to evaluate their effect on macrophage activation. This biomimicry approach was performed by expressing the IgV extracellular domain of CD200 out of the

bacterial system, following previous protocols[104]. A key finding of our research was that whilst macrophages cells treated with uncoated biotinylated lentivirus expressed about two-thirds more *GFP* expression than CD200ED-coated lentivirus, HEK 293T cells treated the same way as the macrophages revealed the same amount of *GFP* expression. This indicated that the CD200R expressed on the surface of the macrophages is essential for regulating the phagocytosis and activation of the macrophages upon CD200 protein binding. These results are consistent with previous findings that CD200 can diminish the phagocytosis by macrophages and escape immunosurveillance[159,166–168]. In addition, our research also found that in two more controls group, coreSA protein only and CD200ED-coreSA, interacted with the nonbiotinylated virus, which further tested the phagocytic resistance of macrophages cells compared to the CD200-decorated lentivirus. We found that controls have higher expression of *GFP* comparing to the virus tagged with the CD200 protein, which indicated none of the controls succeeded in preventing phagocytosis and escaping the clearance of macrophages. This can be therefore explained by how they were either missing the CD200 protein or due to unsuccessful attachment of the CD200 protein on the virus surface. Additionally, the result of anti-phagocytosis mediated by CD200-CD200R interaction was confirmed by blocking CD200 protein immobilized on virus membrane, and CD200R on macrophages surface. Presumably, inhibition of either or both protein moieties resulted in more virus engulfment by macrophages. We also capitalized on how it is known that proinflammatory cytokines are secreted from macrophages in response to pathogens including viruses[116–118]. Here, confirming our other findings, macrophages that were treated with lentivirus-decorated with CD200 extracellular domain protein suppressed the pro-inflammatory cytokine TNF-α and IL-6 compared to biotinylated lentivirus, which showed significantly higher levels of these proinflammatory cytokines.

Chapter 4: Lentivirus Tethered with Ectodomains of CD200 and CD47 Proteins Inhibits Phagocytic Activity by Macrophage

Abstract

CD200 and CD47 are members of immunoglobulin superfamily proteins that have been identified to downregulate the macrophage activation and suppress phagocytic activity, through the binding to CD200R and SIRPα receptors, respectively. This is of interest for gene therapy, because whilst viruses have become a promising approach in the field of gene delivery, virus recognition by the immune system remains a barrier. We therefore investigated employing the anti-inflammatory and anti-phagocytic function of both CD200 and CD47 proteins within virion carriers to result in these carriers being tolerated by the immune system. To approach this, biotinylated viral vectors were added to homogeneous proteins of CD200ED-coreSA and CD47ED-coreSA (1:1 and 3:1 ratios). After biomimicry of the virus surface with the two proteins through biotin-streptavidin binding, J774A.1 macrophages were treated with the modified virus to evaluate phagocytosis resistance. Our results showed that the outcome of immobilizing both proteins of CD200ED and CD47ED on the virus surface suppresses the phagocytic activity. However, this suppression was not significantly different compared with using the CD47ED protein alone. In conclusion, harnessing the CD200ED and CD47ED proteins on lentivirus surfaces downregulates macrophage activation, but to no greater extent than using the CD47ED protein alone.

Introduction

The uptake of cell debris and foreign particles is an efficient process performed by the mononuclear system[169]. Macrophages are generally efficient species, rapidly engulfing foreign micro- and nanoparticles, and whilst important in preventing disease, they therefore present a challenge to medical treatments based on the use of drug carriers[170–172]. To help minimize macrophage clearance of therapeutic particles, various molecules are incorporated on the particles' surfaces. The most commonly applied modification is hydrophilic polyethylene glycol (PEG) chains; incorporating them on the surface of particle effectively put the particle into 'stealth mode', making it less readily detected by macrophages and thereby extending the duration that it circulates in the bloodstream[173,174]. However, while PEG modification does increase the longevity of the particle, it is also associated with reduction of immunological responses as well as delivery efficiency. Moreover, it is not biodegradable, which drawbacks limit the scope of PEGylation[175–177].

An alternative approach is to use CD47 ectodomain protein to modulate the surface of lentiviral vectors. CD47 proteins are 'markers of self' that interact with signal regulatory protein-alpha (SIRPα) on the surface of macrophages. As CD47-abundant erythrocytes are recognized as being 'self', they are not phagocytic targets, and thus avoid macrophage clearance[2]. The effect of the interaction between CD47 and SIRPα is that it enables CD47-decorated viruses to endure in the blood, facilitating delivery of CD47-decorated viruses to tumors[78,178]. Moghimi *et al.* proposed that this function could be manipulated in such a way so as to provide a design option for drug carriers that are capable of evading the immune system, specifically to evade macrophage clearance[179]. Another study reported by Hsu *et al.* showed the antiphagocytic effect on macrophages by expressing the extracellular domain of CD47 fused with streptavidin (CD47-SA) in bacteria and purifying the soluble fusion protein via biotin-avidin affinity purification[109]. The study reported that J774A.1 macrophages cells treated for one hour with the purified soluble CD47-SA protein, followed with treatment of prepared perfluorocarbon-based oxygen carriers for 2 hours post-treatment, and thereafter showed less phagocytosis of particles[109]. The efficacy of CD47-SA to assist in diminishing phagocytosis has also been demonstrated to last for 5 hours by immobilizing 3-μm biotinylated zymosan particles with CD47-SA protein[180].

Much like CD47, the anti-inflammatory transmembrane glycoprotein CD200 is a widely expressed self-protein member of the immunoglobulin superfamily. Various cells express CD200 protein, including cardiomyocytes, endothelial cells, keratinocytes, lymphoid cells (T, B cells), myeloid cells (macrophages, dendritic cells) and neurons[141–143]. Macrophages, microglia and neutrophils express cell surface receptor CD200R that exclusively recognizes CD200[145,146]. Downregulation of macrophage activity is mediated by the interaction between CD200 and CD200R[145]. This capacity is exploited in cancer stem cell (CSC) immunology; CSCs resist immune system responses by expressing CD200 (which inhibits macrophage activity)[147]. This CD200-CD200R inhibitory effect on dendritic cells has been observed in a number of studies[148–150,181]. Most of the research into the interactions between CD200 and CD200R however has centered on reducing the secretion of pro-inflammatory cytokines in myeloid cells; its contribution to minimizing phagocytosis is a more recent area of study.

This study considers assessing the effect of CD200ED-coreSA and CD47ED-coreSA on phagocytic function of macrophages. The two fusion proteins were obtained as thoroughly indicated in Chapter 2 and 3. Binding of the purified CD200ED-coreSA protein and CD47ED-coreSA protein to biotinylated lentiviral vectors were achieved due to the high affinity of core streptavidin to biotin. CD200ED:CD47ED-coated and uncoated virus particles were exposed to macrophage J774A.1 and the interactions were assessed. Our results indicate that CD200ED:CD47ED-coated lentivirus exhibited greater resistance to macrophage activity than uncoated virus particles, however, not significantly greater than the effect of CD47ED-coreSA protein alone.

Methods

Attachment of CD200ED and CD47ED proteins to viral vectors

Purified recombinant proteins of CD200ED-coreSA and CD47ED-coreSA (descried in Chapter 2 and 3) were homogeneously mixed in microcentrifuge tubes with 1:1 ratio and 3:1 ratio (CD200ED:CD47ED). Next, biotinylated lentiviral particles were separately added to each tube and placed under gentle shaking for 1 hour at 4^{o}C. Unbound proteins were removed by washing the lentivirus particles. Afterward, CD200ED:CD47ED-modified

viruses and unmodified viruses were added to J774A.1 macrophages that were previously cultured in 6-well plates. Culture media were replaced 3 hours later and *GFP* expression was evaluated by microplate reader at 72 hours post-infection. HEK 293T cells were used as nonphagocytic cell line control and treated with 1:1 ratio of modified and unmodified virus.

Statistical analysis

The data in this Chapter is presented as the mean ± standard deviation from three independent experiments and analyzed using student *t*-test. *P* value less than 0.05 is considered statistically significant.

Results and discussion

In this study, we inhibited phagocytic clearance of lentiviruses by using two recombinant self proteins. As described previously, the ubiquitously expressed, mammalian cell-surface protein CD47 interacts exclusively with SIRPα present on the surface of dendritic cells and macrophages[2,182]. The effect of this interaction is to inhibit the phagocytosis function of macrophages. This study used CD47 biomimicry to reduce the immune system clearance of lentiviral carriers, thereby promoting vector efficiency[182]. In contrast, CD200 has been reported to regulate myeloid cells, including macrophages, though binding to the CD200 receptor. The interaction of CD200 ligands with CD200 receptors has been well studied[183]. The marker-of-self protein, CD47, is known to prolong blood circulation and therefore enhance drug or gene delivery[172]. In contrast, the anti-inflammatory protein, CD200, has been recognized to inhibit macrophage activation and regulate the immune response. Our aim was to employ the function of the two proteins, CD47ED and CD200ED, within the drug or gene carriers (here, lentivirus) to increase the time and delivery efficiency in the blood circulation. The two purified proteins, CD200ED-coreSA and CD47ED-coreSA, were homogeneously mixed in a sterilized tube prior to the addition of biotinylated viral vectors. We assume that each biotinylated viral vector would equally capture CD200ED and CD47ED proteins though high affinity to the core streptavidin fused with each protein. Phagocytic J774A.1 macrophages, and nonphagocytic HEK 293T cells, were treated with lentivirus co-immobilized with CD200ED:CD47ED (1:1 ratio). The

biomimetic effect of proteins on virus engulfment by the two cell-lines was analyzed by measuring the *GFP* expression at 72 hours post-infection. The HEK 293T cells expressing *GFP* did not exhibit dissimilarity results for both CD200ED:CD47ED-modified and unmodified biotinylated lentivirus (Figure 4.1A), and the fluorescent intensity obtained by the microplate reader was not statically significant (Figure 4.1B). This indicated the CD200 and CD47 ligands failed to bind to the cognate receptors due to the extremely low expression of CD200R and SIRPα receptors[102,184]. In contrast, the amount of *GFP* expression in J774A.1 macrophages was higher in the group treated with unmodified biotinylated lentivirus comparing to macrophages treated with 1:1 ratio of CD200ED:CD47ED-modified lentivirus (Figure 4.2A). Furthermore, this result was confirmed by measuring the *GFP* intensity using the microplate reader, indicating that the macrophages infected with CD200ED:CD47ED-modified lentivirus was ~3-fold less than the unmodified virus (Figure 4.2B). This result was identical to our finding of CD47-modifed virus (discussed in Chapter 2), and that the immobilization of CD200ED on the lentivirus surface revealed no significant effect in this experiment. Based on these results, we hypothesized that increasing the amount of CD200ED protein relative to the CD47 protein (3:1 ratio) might enhance the CD200 effect on the diminution of macrophage's phagocytosis.

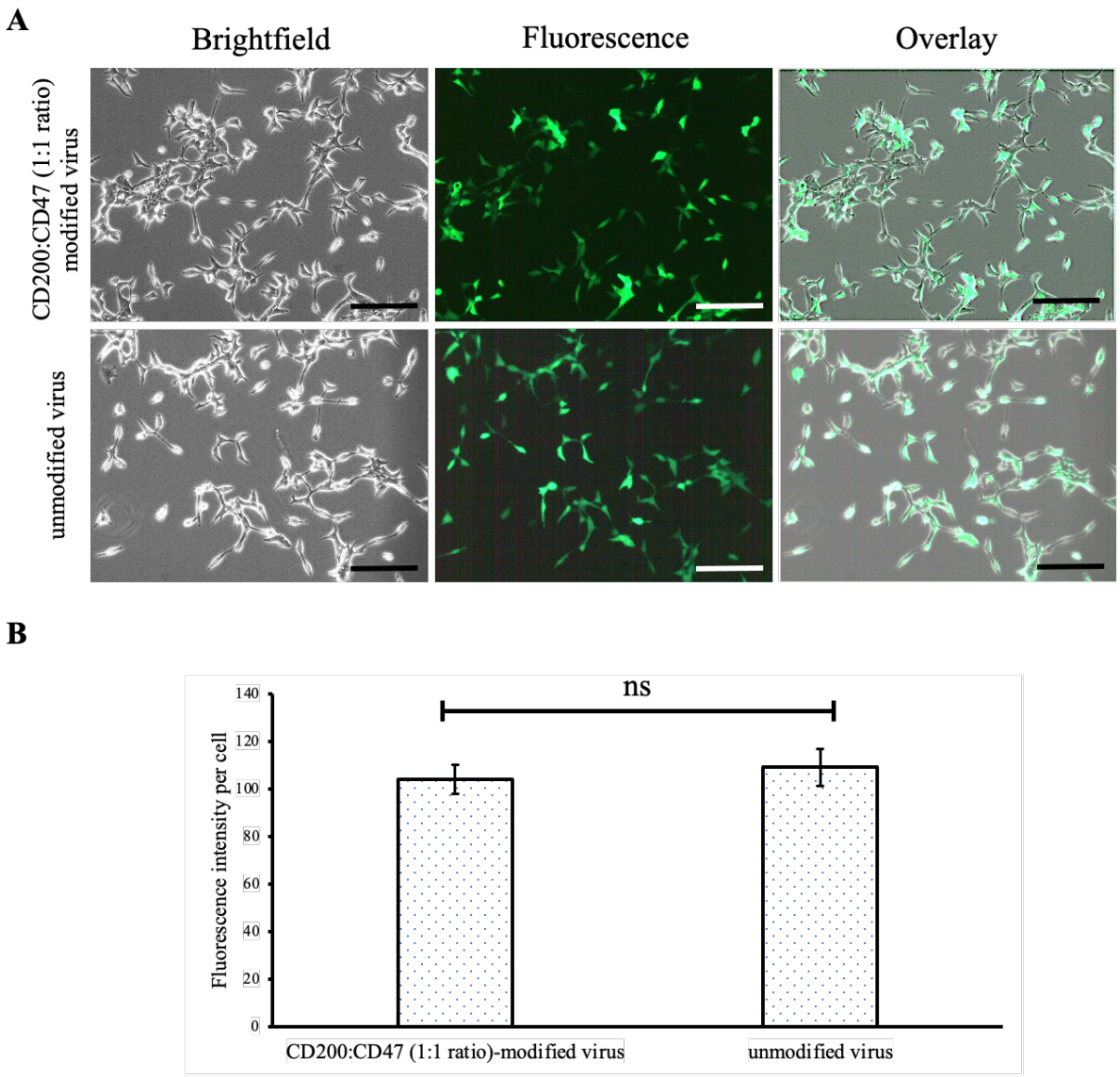

Figure 4.1. HEK 293T cells treated with lentivirus tagged with CD200:CD47 proteins (1:1 ratio). (A) microscopic image of HEK 293T cells treated with 1:1 ratio of CD200:CD47-modified lentivirus and unmodified lentivirus; (B) the fluorescence intensity of *GFP* expression per cell exhibited by modified and unmodified virus. Statistical analysis was performed using student *t*-test and data were presented as mean ± standard deviation (n = 5); which demonstrated insignificant different (ns).

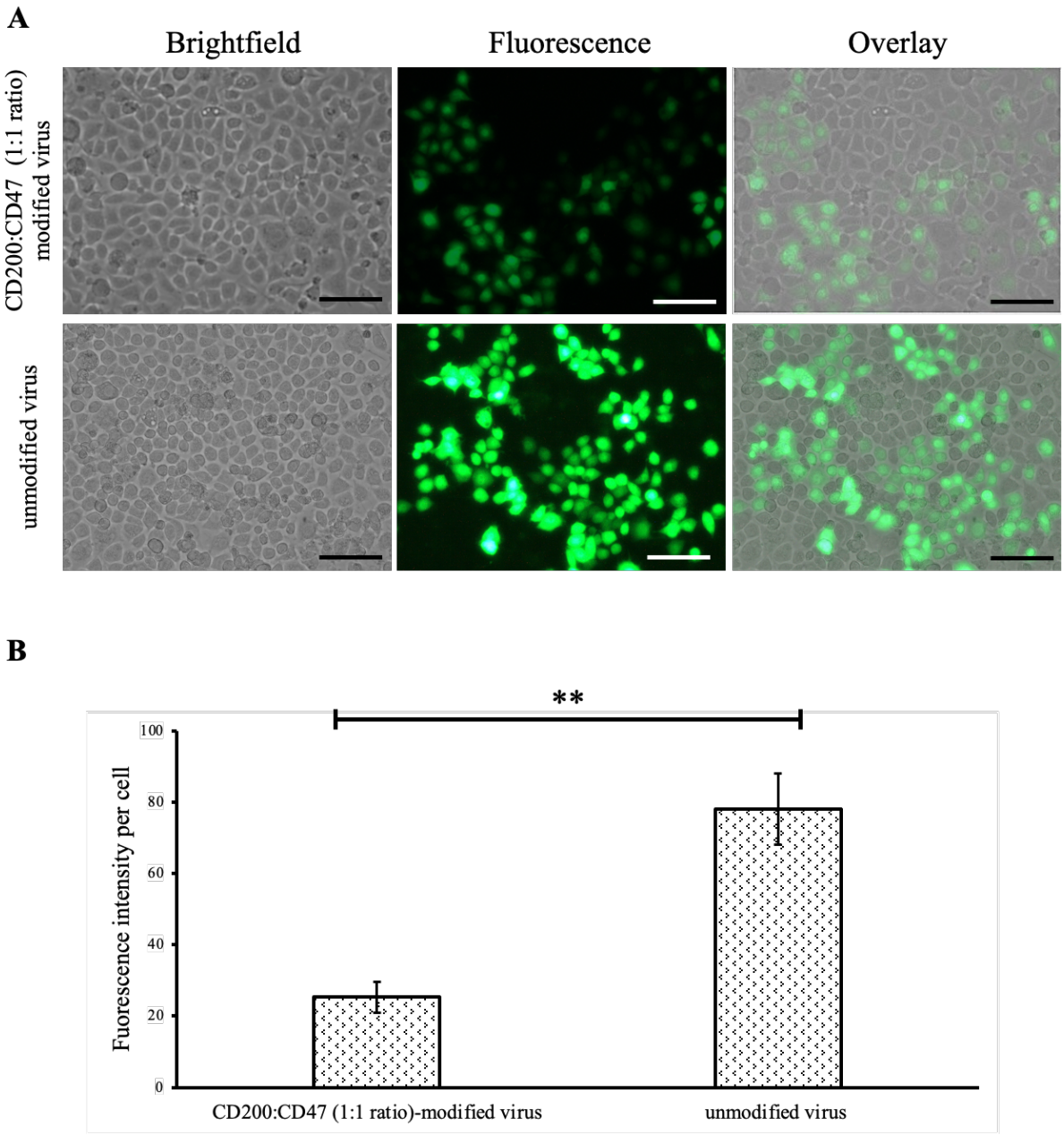

Figure 4.2. J774A.1 macrophages treated with lentivirus tagged with CD200ED:CD47ED proteins (1:1 ratio). (A) microscopic images of J774A.1 cells treated with lentivirus capped with CD200ED:CD47ED proteins (1:1 ratio) and unmodified biotinylated lentivirus; (B) the fluorescence intensity of *GFP* expression per cell for macrophages treated with CD200ED:CD47ED-modified lentivirus and unmodified biotinylated lentivirus. Statistical analysis was performed using student *t*-test and data were presented as mean ± standard deviation (n = 5); ** denotes $P<0.01$.

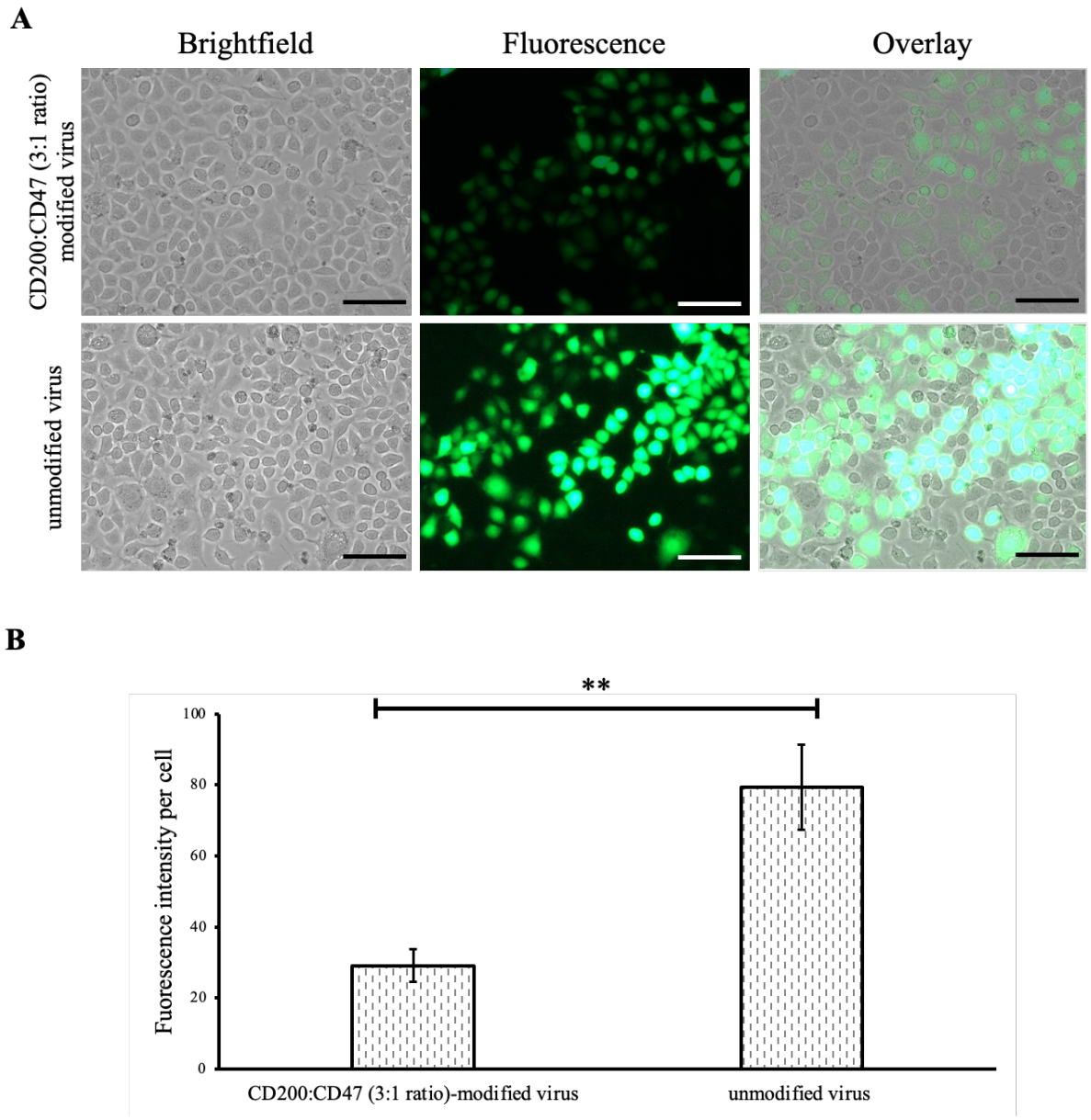

Figure 4.3. J774A.1 macrophages treated with lentivirus tagged with CD200ED:CD47ED proteins (3:1 ratio). (A) microscopic image of J774A.1 cells treated with CD200ED:CD47ED proteins (3:1) ratio and unmodified lentivirus. B) the fluorescence intensity of *GFP* expression per cell showed modified virus group is significantly less than unmodified virus. Statistical analysis was performed using student *t*-test and data were presented as mean ± standard deviation (n = 5); ** denotes $P<0.01$.

J774A.1 macrophages were exposed to the treatment of CD200ED-coreSA and CD47ED-coreSA with a 3:1 ratio tethered on the surface of biotinylated virus, and their effect was assessed by measuring fluorescent intensity of *GFP* expression. J774A.1

macrophages expressing *GFP* at 72 hours post-infection with CD200ED:CD47ED-modified lentivirus (3:1) showed levels of *GFP* were ~3-fold less comparing to unmodified biotinylated lentivirus (Figure 4.3A & B). This finding therefore indicated that increasing the ratio of CD200ED:CD47ED from 1:1 to 3:1 had no discernible effect. A potential explanation for why our hypothesis of increasing the relative ratios of these proteins would enhance the CD200 effect was not supported is due to the affinity binding of CD47 to SIRPα ligand (K_D= 0.22 μM)[185] is higher than the affinity binding between CD200 and CD200R (K_D= 0.4 μM)[186]. Therefore, by the time viral vectors communicate with macrophage, the CD47 ligand recognizes its cognate receptor (i.e., SIRPα) much faster and links to it, which could reduce the chance of CD200 binding to its receptor. Moreover, CD200R expression on a macrophage's surface is not as abundant as SIRPα, which may also limit the interaction of CD200-CD200R. Taken all together, CD200ED and CD47ED proteins tagging the lentiviral vectors on 1:1 or 3:1 ratio did not enhance diminution of phagocytosis above that of the CD47-modified virus. Therefore, we suggest that increasing the amount of CD200 protein on lentivirus surfaces may be more effective by constructing a new vector with fusion genes of CD47ED and CD200ED together. This will double the amount of each protein and might promote reduction of macrophage activity, as well as chronic inflammation.

Chapter 5: Immobilization of CD47 and CD200 Ectodomains on Viral Vectors Enhances Immune Evasion

Abstract

CD47, also known as integrin-associated protein, is expressed on all cells as a marker of self. CD200 is a transmembrane glycoprotein that acts as an immunomodulator. CD47 and CD200 interact with SIRPα and CD200R located on myeloid cells respectively, reducing macrophage activation and consequent inflammation. In this study, lentiviral membrane was capped with fusion protein of CD200 and CD47 ectodomains to downregulate immunoregulation and resist phagocytosis via interacting with CD200R and SIRPα. CD200ED domain, CD47ED domain, and core streptavidin fusion protein (CD200ED-CD47ED-coreSA) was expressed from bacteria transformed with pET-30a(+) vector and transformed into Lemo21(DE3) competent *E. coli* cells. The fusion protein expressing CD200ED-CD47ED-coreSA was purified using his-tag affinity column and characterized by SDS-PAGE and Western blot. The purified protein was immobilized on surface of biotinylated lentivirus through biotin-streptavidin binding. The modified lentivirus was used to infect J774A.1 cells to assess impact on phagocytosis and surrogate markers of inflammation *viz*. cytokines IL-6 and TNF-α. Our results showed the fusion protein was found to bind well to the lentivirus surface. The biotinylated lentivirus particles and the lentivirus immobilized with recombinant fusion protein were found to be infective. We also found that when J774A.1 mouse derived macrophage cells were infected with lentiviruses tethered with CD200ED-CD47ED-coreSA fusion protein, there was five-fold reduction in phagocytosis as compared to the biotinylated lentivirus (control group). Through use of blocking antibodies against CD200, CD47, CD200R, and SIRPα, the antiphagocytic phenotype was rescued. Moreover, J774A.1 macrophages infected with modified biotinylated lentivirus particle resulted in reduced secretion of IL-6 and TNF-α. In conclusion, surface immobilization of fusion protein CD200ED-CD47ED-coreSA on lentivirus particles inhibits their phagocytosis and reduces induction of pro-inflammatory cytokines. The fusion protein (CD200ED-CD47ED) effectively immobilizes on biotinylated lentiviral particles attributing stealthy onto the lentiviral nanoparticles.

Introduction

Viral vectors effectively modify eukaryotic cells due to their inherent ability to transfect host cells to replicate. This ability of viruses makes them suitable for gene therapy applications and thus makes them optimal vectors for gene delivery[187]. One such group of viruses extensively used in research and industry is the lentivirus. Lentiviruses can replicate in dividing and non-dividing cells, and transfect large transgenes with higher efficiency and stable expression[188]. Despite low immunogenicity and reduced side effects, viral vectors often face risks of elimination by the host immune surveillance. Gene delivery methods have adopted stealthy functionalization to mitigate phagocytic clearance for the enhancement of targeted delivery. Two important attributes of stealth functionalization include remaining inconspicuous to the mammalian host and a consequent evasion of host immune response[22]. Several studies have explored the role of varied biomimetic approaches for the same[18]. Coating of vectors with host cell membranes or membrane components have been previously undertaken[77,189–191], including the role of CD200 and CD47 that have gained significant prominence.

CD200, which interacts with CD200 receptor, belongs to the immunoglobulin superfamily and is expressed on a wide range of host cells such as the cells of the lymphoid and myeloid lineage, the cardiomyocytes, neurons, keratinocytes, and the endothelial cells[152]. The applicability of CD200 as a biomimetic molecule conferring stealth functionalization has been assessed for nanoparticles. It was reported that nanoparticles coated with CD200 diminished phagocytosis and dampened pro-inflammatory response[158]. Another study found that CD200-coated poly(lactic-co-glycolic acid) particles diminished production of proinflammatory cytokine TNF-α and increased production of anti-inflammatory cytokine IL-10[192]. In specific disease models, expression of CD200 been associated with immune modulation measured as ability to subvert inflammatory immune responses. For instance, CD200 regulated IL-6 production, modulates expression of myeloid derived suppressor cells (MDSCs)[193,194] in pancreatic tumors. A deficient expression of CD200-CD200R results in an anti-inflammatory response in the brain contributing to chronic immune insufficiency and thus disease progression[195,196]. On the other expression of CD200 reported as a pro-survival mechanism adopted by the Huntington's neurons[197].

Similarly, CD47, also known as integrin-associated protein, is a self-cell marker expressed on myeloid cells, which mediates its action by interacting with SIRPα (*a.k.a.* CD172α)[113]. Independently, these ligand-receptor interaction is known to exhibit antiphagocytic effect thereby deregulating activation of the mononuclear phagocyte system and effective evasion of downstream immune signaling mechanisms. CD47 overexpression has been shown in several cancers, which allow them to escape from immunosurveillance. However, blocking of CD47 resulted in reversion of phagocytosis inhibition and consequent clearance of tumor cells[198,199]. For instance, Sosale *et. al.*[102] demonstrated human CD47 expressing lentiviral vectors (hCD47-lenti) were used for targeting lung carcinomas in an *in-vivo* model. The study found that hCD47-lenti prolonged blood circulation and gene delivery to lung cancer xenografts. The hCD47-lenti transduced ~3 fold lower macrophages in comparison to control lentiviruses. The study also showed the efficacy of hCD47-lenti in suppressing phagocytosis mediated by Kupffer cells, splenic macrophages, and bone derived macrophages. In non-human primates, hCD47-lenti could overcome phagocytosis with high transduction efficacy and reduced toxicity[103].

In this Chapter, we are exploring the combinatorial effect of CD200 and CD47 on immune modulation for lentivirus-mediated drug delivery. Further, studies with CD200 or CD47 are mostly undertaken with synthetic nanoparticles for exploration of targeted drug delivery whereas its application in gene delivery remains under explored. Moreover, the modification of lentiviral surfaces involves genetic recombineering of the viruses, which are expensive, and time consuming. In the current study we proposed the above gap in literature by creating a fusion protein of extracellular domain of CD200 and CD47 containing a core streptavidin domain. This domain helps immobilize the recombinant protein on the biotinylated lentiviral surface. The ability of the fusion protein (CD200ED-CD47ED-coreSA) to evade host cell immune response and consequently dampen proinflammatory cytokine response *in vitro* was also assessed. We were able to generate a stable construct which was easily purified and immobilized on lentivirus surface. Functionally, the particles were able to evade phagocytosis by the macrophages and dampen induction of proinflammatory cytokine markers. We thus conclude that use of CD200ED-CD47ED-coreSA fusion protein when immobilized on lentiviral surfaces allows targeted gene delivery with diminution of phagocytosis and anti-inflammation by macrophages.

Methods

Construction of plasmids encoding CD200ED and CD47ED fusion genes

Two separate plasmids were constructed for this study to evaluate the effect of viral vector capped with CD200ED and CD47ED on immunoregulatory and phagocytic activity of macrophage. The ectodomains of mouse CD200 and CD47 were polymerase chain reaction (PCR) amplified from commercially available clones of full-length genes in pCMV-SPORT6 vectors, which were purchased from the Harvard Medical School (Boston, MA). CoreSA DNA sequence was PCR amplified from pSTE2-215 (yol) plasmid[105]. The first orientation was the pME008 plasmid encoding CD200ED-CD47ED-coreSA, constructed by cloning the sequence of CD200ED as described previously in Chapter 3, and inserting into the previously constructed pME006 plasmid, which encodes CD47ED-coreSA (Section 2.3.1). The pME006 plasmid (vector) and CD200ED gene (insert) were cut with restriction enzymes BamHI and EcoRV and ligated together to get plasmid pME008 (Figure 5.1 A & B). The second orientation was constructing the pME009 plasmid, which separates CD200ED and CD47ED with the coreSA DNA sequence to release a final product of CD200ED-coreSA-CD47ED fusion gene as shown in Figure 5.6 B. To explain, the DNA sequences of CD47ED gene was PCR amplified using forward (5'– GCGGGAATTCCTACTGTTTAGTAACGTCAAC –3') and revers ('5'– TTAACTCGAGTCCTTTCTCCTCCTCGTAAG –3') primers, and cloned into the plasmid vector pET30a(+) in between XhoI and EcoRI. Next, the DNA sequence of coreSA gene was amplified by PCR using sense (5'– ATATTGGATCCGGTGCTGCTGAAGCAGGTA –3') and antisense (TATATAAAGAATTCGGAGGCGGCGGACGGC) primers, and cloned into the plasmid pET-30a(+)-CD47ED vector in between EcoRI and BamHI. Lastly, the sequence of CD200ED gene was amplified using the same forward and reverse primers mentioned in Section 3.3.1 and cloned into the plasmid encoding pET30(+)-CD47ED-coreSA in between the BamHI and EcoRV restriction sites. For all three genes, PCRs were performed with Phusion DNA polymerase in a Bio-Rad Thermal cycler with an initial denaturation of 98°C for 30 s and then 30 cycles of denaturation at 98°C for 10s, annealing at 60°C for 15 s, and extension at 72°C for 15 s. Final extension was performed at 72°C for 5 min. The PCR

products were purified using a Monarch PCR DNA cleanup kit and then analyzed by 1% agarose gel electrophoresis (Figure 5.6 B).

Expression and purification of the CD200ED-CD47ED-core SA fusion protein.

T7 Lemo21(DE3) competent *E. coli* cells were transformed with pME008 plasmid encoding CD200ED-CD47ED-coreSA and selected by growth on agar plates containing 50 μg mL^{-1} of kanamycin. A single colony was picked and grown in a suspension of 5 mL of lysogeny broth (LB) supplemented with 50 μgmL^{-1} kanamycin and shaken overnight at 230 rpm at 37°C. The starter culture (1 mL) was diluted in 1 L of LB medium containing 0.5 mM of L-rhamnose and 50 μg mL^{-1} of kanamycin and incubated at 37°C with shaking at 225 rpm. The optical density (OD) was monitored at a wavelength of 600 nm. When the OD of culture reached 0.6 – 0.8, the temperature of the shaking incubator was reduced to 18°C and subsequently cultures were induced with 0.4 mM Isopropyl β-D-1-thiogalactopyranoside (IPTG). Thereafter, the cells were shaken at 225 rpm overnight and harvested by refrigerated centrifugation at 4500 g for 20 min. Cell pellets were resuspended in proprietary nonionic detergent (B-PER) containing 50 mM Tris-HCl, and 1× EDTA-free Halt protease inhibitor (pH 7.5) in a ratio of 5 mL/g and incubated at RT for 15 min. Cells were placed on ice and disrupted by sonication for 30 min with power set at 5 (Misonix, NY), followed by incubating on ice for 20 more min. Soluble protein was isolated by refrigerated centrifugation at 18,000 xg for 20 min and the crude protein was purified using immobilized metal affinity chromatography (IMAC) packed with HisPur™ cobalt nitrilotriacetic acid (Co-NTA) resin. According to the manufacture company, crude protein was mixed with equal volumes of equilibrium buffer before loading on to the Co-NTA resin. The resin was gently shaken at 4°C for a minimum of 1 hour to enhance the binding of the CD200ED-CD47ED-coreSA fusion protein to the histidine-tagged resin. Unbound proteins were allowed to flow-through, and the resin was washed with washing buffer (10 mM imidazole in 1x PBS, pH 7.4) for five times. The target protein (CD200ED-CD47ED-coreSA) was collected with one resin-bed volumes using elution buffer (250 mM imidazole, 1x PBS, pH 7.4) until the absorbance at 280 nm returned to baseline. The purified protein fractions were concentrated with protein concentrator PES (MWCO = 10 kDa). The concentration of the fusion protein was measured

using BCA assay. Similarly, the pME009 plasmid encoding the CD200ED-coreSA-CD47ED were overexpressed and purified following the aforementioned protocol.

SDS-PAGE and western blot analysis.

The crude protein from the bacterial lysates and the purified CD200ED-CD47ED-coreSA fusion protein were characterized by SDS-PAGE. Samples were mixed with equal volumes of 2x Laemmli sample buffer containing 5% (v/v) of 2-mercaptoethanol. The samples were heated at 95°C for 5 min and run on 12% polyacrylamide Mini-PROTEAN Tetra handcast systems gels, which was performed in 1x of Tris-glycine electrode buffer at 200V for 40 min. The gel was stained with Coomassie brilliant blue R250 staining solution containing 40% (v/v) methanol and 10% (v/v) acetic acid for a minimum of 3 hours. The gel was de-stained with fast-destaining solution containing 40% (v/v) methanol and 10% (v/v) acetic acid for 1 hour at RT, and then gel was incubated overnight in slow-destaining solution containing 10% (v/v) methanol and 10% (v/v) acetic acid. Similarly, the CD200ED-coreSA-CD47ED recombinant protein was characterized by SDS-PAGE following the aforementioned protocol. For Western blot analysis, four samples of the purified fusion protein (CD200ED-CD47ED-coreSA) were separately transferred from the SDS-PAGE to a PVDF membrane using Trans-Blot® semi-dry system (Bio-Rad) set up at 20 V for 1 hour. The membranes were then probed in blocking buffer (5% (w/v) BSA in TBS with 0.1% tween-20 (TBST)) for 1 hour at RT under gentle shaking condition, followed by three washes with TBST buffer for 5 min each. Then, the membranes were separately immersed in primary antibodies solution of anti-mouse CD200 monoclonal antibody, anti-mouse CD47 monoclonal antibody, anti-streptavidin monoclonal antibody and anti-histag monoclonal antibody overnight at 4°C. Following incubation, the membrane was washed thrice at RT for 5 min with TBST, before incubating in a 1: 1000 dilution of anti-mouse IgG-HRP conjugate for 1 hour at RT. Bound HRP, representing the CD200ED-CD47ED-coreSA fusion protein, was detected by chemiluminescent imaging of the ECL substrate (PXi, Syngene, MD, USA).

Preparation and characterization of biotinylated lentivirus tagged with CD200ED-CD47ED-coreSA fusion protein

The biotinylated lentivirus was mixed with 1 mL of the purified fusion protein and incubated under gentle shaking at 4°C to enhance linking of streptavidin from the fusion protein to the biotin lipid anchor on the membrane of lentivirus. Unbound protein was removed by washing three times. Surface modification of biotinylated lentiviral vectors with CD200ED-CD47ED-coreSA fusion protein was characterized by dot blot analysis. Briefly, 5 μL of biotinylated lentivirus tethered with CD200ED-CD47ED-coreSA fusion protein was added to two PVDF membranes. The membranes were blocked separately with blocking buffer for 1 hour at RT, and then incubated with primary antibodies solution of anti-mouse CD47 monoclonal antibody or anti-mouse CD200 monoclonal antibody. After washing for three times with TBST, membranes were probed separately into secondary antibody (mouse IgG HRP conjugated antibody). The membranes were also developed using the chemiluminescent ECL substrate and chemiluminescent images were recorded. Biotinylated lentivirus and soluble CD200ED-CD47ED-coreSA fusion protein were added to membranes as negative and positive controls.

Phagocytosis assay of biotinylated lentivirus tagged with CD200ED-CD47ED-coreSA

J774A.1 macrophage cells were cultured in a 6-well tissue culture plate and maintained in DMEM supplemented with 10% FBS and 1% penicillin streptomycin. The cells were incubated at 37°C in a 5% CO_2 incubator. The macrophages were infected with unmodified and fusion protein (CD200ED-CD47ED-coreSA) modified lentiviral vectors for 3 hours, and then cells were washed with 1x PBS to remove undigested lentiviral vectors and replenished with fresh culture medium. The cells were analyzed at 72 hours post-infection to assess the extent of phagocytosis. Phagocytic efficacies of J774A.1 cells was also evaluated by treatment with biotinylated lentivirus capped with CD200ED-coreSA-CD47ED; a different fusion protein orientation where the two ectodomain of CD200 and CD47 were separated with coreSA. Biotinylated lentivirus and coreSA-modified virus were used as

controls. The fluorescent intensity was evaluated using flow cytometer to determine viral engulfment by macrophages.

Ligands and receptors inhibition assay

Phenotype rescue experiments were undertaken to confirm the role of the ectodomains of CD47 and CD200 in the inhibition of phagocytosis. Briefly, J774A.1 macrophages were treated with anti-CD200R antibodies, anti-SIRPα or both (anti-CD200R and anti-SIRPα antibodies) for an hour to block the respective receptors. The cells were washed with 1x PBS and infected with biotinylated lentivirus tagged with CD200ED-CD47ED-coreSA fusion protein. Simultaneously, biotinylated lentiviruses tethered with CD200ED-CD47ED-coreSA fusion protein were treated with anti-CD200 and anti-CD47 or both (anti-CD200 and anti-CD47) antibodies for an hour, to block the ligands on the surface of the modified vector, prior to infect J774A.1 macrophages. Cultured J774A.1 cells were separately treated with the blocked biomimetic proteins immobilized on viral vectors. The fluorescent intensity was qualitatively and quantitatively analyzed using microscopic imaging and microplate readers, respectively.

Flow cytometry

Flow cytometry was used to assess the phagocytic and infection rates of the CD200ED-CD47ED-coreSA-tagged and untagged lentivirus infecting macrophage cells. The level of GFP was determined by flow cytometry as a marker for virus infectivity. The macrophages and control cells were harvested by trypsinization from the culture dishes and centrifuged at 400 xg for 5 min, thereafter, resuspended in 1x PBS. A minimum of 20,000 events were recorded for each preparation in the flow cytometer.

The effect of CD200ED-CD47ED on the IL-6 and TNF-α secretion from J774A.1 macrophage.

J774A.1 macrophages were seeded at a density of 5×10^4 cells cm^{-2} in 6-well plates. The cells were treated with unmodified lentiviral particles or fusion protein modified lentiviral particles for 18 h. cell culture supernatants were collected and stored at -80°C until

cytokine estimation using commercial ELISA. As per manufacturer's instructions, 100 µL of coating buffer containing either IL-6 or TNF-α antibody were added to each well of a 96 well plate. The plated were incubated at 4°C for overnight. The coating solution was removed, and the wells were washed thrice with a wash buffer (PBS + 0.05% Tween 20), followed by blocking with 200 µL 1× ELISPOT diluent per well for 1 hour at RT. The wells were washed thrice, as before, and 100 µL of culture media or appropriate standards and controls were added to the test plate for 2 hours at RT. Following removal of samples, the plate was again washed thrice and the IL-6 and TNF-α detection antibodies prepared in ELISPOT diluent were added at 100 µL per well for one hour at RT. The detection antibodies were removed, and the wells washed thrice, as before. 100 µL streptavidin-HRP in ELISPOT diluent was added and incubated at RT for 30 min. Following removal of the conjugate, the wells were washed five times, and 100 µL of 1× TMB solution was added to each well for 15 min at RT. Addition of 50 µL per well of 1 M phosphoric acid stopped the reaction. The resultant absorbance at 450 nm was determined on a microplate reader (SpectraMax M2e). The concentrations of IL-6 and TNF-α in the culture media were determined using the standard curves.

Statistical analysis

All data are presented as the mean ± standard deviation from at least three independent experiments and analyzed using one-way analysis of variance (ANOVA), followed by Tukey multiple comparisons post hoc tests in between experimental groups. *P* value less than 0.05 is considered statistically significant.

Results

Expression and purification of CD200ED-CD47ED-coreSA fusion protein

The gene sequence encoding ectodomain of CD200 (CD200ED), ectodomain of CD47 (CD47ED), and coreSA were PCR amplified from plasmid pME008. The results were verified by agarose gel electrophoresis which showed bands for coreSA at ~0.4 kb (384 bp), CD47ED at ~0.4kb (397 bp) and CD200ED at ~0.3 kb (291 bp) (Figure 5.1B). The plasmid construct pME008 produces the coreSA gene sequence (~14.2 kDa), CD47ED (~14.6 kDa),

and CD200ECD (~10.77 kDa) was estimated to produce a protein with molecular weight of ~ 40 kDa.

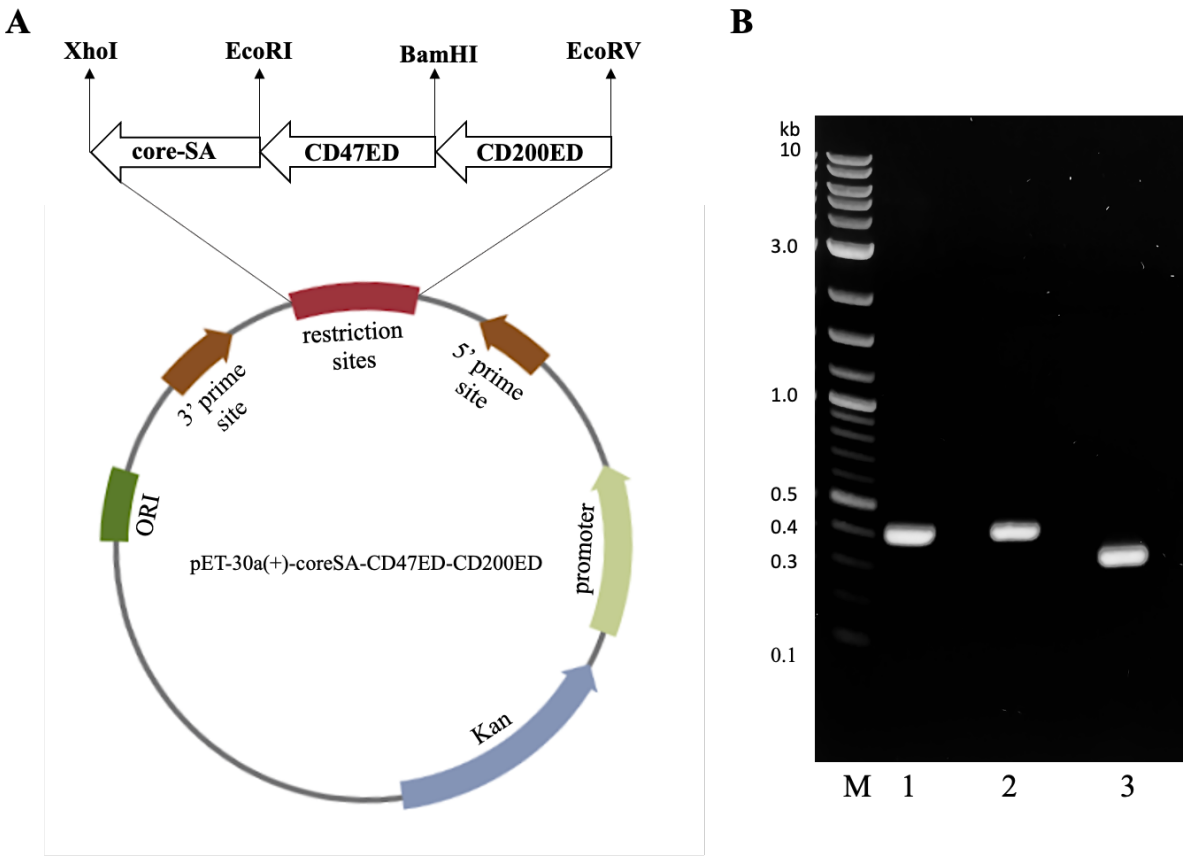

Figure 5.1. Plasmid map and PCR amplification of CD200-CD47 fusion gene. (A) vector map of plasmid pET-30a(+) showing cloning site of both genes of interest gene core streptavidin (coreSA), ectodomain of mouse CD47 (CD47ED), and ectodomain of mouse CD200 (CD200ED) in between respective restriction sites; (B) DNA gel electrophoresis of PCR products of coreSA in lane 1, CD47ED in lane 2, CD200ED in lane 3; M reflects the ladder.

SDS-PAGE analysis confirmed the expression of 40 kDa protein from crude cell lysate of pME008 transformed bacteria induced in the presence of IPTG (Figure 5.2B, lane 1). The purified CD200ED-CD47ED-coreSA fusion protein was characterized by a single band around the target location of ~40 kDa in the SDS-PAGE (Figure 5.2B, lane 2). The protein was eluted from IMAC using a buffer containing 250 mM imidazole. Most of the protein was eluted in the second fraction as shown in the elution profile in Figure 5.2A. The protein concentration of the eluted fraction was estimated to be 486 ± 29 μg mL^{-1} using the bicinchoninic acid (BCA) assay. The specificity of the overexpressed and purified protein

was further confirmed using Western blot analysis. As shown in Figure 5.2C, the fusion protein was detected by single band ~40 kDa using anti-CD200, anti-CD47, anti-streptavidin, and anti-histag antibodies. Dot blot analysis using anti-CD200 antibody (Figure 5.2E) and and-CD47 antibody (Figure 5.2D) confirmed the attachment of CD200ED-CD47ED-coreSA fusion protein on biotinylated lentiviral particles. the unmodified biotinylated lentiviral particles (negative control) exhibited no dot for both antibodies, which indicated the lack of protein on their surface. However, the soluble fusion protein (positive control) showed no difference in size of fusion protein coated on the surface of lentivirus (Figure 5.2D and Figure 5.2E). These results indicated that CD200ED-CD47ED fusion proteins were successfully tagged on the surface of viral vectors.

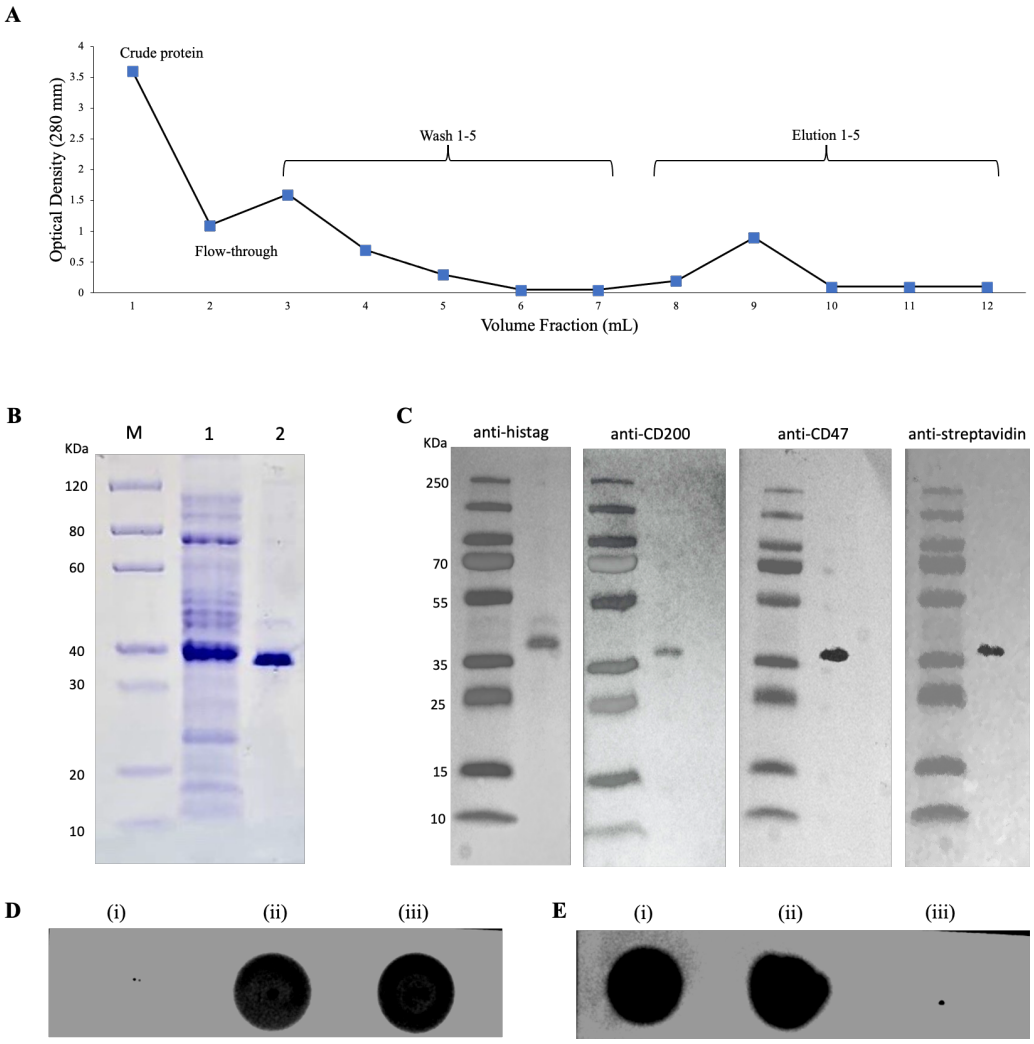

Figure 5.2. Characterization of CD200ED-CD47ED-coreSA fusion protein. (A) elution profile of the protein purification process showing that most of the target protein eluted at the fraction 9; (B)

SDS-PAGE analysis showing the protein marker (lane M), soluble crude protein with overexpressed fusion protein around 40 kDa (lane 1), and purified concentrated fusion protein ~ 40 kDa (lane 2); (C) Western blot analysis revealing reactivity of anti-histag antibody, anti-CD200 antibody, anti-CD47 antibody and anti-streptavidin antibody against the purified fusion protein. (D) dot blot assay was performed to assess the presence of the CD47ED protein on the surface of lentivirus modified with CD200ED-CD47ED-coreSA fusion protein. (i) unmodified biotinylated lentivirus (negative control), (ii) CD200ED-CD47ED-modified lentivirus, and (iii) soluble CD47ED protein (positive control) blotted on the membrane and run against anti-CD47 monoclonal antibody. The result showed CD47ED is anchored on the modified lentivirus by detecting strong dot in CD47ED-modifed virus (ii) as well as in the CD200ED-CD47ED fusion protein (iii). However, unmodified biotinylated lentivirus (i) showed no CD47ED signal. (E) dot blot assay against anti-CD200 monoclonal antibody showing biotinylated lentiviral particles can bind CD200ED-CD47ED fusion protein (ii) via biotin-streptavidin, while unmodified biotinylated lentivirus (iii) (negative control) revealing no CD200ED signal. Here, soluble CD200ED was used as a positive control (i).

Effect of fusion protein on phagocytosis by J774A.1 macrophages

The role of CD200ED-CD47ED-coreSA fusion protein on inhibiting phagocytosis was confirmed through *in vitro* functional studies. J774A.1 macrophage cells were infected with biotinylated lentiviruses tagged with fusion protein (CD200ED-CD47ED-coreSA) and nontagged biotinylated lentiviral particles as control. Through fluorescence microscopy we found that whilst, biotinylated lentiviral particles were readily taken up by J774A.1 macrophages, the fusion protein modified biotinylated lentivirus were much less phagocytosed by the macrophages (Figure 5.3A). Flow cytometer analysis confirmed a reduced expression of *GFP* by macrophages cells, which demonstrated that the untreated negative control group revealed 0.18% (5.3B), the group treated with fusion protein modified biotinylated lentiviral particles express 27.7% (Figure 5.3E), and unmodified biotinylated lentiviral particles showed higher *GFP* expression of 62.2% (5.3C). Through plate reader, the fluorescence illustrated about ~5-folds decrease in the uptake of fusion protein modified biotinylated lentiviral particles by J744A.1 macrophages (Figure 5.3F). To further ascertain that the anti-phagocytic effect was a consequence of CD200ED-CD47ED and not contributed in part by coreSA, J774A.1 macrophages were treated with biotinylated lentiviral particles modified with coreSA only, which revealed no anti-phagocytic effect. The observation was ascertained using fluorescence microscopy (Figure 5.3A, ii) and flow cytometry (Figure 5.3D), which revealed no significant difference in uptake of nonbiotinylated lentiviral particles and biotinylated lentiviral particles modified with coreSA (Figure 5.3F). Moreover, the flow cytometer histogram showed MFI = $1.39\times10^6 \pm 6{,}816$ for unmodified biotinylated

virus, MFI = $1.31\times10^6 \pm 7{,}422$ for coreSA-modified virus and MFI = $4.82\times10^5 \pm 2{,}063$ for CD200ED-CD47ED-modified virus (data not shown). Judging from these results, fusion protein modified virus should be tolerated by the immune system by suppressing macrophages engulfment much more comparing to unmodified lentivirus.

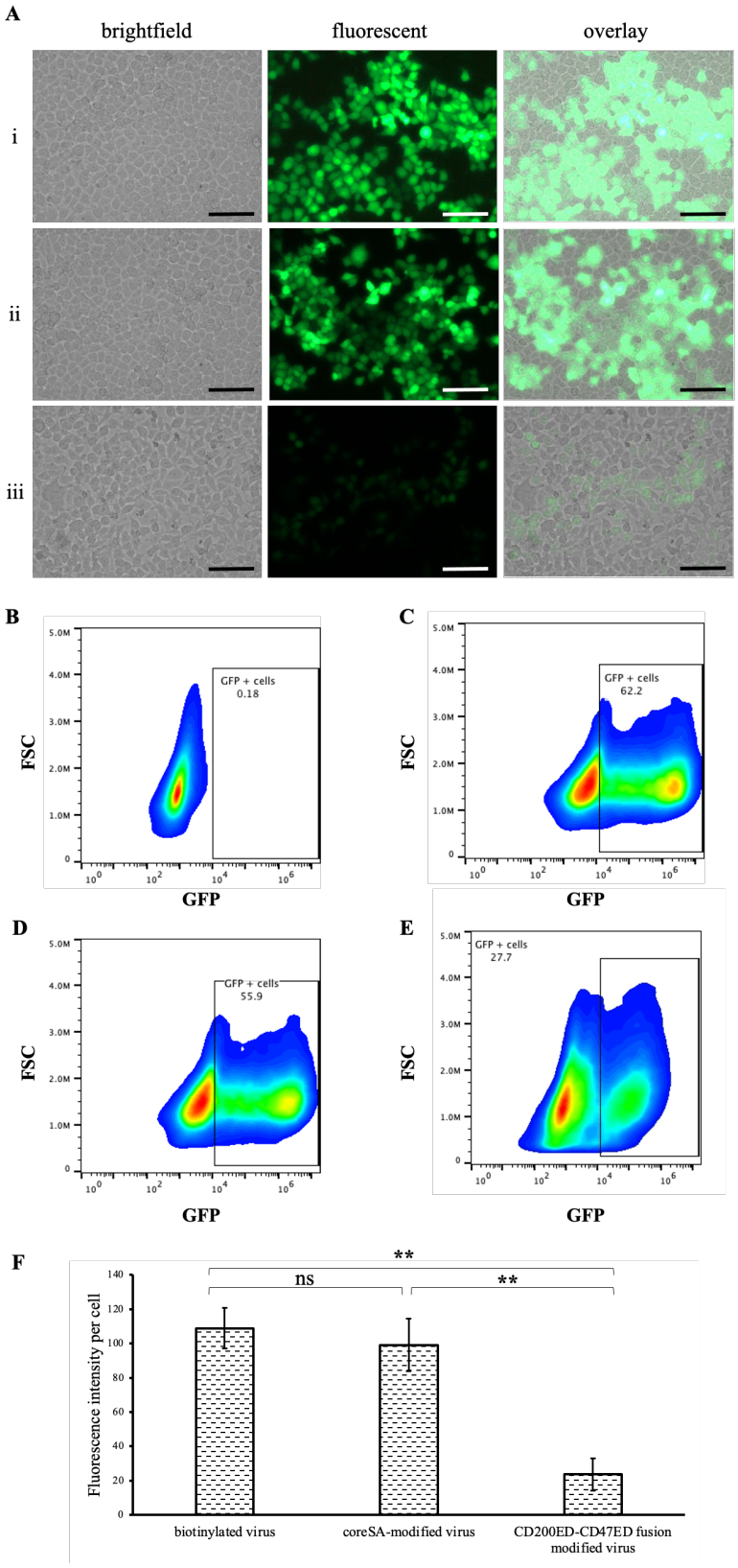

Figure 5.3. Reduced macrophage phagocytosis of lentivirus tethered with CD200ED-CD47ED fusion protein. (A) showing brightfield, fluorescent, and overlay images of J774A.1 macrophage cells

ingested (i) biotinylated lentivirus, (ii) coreSA-biotinylated lentivirus, and (iii) CD200ED-CD47ED-biotinylated lentivirus, respectively. Scale bar denotes 100 μm; (B-E) density plot of macrophages expressing *GFP* using flow cytometer – (B) untreated J774A.1 macrophages (negative control), (C) J774A.1 macrophages treated with unmodified biotinylated lentivirus (positive control), (D) J774A.1 macrophages treated with coreSA-modified biotinylated lentivirus, and (E) J774A.1 macrophages treated with CD200ED-CD47-fusion modified biotinylated lentivirus; (F) measurement of relative fluorescence intensity per cell using ImageJ for J774A.1 macrophages treated with biotinylated lentivirus, coreSA-biotinylated lentivirus, and CD200ED-CD47ED-biotinylated lentivirus at 72 hours post-treatment. Statistical analysis was performed using one-way ANOVA followed by Tukey post hoc multiple comparisons test and data were presented as mean ± standard deviation (n = 5); **Denotes $P<0.01$.

Ligand-receptor blocking assay

To evaluate the importance of CD200 and CD47 on macrophage activation and resistance to phagocytosis, we undertook a two-way phenotype rescue assay *in vitro.* First, we blocked the protein expressed on the biotinylated lentivirus using anti-CD200 and anti-CD47 monoclonal antibodies separately and together, prior to infect J774A.1 macrophages cells. It was found that blocking only CD47 (Figure 5.4A, ii) enhanced uptake more than blocking only CD200 (Figure 5.4A, i). Whereas the intensity of *GFP* expression increased significantly when both surface proteins were blocked (Figure 5.4A, iii). Second, we blocked corresponding receptors to the biomimetic proteins located on the J774A.1 using antibodies against CD200R and SIRPα. Blocking the CD200R prevents the CD200-CD200R binding (but not affecting the CD47-SIRPα binding) and therefore, the CD200 protein functionally is not active. In contrast, blocking the SIRPα effect only its interaction with CD47 protein, but does not affect the CD200-CD200R interaction and functionality. Expectedly, blocking of the receptors *viz* CD200R or SIRPα resulted in an increased uptake of the biotinylated lentiviral particles by J774A.1 (Figure 5.4B, i & ii and 5.4C) and exhibiting much higher intensity of *GFP* expression when blocking both receptors (Figure 5.4B, iii and 5.4C).

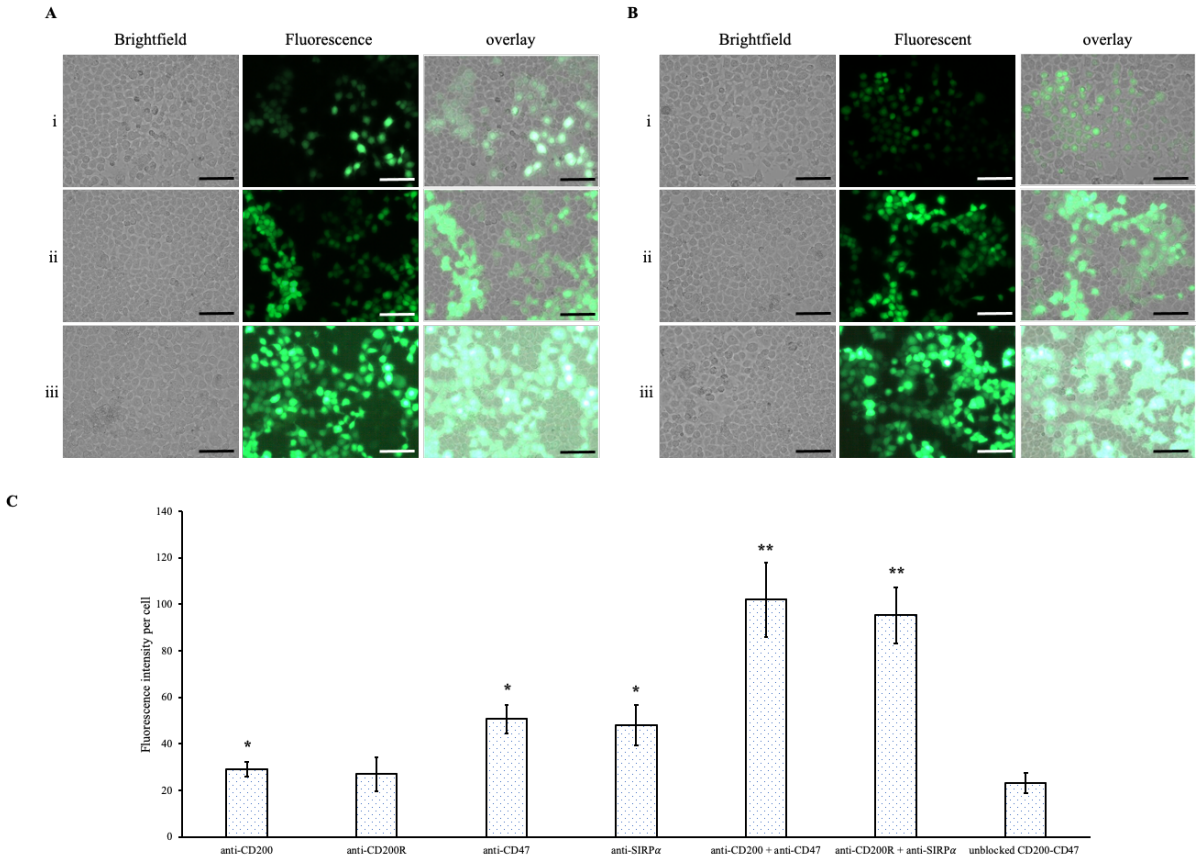

Figure 5.4. Inhibition of macrophage phagocytosis via CD200ED-CD47ED/SIRPα-CD200R axis. (A) showing brightfield, fluorescence, and overlay images of J774A.1 macrophages infected with CD200ED-CD47ED-modified lentivirus with (i) blocking CD200ED protein, (ii) blocking CD47ED protein, (iii) blocking CD200ED and CD47ED proteins. (B) showing brightfield, fluorescence, and overlay images of CD200ED-CD47ED-modified lentivirus added to J774A.1 macrophages blocked with (i) anti-CD200R receptor, (ii) anti-SIRPα receptor, (iii) or blocked with anti-CD200R and anti-SIRPα receptors together; Scale bar denotes 100 μm (C) fluorescence intensity per cell of J774A.1 macrophages incubated with and without antibodies blocking either ligand and/or receptors of CD200, CD47, CD200R, or SIRPα, then treated with CD200ED-CD47ED-tethered lentivirus. Statistical analysis was performed using one-way ANOVA followed by Tukey post hoc multiple comparisons test and data were presented as mean ± standard deviation (n = 5). **P*<0.05 and ***P*<0.01 comparing to unblocked CD200ED-CD47ED-fusion modified virus.

Induction of pro-inflammatory cytokines IL-6 and TNF-α from J774A.1 macrophages.

The levels of IL-6 cytokine induced by either biotinylated lentivirus coated with CD200ED or CD47ED were not statically significant comparing to cytokines induced by virus tethered with the CD200-CD47 fusion protein (Figure 5.5A). In contrast, the secretion of TNF-α from CD47ED-modifed virus was statically significant (*P*<0.05) comparing to CD200ED-CD47ED-coreSA modified virus group. However, CD200ED-modifed virus was

not showing significant secretion of TNF-α. The biotinylated lentivirus particles (unmodified with biomimetic proteins) induced significantly higher amounts of both IL-6 (48 ± 6 pg/mL) and TNF-α (1216 ± 121 pg/mL) comparing to CD200ED-, CD47ED- and CD200ED-CD47ED-coreSA modified virus. J774A.1 macrophages treated with virus tagged with CD200ED-CD47ED fusion protein secreted 20 ± 8 pg/mL for IL-6 and 663 ± 127 pg/mL for TNFα, which is about 58.3% and 45.5% less than the levels of IL-6 and TNF-α secreted by biotinlyted lentiviurs, respectively (Figure 5.5 A-B).

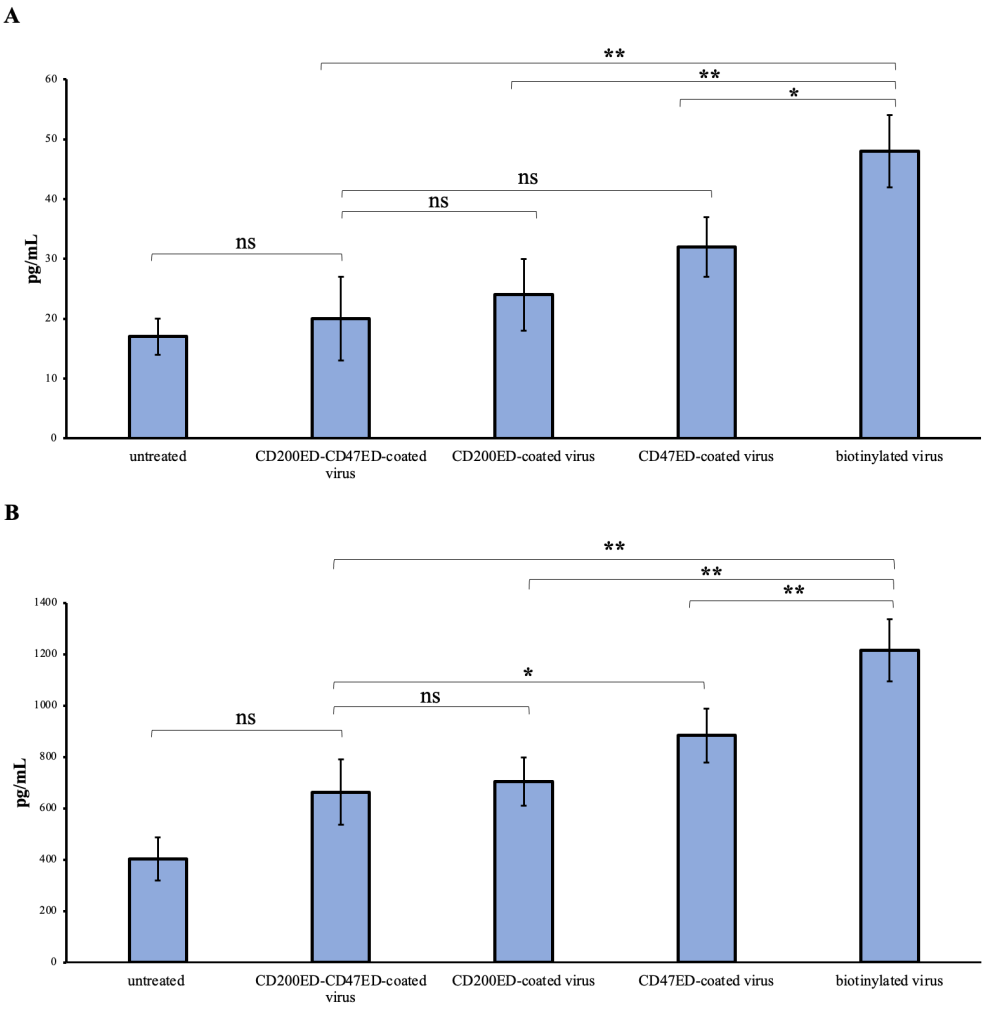

Figure 5.5. IL-6 and TNF-α secreted by J774A.1 macrophages. Pro-inflammatory cytokines secretion of IL-6 (A) and TNF-α (B) from macrophages challenged with untreated, CD200ED-CD47ED-coated lentivirus, CD200ED-coated virus, CD47ED-coated virus, and biotinylated lentivirus for 18 hours. Statistical analyses were measured using one-way ANOVA and data were presented as mean ± standard deviation; * and ** denotes $P<0.05$ and $P<0.01$, respectively.

To understand the ligand-receptor binding effect on phagocytic activity of macrophages, a slightly modified vector was constructed and expressed with different orientation with the two biomimetic proteins being separated by coreSA (CD200ED-coreSA-CD47ED) (Figure 5.6 A&B). The purified fusion protein (~40 kDa) was used to modify the surface of biotinylated lentivirus particles and infected J774A.1 macrophages (Figure 5.6C). Even when the CD200ED and CD47ED were separated by coreSA protein, it did not influence the phagocytic infectivity of J774A.1 cells. Fluorescence microscopy revealed reduced uptake of biotinylated lentiviral particles modified with CD200ED-coreSA-CD47ED protein (Figure 5.7A, iii). Consequently, a significant reduction in the mean fluorescence intensity ($P< 0.05$) was also observed (Figure 5.7B)

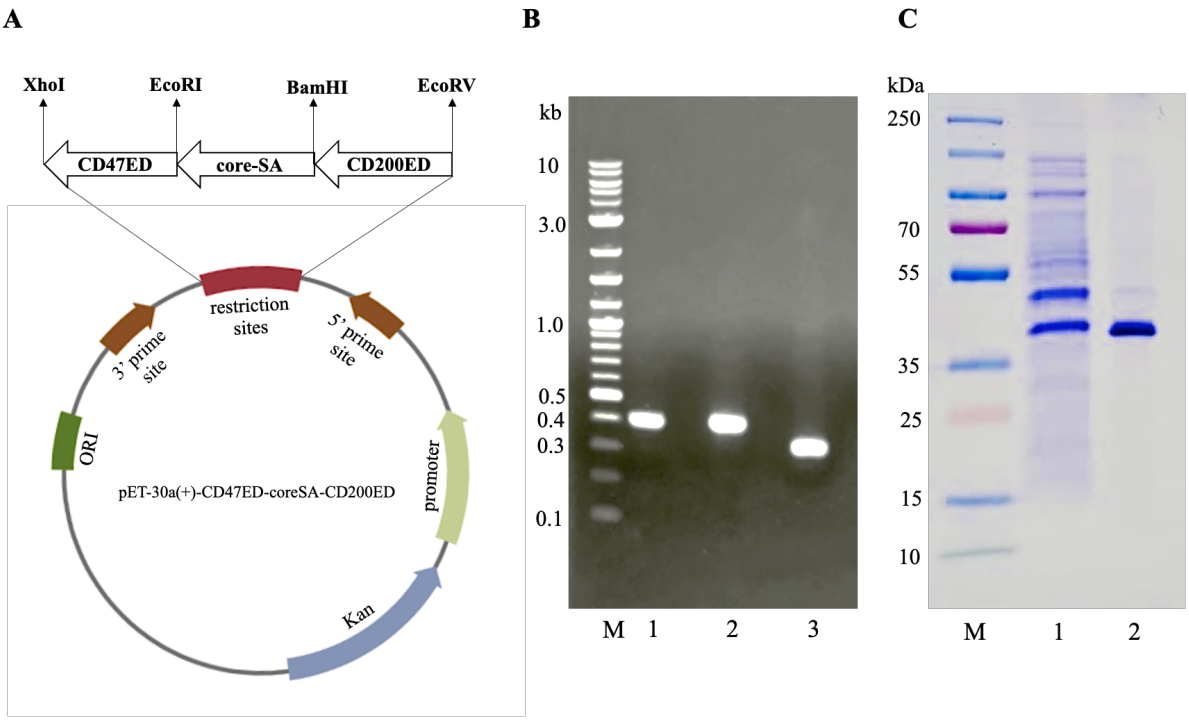

Figure 5.6. Plasmid map and PCR amplification of genes of interest. (A) vector map of plasmid pET-30a(+) showing cloning site of the three genes of interest; ectodomain of mouse CD47 (CD47ED), core streptavidin (coreSA) and ectodomain of mouse CD200ED (CD200ED) in between respective restriction sites; (B) DNA gel electrophoresis of PCR products of CD47ED in lane 1, coreSA in lane 2, CD200ED in lane 3; M reflects the ladder; (C) SDS-PAGE image showing the protein marker (lane M), soluble crude protein expressing fusion protein around 40 kDa (lane 1), and purified concentrated fusion protein ~ 40 kDa (lane 2).

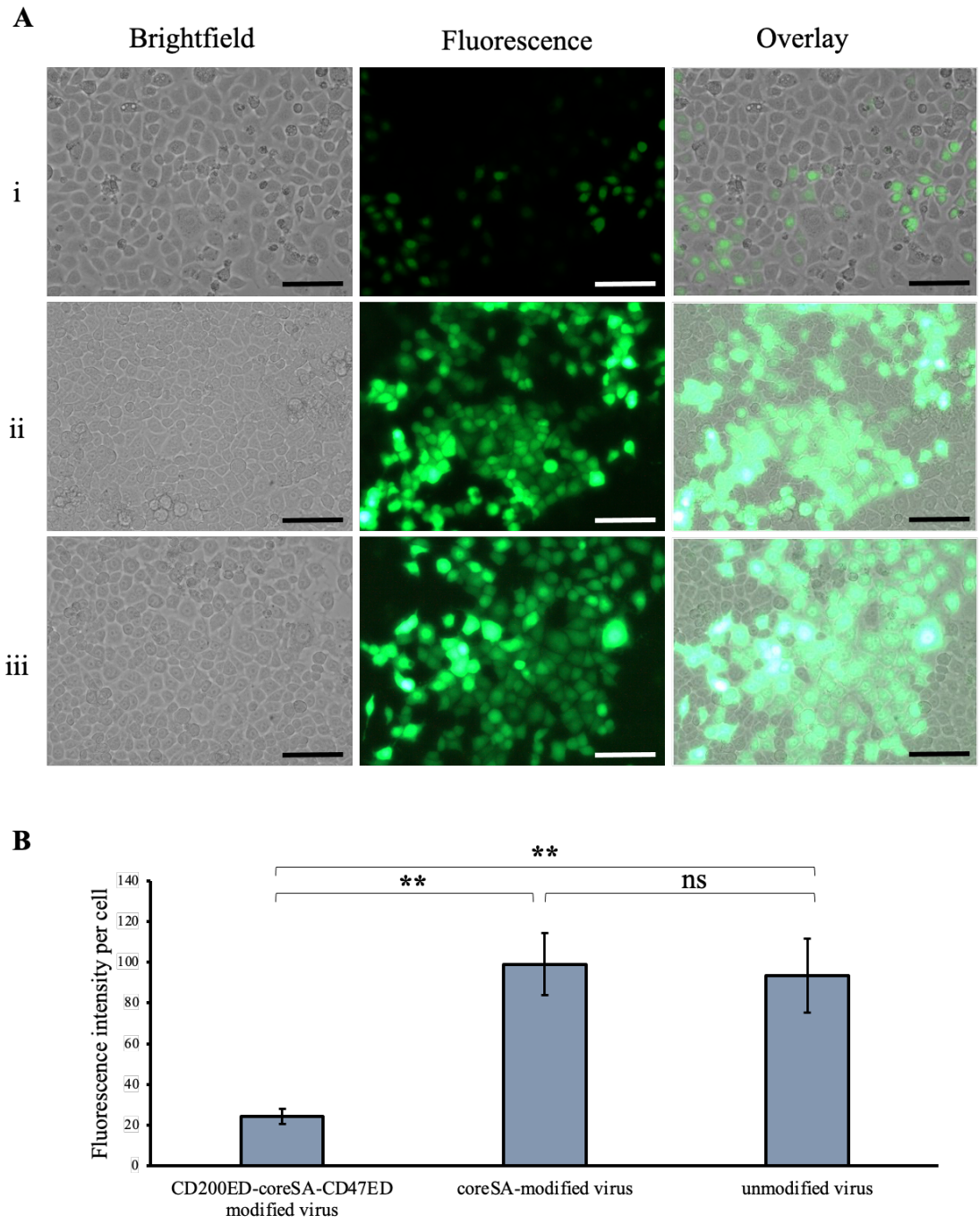

Figure 5.7. phagocytic effect of separating CD200 ectodomain and CD47 ectodomain with coreSA protein. Macrophages treated with lentivirus tagged with CD200ED-coreSA-CD47ED fusion protein. (A) showing brightfield, fluorescent, and overlay images of J774A.1 macrophage cells ingested (i) CD200ED-coreSA-CD47ED-biotinylated lentivirus, (ii) coreSA-biotinylated lentivirus, and (iii) biotinylated lentivirus, respectively; (B) measurement of fluorescence intensity per cell of J774A.1 macrophages treated with CD200ED-coreSA-CD47ED-biotinylated lentivirus, coreSA-biotinylated lentivirus, and biotinylated lentivirus at 72 hours post-treatment. Scale bar denotes 100 μm and data were presented as mean ± standard deviation (n = 5). **Denotes $P<0.01$ comparing to CD200ED-coreSA-CD47ED-modified lentivirus.

Discussion

In the current study, extracellular domains of CD200 and extracellular domain of CD47 were immobilized on the surface of biotinylated lentiviruses through a core streptavidin (coreSA) domain. The ability of the fusion protein (CD200ED-CD47ED-coreSA) in overcoming macrophage mediated phagocytosis and targeted gene delivery was assessed. The role of CD200 and CD47 in mediating stealth functionalization for drug delivery has been explored previously[102,103,158]. However, our study is a preliminary demonstration of the interaction of CD200 and CD47 fusion protein, its ability to mimic biological systems and confer the stealthy functionality on drug carriers. The fusion protein was cloned, expressed, and purified using the bacterial cloning vectors. The genetic chimera was constructed using only the extracellular domains of the CD200, CD47 and the domain of core streptavidin. It has previously been shown that the extracellular domains of CD200[200,201] and CD47[202] retain functionality required for binding to and phosphorylation of their cognate receptors. Additionally, it has also been shown that core streptavidin is more soluble than full length streptavidin, which tends to form higher order aggregates[119]. The use of extracellular domains of CD200 and CD47 along with core streptavidin allowed easy purification of a low molecular weight recombinant fusion protein.

Whilst conformational changes in synthetic nanoparticles for enhanced surface binding are plausible[158], it is less feasible with biological vectors such as viruses and bacteria[203]. Immobilization of biological vectors must be undertaken by achieving a balance between available surface area and maintenance of structural integrity[203]. Dot blot assays confirmed that the fusion protein was appropriately immobilized on the biotinylated lentiviral surface. To ensure that immobilized viral particles retained functionality, we assessed their infectivity in HEK 293T cells. Surface modified and non-modified lentivirions were both found to be equally up taken by the HEK 293T cells. It is thus likely that surface modification of the bio-vector has not disrupted the infectivity of the lentiviral particle and allows for effective gene transfer.

To further assess if the functionality of fusion protein is integrative, J774A.1 macrophages were employed. Infection of J774A.1 macrophages with fusion protein immobilized lentiviruses resulted in inhibition of phagocytosis and dampening of

proinflammatory cytokine responses. Whilst the individual extracellular domain of CD47 or CD200 did inhibit phagocytosis (shown in Chapter 2 and 3), the combined effect of phagocytosis evasion was significantly higher when biotinylated lentiviruses were immobilized with the fusion protein (i.e., containing both ectodomains of CD200 and CD47). A previously undertaken study immobilized the surface of poly(lactic-co-glycolic acid) (PLGA) nanoparticles with CD200. The modification was applied to several geometries of the particle and was found to result in reduced phagocytosis and consequent suppression of proinflammatory cytokines (TNF-α) with an increased secretion of anti-inflammatory cytokines (namely IL-10)[192]. Similarly when nano- and micro-sized polystyrene particles were coated with CD200 it was found to result in diminished phagocytosis and a decreased secretion of TNF-α[158]. Similarly in an Alzheimer's disease model CD47ED conjugated PLGA particles were able to resist phagocytosis and increased the half-life of the particles in blood circulation[204]. PEGylated nanoparticles co-coupled with CD47 displayed reduced cellular uptake by macrophages *in vitro* and *in vivo*[205]. *In-vivo* models in non-human primates confirmed the ability of CD47-modified lentiviral particles to evade phagocytosis with high transduction efficacy[103].

While inhibition of phagocytosis is a significant aspect of stealthing, post phagocytic events include evocation of an inflammatory immune response. The protective nature of proinflammatory immune responses assist antigenic clearance[206]. However, we found that along with inhibition of phagocytosis, there was a significant reduction in induction of pro-inflammatory cytokines IL-6 and TNF-α. Our findings are consistent with previous results illustrating the repression of pro-inflammatory cytokines upon CD47 binding to SIRPα[102,103,205] and CD200 interaction with CD200R[158,192]. The rescue of phenotype upon blocking of the respective ligands viz, CD200, CD47 and their cognate receptors CD200R, SIRPα (CD172α) confirmed that phagocytosis is mediated through the classical pathway[108,113,155,161] and is also not contributed by the coreSA domain in the fusion protein. A blocked CD200 receptor resulted in a lower fluorescence intensity in comparison to a blocked CD47 receptor indicating a higher phagocytic index. It is likely that the surface of J774A.1 cells has differential turnover of receptors CD200R and CD172α resulting in this differential phenotype. It is also consistent with the previous findings in Chapter 2 and 3 that

CD47-CD172α interaction led to stronger antiphagocytic feature than CD200-CD200R interaction.

Chapter 6: Conclusion and Future Directions

Significant advancements have been made in the design of engineered nanoparticles in the past few decades. Despite these advancements, synthetic systems do not match the complexity of natural cells. The development of efficient therapeutic delivery vehicles requires evasion of the mononuclear phagocyte system, localization to the target sites, and sustained delivery. Inspired by the way innate biological cells from our body can accomplish complex tasks daily in the body, the biomimetic approach to engineering delivery systems has expanded rapidly. Delivery carriers based on viral vectors' stealth mimicry have shown to offer a certain degree of immune evasion. However, there remains obstacles to efficient delivery, and delivery mechanisms used by biological carriers is yet to be fully understood. Greater understanding will allow researchers to develop new and improved synthetic techniques based on innate biological cells. The field of nanobiotechnology continues to develop to accommodate the ever-expanding dynamism of therapeutic discovery. There are multiple combinations of chemical and bio-inspired molecules that aid better uptake and efficacy of nanoparticles. The choice of the coating is dependent on the target tissue, the immune barrier that needs to be overcome, and the ease of synthesis. Personalized medicine may thus not only refer to personalized therapeutics but also encompass delivery suited for the condition to be treated. More compelling data in favor of these newly devised strategies may enhance the speed of securing their regulatory approvals and benefit clinical applications.

Nanoparticle-based drug delivery systems, which involve viral or nonviral vectors, offer the advantage of being small, having high solubility, and higher efficacy compared with many other drug delivery systems. However, these structures still face the risk of rapid clearance by an active immune system. This rapid clearance can result in therapeutics being inappropriately or under-utilized. Immune evasion of nanoparticles can be achieved through surface modification either by chemical or biological means. Chemical methods involve surface modification through molecules that have high hydrophilicity or no surface charge whereas biological methods involve mainly a mimicry of naturally occurring biological systems that confer the NPs with stealth functionalities that enable them to evade

detection by the immune system. This dissertation investigates biological modifications adopted to build resilient lentivirus nanoparticles.

This study provides a preliminary report on immobilization of ectodomain of mouse CD47 on the lentiviral outer membrane to assess evasion of macrophage phagocytosis. Using recombineering to functionalize lentivirus presents a novel approach to biomimicry that does not involve genetic engineering of lentiviruses. The surface immobilization of viral vectors with CD47 ectodomain can provide an alternative approach to endow therapeutic viruses with stealth functionalization and achieve prolonged blood circulation for enhanced drug targeting. Similarly, modified lentiviral particles with the extracellular domain of CD200 expressed along with the core domain of streptavidin demonstrated efficacy in delivering the green fluorescence protein (*GFP*) gene, and could inhibit phagocytosis mediated by mouse macrophages, and dampened pro-inflammatory responses as measured using concentrations of IL-6 and TNFα, the sentinel marker of pro-inflammation. Whilst this study provides preliminary evidence towards the modification of lentiviruses for stealth functionalization, the functionality of the particles along with their stability *in vivo* needs further investigation. Moreover, our study is preliminary evidence for immobilization mediated surface modulation of lentiviral particles using a fusion protein bearing two extracellular domains. While individually the molecules have been assessed for their ability to evade host immune responses, the combined effect of the fusion proteins was significantly higher. The study presents a novel notion to modulate nanoparticle surfaces to mimic biological systems and achieve better stealth functionalization.

CD200 protein contains two immunoglobulin domain, Ig-variant (IgV) and Ig-constant (IgC2). In a previous study by Zhang *et al*. the two extracellular domains of CD200 protein (IgV and IgC2) immobilized on the surface of biotinylated polystyrene particles reduced phagocytosis and downregulated macrophage activation[158]. In this dissertation, the effect of the IgV extracellular domain on regulation of macrophages was investigated, where co-expression of IgV CD200 and IgV CD47 proteins demonstrated a promising approach for virotherapuetic use. Further investigation of expressing the two extracellular domains of CD200 along with CD47 is needed. The interaction and immobilization of proteins with ligands and particles' surface must be analyzed using surface plasmon resonance (SPR)

technique, which would provide better understanding of domains binding and function. Moreover, this study is a proof-of-concept, and thus further research is required involving experimental validation for human CD200 extracellular domain (IgV and IgC2) and CD47 protein extracellular domains, human-derived primary macrophages, and *in vivo* experiments.

Additionally, Implanted materials are considered to be foreign to the body, leading to the body responding with macrophages and subjecting such materials to elimination by the immune system[207]. The effect of surface modification on macrophages and the immune response has attracted research attention in various areas including tissue engineering, biomaterials and implanted materials or medical devices. Stachelek *et al.,* reported that polymeric biomaterials functionalized with CD47 protein effectively reduces inflammatory cell attachments[111]. In contrast, CD200 extracellular domain was found to delay macrophage attachment into tissue-culture treated polystyrene (TCPS)[208]. Therefore, the effect of modifying biomaterial surfaces with CD200 and CD47 extracellular domains and their co-expression, along with their stability *in vivo,* needs further investigation. Moreover, the mechanistic and systemic effect of each CD47, CD200, and CD200-CD47 fusion protein remain unclear and should be investigated. The time it takes phagocytosis-resistant effect last long for the CD47, CD200, and CD200-CD47 fusion protein are not understood and must be assessed as well.

Lastly, since CD47 protein is an integrin-associated protein[121], it remains to be investigated whether the CD47 protein has effect on the overexpression of the integrin $\alpha_v\beta_3$ on tumor metastasis and angiogenesis[209]. Moreover, adenocarcinomic human alveolar basal epithelial cells (A549 cells) with high level of integrin $\alpha_v\beta_3$ might enhance the infectivity of lentiviral vectors tagged with CD47 protein in compare with A549 cells of blocked integrin $\alpha_v\beta_3$. In short, 'marker of self' CD47 protein function may not be limited to anti-phagocytosis but could also suppress tumor angiogenesis by targeting drug carriers onto epithelial cells bearing with high expression of integrin $\alpha_v\beta_3$.

Literature Cited

1. Halma C, Daha MR, van Es LA. In vivo clearance by the mononuclear phagocyte system in humans: an overview of methods and their interpretation. *Clin Exp Immunol*. 1992;89(1):1-7. doi:10.1111/j.1365-2249.1992.tb06868.x

2. Oldenborg PA, Zheleznyak A, Fang YF, Lagenaur CF, Gresham HD, Lindberg FP. Role of CD47 as a marker of self on red blood cells. *Science (80-)*. 2000;288(5473):2051-2054. doi:10.1126/science.288.5473.2051

3. Yong S-B, Song Y, Kim HJ, Ain QU, Kim Y-H. Mononuclear phagocytes as a target, not a barrier, for drug delivery. *J Control Release*. 2017;259:53-61. doi:https://doi.org/10.1016/j.jconrel.2017.01.024

4. Müller RH, Mäder K, Gohla S. Solid lipid nanoparticles (SLN) for controlled drug delivery - A review of the state of the art. *Eur J Pharm Biopharm*. 2000;50(1):161-177. doi:10.1016/S0939-6411(00)00087-4

5. Kalachandra S, Takamata T, Lin DM, Snyder EA, Webster-Cyriaque J. Stability and release of antiviral drugs from ethylene vinyl acetate (EVA) copolymer. *J Mater Sci Mater Med*. 2006;17(12):1227-1236. doi:10.1007/s10856-006-0596-6

6. Farokhzad OC, Langer R. Nanomedicine: Developing smarter therapeutic and diagnostic modalities. *Adv Drug Deliv Rev*. 2006;58(14):1456-1459. doi:10.1016/j.addr.2006.09.011

7. Salmaso S, Caliceti P. Stealth properties to improve therapeutic efficacy of drug nanocarriers. *J Drug Deliv*. 2013;2013:374252. doi:10.1155/2013/374252

8. Duncan R, Vicent MJ. Polymer therapeutics-prospects for 21st century: The end of the beginning. *Adv Drug Deliv Rev*. 2013;65(1):60-70. doi:10.1016/j.addr.2012.08.012

9. Kaminskas LM, McLeod VM, Kelly BD, et al. Doxorubicin-Conjugated PEGylated Dendrimers Show Similar Tumoricidal Activity but Lower Systemic Toxicity When Compared to PEGylated Liposome and Solution Formulations in Mouse and Rat Tumor Models. *Mol Pharm*. 2012;9(3):422-432. doi:10.1021/mp200522d

10. Plummer R, Wilson RH, Calvert H, et al. A Phase i clinical study of cisplatin-incorporated polymeric micelles (NC-6004) in patients with solid tumours. *Br J Cancer*. 2011;104(4):593-598. doi:10.1038/bjc.2011.6

11. Thomas OS, Weber W. Overcoming Physiological Barriers to Nanoparticle Delivery-Are We There Yet? *Front Bioeng Biotechnol*. 2019;7:415. doi:10.3389/fbioe.2019.00415

12. Kluin OS, van der Mei HC, Busscher HJ, Neut D. Biodegradable vs non-biodegradable antibiotic delivery devices in the treatment of osteomyelitis. *Expert Opin Drug Deliv*. 2013;10(3):341-351. doi:10.1517/17425247.2013.751371

13. Kaestner L, Bogdanova A. Editorial: The Red Cell Life-Cycle From Erythropoiesis to Clearance. *Front Physiol*. 2018;9:1537. doi:10.3389/fphys.2018.01537

14. Rizvi SAA, Saleh AM. Applications of nanoparticle systems in drug delivery technology. *Saudi Pharm J*. 2018;26(1):64-70. doi:10.1016/j.jsps.2017.10.012

15. Mazumdar S, Chitkara D, Mittal A. Exploration and insights into the cellular internalization and intracellular fate of amphiphilic polymeric nanocarriers. *Acta Pharm Sin B*. 2021;11(4):903-924. doi:10.1016/j.apsb.2021.02.019

16. Azad N, Rojanasakul Y. Macromolecular Drug Delivery. In: ; 2008:293-323. doi:10.1007/978-1-59745-532-9_14

17. Petros RA, Desimone JM. Strategies in the design of nanoparticles for therapeutic applications. *Nat Rev Drug Discov*. 2010;9(8):615-627. doi:10.1038/nrd2591

18. Yoo JW, Irvine DJ, Discher DE, Mitragotri S. Bio-inspired, bioengineered and biomimetic drug delivery carriers. *Nat Rev Drug Discov*. 2011;10(7):521-535. doi:10.1038/nrd3499

19. Marshall JS, Warrington R, Watson W, Kim HL. An introduction to immunology and immunopathology. *Allergy, Asthma Clin Immunol*. 2018;14(2):49. doi:10.1186/s13223-018-0278-1

20. Hume DA. The mononuclear phagocyte system. *Curr Opin Immunol*. 2006;18(1):49-53. doi:https://doi.org/10.1016/j.coi.2005.11.008

21. Yona S, Gordon S. From the Reticuloendothelial to Mononuclear Phagocyte System – The Unaccounted Years. *Front Immunol*. 2015;6(JUL):328. doi:10.3389/fimmu.2015.00328

22. Fam SY, Chee CF, Yong CY, Ho KL, Mariatulqabtiah AR, Tan WS. Stealth coating of Nanoparticles in drug-delivery systems. *Nanomaterials*. 2020;10(4):1-18. doi:10.3390/nano10040787

23. Gustafson HH, Holt-Casper D, Grainger DW, Ghandehari H. Nanoparticle uptake: The phagocyte problem. *Nano Today*. 2015;10(4):487-510. doi:10.1016/j.nantod.2015.06.006

24. Park EJ, Choi J, Lee KC, Na DH. Emerging PEGylated non-biologic drugs. *Expert Opin Emerg Drugs*. 2019;24(2):107-119. doi:10.1080/14728214.2019.1604684

25. Milton Harris J, Chess RB. Effect of pegylation on pharmaceuticals. *Nat Rev Drug Discov*. 2003;2(3):214-221. doi:10.1038/nrd1033

26. Garay RP, El-Gewely R, Armstrong JK, Garratty G, Richette P. Antibodies against polyethylene glycol in healthy subjects and in patients treated with PEG-conjugated agents. Published online 2012. doi:10.1517/17425247.2012.720969

27. Kozma GT, Shimizu T, Ishida T, Szebeni J. Anti-PEG antibodies: Properties, formation, testing and role in adverse immune reactions to PEGylated nano-biopharmaceuticals. *Adv Drug Deliv Rev*. 2020;154-155:163-175. doi:10.1016/j.addr.2020.07.024

28. Wang X, Ishida T, Kiwada H. Anti-PEG IgM elicited by injection of liposomes is involved in the enhanced blood clearance of a subsequent dose of PEGylated liposomes. *J Control Release*. 2007;119(2):236-244. doi:https://doi.org/10.1016/j.jconrel.2007.02.010

29. Yang Q, Lai SK. Anti-PEG immunity: Emergence, characteristics, and unaddressed questions. *Wiley Interdiscip Rev Nanomedicine Nanobiotechnology*. 2015;7(5):655-677. doi:10.1002/wnan.1339

30. Gonçalves GAR, Paiva R de MA. Gene therapy: advances, challenges and perspectives. *Einstein (São Paulo)*. 2017;15(3):369-375. doi:10.1590/s1679-45082017rb4024

31. Gyngell C, Douglas T, Savulescu J. The Ethics of Germline Gene Editing. *J Appl Philos*. 2017;34(4):498-513. doi:10.1111/japp.12249

32. Evans JH. Setting ethical limits on human gene editing after the fall of the somatic/germline barrier. *Proc Natl Acad Sci*. 2021;118(22):e2004837117. doi:10.1073/pnas.2004837117

33. Sung YK, Kim SW. Recent advances in the development of gene delivery systems. *Biomater Res*. 2019;23(1):1-7. doi:10.1186/s40824-019-0156-z

34. Shoeb E, Hefferon K. Future of cancer immunotherapy using plant virus-based nanoparticles. *Futur Sci OA*. 2019;5(7):FSO401. doi:10.2144/fsoa-2019-0001

35. Mali S. Delivery systems for gene therapy. *Indian J Hum Genet*. 2013;19(1):3-8. doi:10.4103/0971-6866.112870

36. Sokullu E, Abyaneh HS, Gauthier MA. Plant/bacterial virus-based drug discovery, drug delivery, and therapeutics. *Pharmaceutics*. 2019;11(5). doi:10.3390/pharmaceutics11050211

37. Dong X. Current strategies for brain drug delivery. *Theranostics*. 2018;8(6):1481-1493. doi:10.7150/thno.21254

38. Kouraklis G. Progress in cancer gene therapy. *Acta Oncol (Madr)*. 1999;38(6):675-683. doi:10.1080/028418699432815

39. Letvin NL. Progress in the Development of an HIV-1 Vaccine. *Science (80-)*. 1998;280(5371):1875 LP - 1880. doi:10.1126/science.280.5371.1875

40. Emeagi PU, Goyvaerts C, Maenhout S, Pen J, Thielemans K, Breckpot K. Lentiviral Vectors: A Versatile Tool to Fight Cancer. *Curr Mol Med*. 2013;13(4):602-625. doi:10.2174/1566524011313040011

41. Miller AD. Retrovirus Packaging Cells. *Hum Gene Ther*. 1990;1(1):5-14. doi:10.1089/hum.1990.1.1-5

42. Roldão A, Mellado MCM, Castilho LR, Carrondo MJT, Alves PM. Virus-like particles in vaccine development. *Expert Rev Vaccines*. 2010;9(10):1149-1176. doi:10.1586/erv.10.115

43. Finbloom J, Aanei I, Bernard J, et al. Evaluation of Three Morphologically Distinct Virus-Like Particles as Nanocarriers for Convection-Enhanced Drug Delivery to Glioblastoma. *Nanomaterials*. 2018;8(12):1007. doi:10.3390/nano8121007

44. Fu Y, Li J. A novel delivery platform based on Bacteriophage MS2 virus-like particles. *Virus Res*. 2016;211:9-16. doi:10.1016/j.virusres.2015.08.022

45. Chung YH, Cai H, Steinmetz NF. Viral nanoparticles for drug delivery, imaging, immunotherapy, and theranostic applications. *Adv Drug Deliv Rev*. 2020;156:214-235. doi:10.1016/j.addr.2020.06.024

46. Noad R, Roy P. Virus-like particles as immunogens. *Trends Microbiol*. 2003;11(9):438-444. doi:10.1016/S0966-842X(03)00208-7

47. Ihler GM, Glew RH, Schnure FW. Enzyme loading of erythrocytes. *Proc Natl Acad Sci U S A*. 1973;70(9):2663-2666. doi:10.1073/pnas.70.9.2663

48. Jiang Y, Jahagirdar BN, Reinhardt RL, et al. Erratum: Pluripotency of mesenchymal stem cells derived from adult marrow (Nature (2002) 418 (41-49) DOI: 10.1038/nature00870). *Nature*. 2007;447(7146):879-880. doi:10.1038/nature05812

49. Corsten MF, Shah K. Therapeutic stem-cells for cancer treatment: hopes and hurdles in tactical warfare. *Lancet Oncol*. 2008;9(4):376-384. doi:10.1016/S1470-2045(08)70099-8

50. Cihova M, Altanerova V, Altaner C. Stem Cell Based Cancer Gene Therapy. *Mol Pharm*. 2011;8(5):1480-1487. doi:10.1021/mp200151a |

51. Oldenborg P-A. CD47: A Cell Surface Glycoprotein Which Regulates Multiple Functions of Hematopoietic Cells in Health and Disease. *ISRN Hematol*. 2013;2013:1-19. doi:10.1155/2013/614619

52. Marin V, Dander E, Biagi E, et al. Characterization of in vitro migratory properties of anti-CD19 chimeric receptor-redirected CIK cells for their potential use in B-ALL immunotherapy. *Exp Hematol*. 2006;34(9):1218-1228. doi:10.1016/j.exphem.2006.05.004

53. Kloss CC, Condomines M, Cartellieri M, Bachmann M, Sadelain M. Combinatorial antigen recognition with balanced signaling promotes selective tumor eradication by engineered T cells. *Nat Biotechnol*. 2013;31(1):71-75. doi:10.1038/nbt.2459

54. Yu H, Yang Z, Li F, Xu L, Sun Y. Cell-mediated targeting drugs delivery systems. *Drug Deliv*. 2020;27(1):1425-1437. doi:10.1080/10717544.2020.1831103

55. Nakamura K, Ito Y, Kawano Y, et al. Antitumor effect of genetically engineered mesenchymal stem cells in a rat glioma model. *Gene Ther*. 2004;11(14):1155-1164. doi:10.1038/sj.gt.3302276

56. A Review Nanoerythrosomes: Milestone In Novel Drug Delivery System | Asian Journal of Pharmaceutical Research and Development.

57. Chhabria V, Beeton S. Development of nanosponges from erythrocyte ghosts for removal of streptolysin-O from mammalian blood. *Nanomedicine*. 2016;11(21):2797-2807. doi:10.2217/nnm-2016-0180

58. Hu CMJ, Fang RH, Zhang L. Erythrocyte-inspired delivery systems. *Adv Healthc Mater*. 2012;1(5):537-547. doi:10.1002/adhm.201200138

59. Bax BE, Bain MD, Talbot PJ, Parker-Williams EJ, Chalmers RA. Survival of human carrier erythrocytes in vivo. *Clin Sci*. 1999;96(2):171-178. doi:10.1042/cs0960171

60. Byun HM, Suh D, Yoon H, et al. Erythrocyte ghost-mediated gene delivery for prolonged and blood-targeted expression. *Gene Ther*. 2004;11(5):492-496. doi:10.1038/sj.gt.3302180

61. Doshi N, Zahr AS, Bhaskar S, Lahann J, Mitragotri S. Red blood cell-mimicking synthetic biomaterial particles. *Proc Natl Acad Sci U S A*. 2009;106(51):21495-21499. doi:10.1073/pnas.0907127106

62. Merkel TJ, Jones SW, Herlihy KP, et al. Using mechanobiological mimicry of red blood cells to extend circulation times of hydrogel microparticles. *Proc Natl Acad Sci U S A*. 2011;108(2):586-591. doi:10.1073/pnas.1010013108

63. Li R, He Y, Zhang S, Qin J, Wang J. Cell membrane-based nanoparticles: a new biomimetic platform for tumor diagnosis and treatment. *Acta Pharm Sin B*. 2018;8(1):14-22. doi:10.1016/j.apsb.2017.11.009

64. Toledano Furman NE, Lupu-Haber Y, Bronshtein T, et al. Reconstructed stem cell nanoghosts: A natural tumor targeting platform. *Nano Lett*. 2013;13(7):3248-3255. doi:10.1021/nl401376w

65. Kaneti L, Bronshtein T, Malkah Dayan N, et al. Nanoghosts as a Novel Natural Nonviral Gene Delivery Platform Safely Targeting Multiple Cancers. *Nano Lett*. 2016;16(3):1574-1582. doi:10.1021/acs.nanolett.5b04237

66. Lupu-Haber Y, Bronshtein T, Shalom-Luxenburg H, et al. Pretreating Mesenchymal Stem Cells with Cancer Conditioned-Media or Proinflammatory Cytokines Changes the Tumor and Immune Targeting by Nanoghosts Derived from these Cells. *Adv Healthc Mater*. 2019;8(10):1-8. doi:10.1002/adhm.201801589

67. Barclay TG, Day CM, Petrovsky N, Garg S. Review of polysaccharide particle-based functional drug delivery. *Carbohydr Polym*. 2019;221:94-112. doi:10.1016/j.carbpol.2019.05.067

68. Zhang L, Li R, Chen H, et al. Human cytotoxic T-lymphocyte membrane-camouflaged nanoparticles combined with low-dose irradiation: A new approach to enhance drug targeting in gastric cancer. *Int J Nanomedicine*. 2017;12:2129-2142. doi:10.2147/IJN.S126016

69. Gao C, Huang Q, Liu C, et al. Treatment of atherosclerosis by macrophage-biomimetic nanoparticles via targeted pharmacotherapy and sequestration of proinflammatory cytokines. *Nat Commun*. 2020;11(1):1-14. doi:10.1038/s41467-020-16439-7

70. Huang Y, Gao X, Chen J. Leukocyte-derived biomimetic nanoparticulate drug delivery systems for cancer therapy. *Acta Pharm Sin B*. 2018;8(1):4-13. doi:10.1016/j.apsb.2017.12.001

71. Sun K, Yu W, Ji B, et al. Saikosaponin D loaded macrophage membrane-biomimetic nanoparticles target angiogenic signaling for breast cancer therapy. *Appl Mater Today*. 2020;18:100505. doi:10.1016/j.apmt.2019.100505

72. Kang T, Zhu Q, Wei D, et al. Nanoparticles Coated with Neutrophil Membranes Can Effectively Treat Cancer Metastasis. *ACS Nano*. 2017;11(2):1397-1411. doi:10.1021/acsnano.6b06477

73. Jiménez-Jiménez C, Manzano M, Vallet-Regí M. Nanoparticles coated with cell membranes for biomedical applications. *Biology (Basel)*. 2020;9(11):1-17. doi:10.3390/biology9110406

74. Wang S, Duan Y, Zhang Q, et al. Drug Targeting via Platelet Membrane–Coated Nanoparticles. *Small Struct*. 2020;1(1):2000018. doi:10.1002/sstr.202000018

75. Chen HY, Deng J, Wang Y, Wu CQ, Li X, Dai HW. Hybrid cell membrane-coated nanoparticles: A multifunctional biomimetic platform for cancer diagnosis and therapy. *Acta Biomater*. 2020;112:1-13. doi:10.1016/j.actbio.2020.05.028

76. Gong C, Yu X, You B, et al. Macrophage-cancer hybrid membrane-coated nanoparticles for targeting lung metastasis in breast cancer therapy. *J Nanobiotechnology*. 2020;18(1):92. doi:10.1186/s12951-020-00649-8

77. Jin J, Bhujwalla ZM. Biomimetic Nanoparticles Camouflaged in Cancer Cell Membranes and Their Applications in Cancer Theranostics. *Front Oncol*. 2020;9:1560. doi:10.3389/fonc.2019.01560

78. Qie Y, Yuan H, Von Roemeling CA, et al. Surface modification of nanoparticles enables selective evasion of phagocytic clearance by distinct macrophage phenotypes. *Sci Rep*. 2016;6(May):1-11. doi:10.1038/srep26269

79. Mariam J, Sivakami S, Dongre PM. Albumin corona on nanoparticles – a strategic approach in drug delivery. *Drug Deliv*. 2016;23(8):2668-2676. doi:10.3109/10717544.2015.1048488

80. Discher DE, Andrechak JC, Dooling LJ. The macrophage checkpoint CD47 : SIRPa for recognition of "self" cells: from clinical trials of blocking antibodies to mechanobiological fundamentals. doi:10.1098/rstb.2018.0217

81. Lundstrom K. Viral Vectors in Gene Therapy. *Dis (Basel, Switzerland)*. 2018;6(2):42. doi:10.3390/diseases6020042

82. Morizono K, Chen ISY. Targeted Gene Delivery by Intravenous Injection of Retroviral Vectors. *Cell Cycle*. 2005;4(7):854-856. doi:10.4161/cc.4.7.1789

83. Carbonaro-Sarracino DA, Tarantal AF, Lee CCI, et al. Dosing and Re-Administration of Lentiviral Vector for In Vivo Gene Therapy in Rhesus Monkeys and ADA-Deficient Mice. *Mol Ther - Methods Clin Dev*. 2020;16:78-93. doi:10.1016/j.omtm.2019.11.004

84. Worgall S, Wolff G, Falck-Pedersen E, Crystal RG. Innate Immune Mechanisms Dominate Elimination of Adenoviral Vectors Following In Vivo Administration. *Hum Gene Ther*. 1997;8(1):37-44. doi:10.1089/hum.1997.8.1-37

85. Ye X, Jerebtsova M, Ray PE. Liver Bypass Significantly Increases the Transduction Efficiency of Recombinant Adenoviral Vectors in the Lung, Intestine, and Kidney. *Hum Gene Ther*. 2000;11(4):621-627. doi:10.1089/10430340050015806

86. García-Castro J, Alemany R, Cascalló M, et al. Treatment of metastatic neuroblastoma with systemic oncolytic virotherapy delivered by autologous mesenchymal stem cells: an exploratory study. *Cancer Gene Ther*. 2010;17(7):476-483. doi:10.1038/cgt.2010.4

87. Mayor P, Starbuck K, Zsiros E. Adoptive cell transfer using autologous tumor infiltrating lymphocytes in gynecologic malignancies. *Gynecol Oncol*. 2018;150(2):361-369. doi:10.1016/j.ygyno.2018.05.024

88. Tesfay MZ, Kirk AC, Hadac EM, et al. PEGylation of Vesicular Stomatitis Virus Extends Virus Persistence in Blood Circulation of Passively Immunized Mice. *J Virol*. 2013;87(7):3752 LP - 3759. doi:10.1128/JVI.02832-12

89. Croyle MA, Callahan SM, Auricchio A, et al. PEGylation of a vesicular stomatitis virus G pseudotyped lentivirus vector prevents inactivation in serum. *J Virol*. 2004;78(2):912-921. doi:10.1128/jvi.78.2.912-921.2004

90. Fisher KD, Seymour LW. HPMA copolymers for masking and retargeting of therapeutic viruses. *Adv Drug Deliv Rev*. 2010;62(2):240-245. doi:https://doi.org/10.1016/j.addr.2009.12.003

91. Morrison J, Briggs SS, Green N, et al. Virotherapy of ovarian cancer with polymer-cloaked adenovirus retargeted to the epidermal growth factor receptor. *Mol Ther*. 2008;16(2):244-251. doi:10.1038/sj.mt.6300363

92. Eto Y, Yoshioka Y, Mukai Y, Okada N, Nakagawa S. Development of PEGylated adenovirus vector with targeting ligand. *Int J Pharm*. 2008;354(1):3-8. doi:https://doi.org/10.1016/j.ijpharm.2007.08.025

93. Doronin K, Shashkova E V, May SM, Hofherr SE, Barry MA. Chemical Modification with High Molecular Weight Polyethylene Glycol Reduces Transduction of Hepatocytes and Increases Efficacy of Intravenously Delivered Oncolytic Adenovirus. *Hum Gene Ther*. 2009;20(9):975-988. doi:10.1089/hum.2009.028

94. Green NK, Herbert CW, Hale SJ, et al. Extended plasma circulation time and decreased toxicity of polymer-coated adenovirus. *Gene Ther*. 2004;11(16):1256-1263. doi:10.1038/sj.gt.3302295

95. Alemany R, Suzuki K, Curiel DT. Blood clearance rates of adenovirus type 5 in mice. *J Gen Virol*. 2000;81(11):2605-2609. doi:10.1099/0022-1317-81-11-2605

96. Wang H, VerHalen J, Madariaga ML, et al. Attenuation of phagocytosis of xenogeneic cells by manipulating CD47. *Blood*. 2006;109(2):836-842. doi:10.1182/blood-2006-04-019794

97. Matozaki T, Murata Y, Okazawa H, Ohnishi H. Functions and molecular mechanisms of the CD47-SIRPα signalling pathway. *Trends Cell Biol*. 2009;19(2):72-80. doi:10.1016/j.tcb.2008.12.001

98. Jaiswal S, Chao MP, Majeti R, Weissman IL. Macrophages as mediators of tumor immunosurveillance. *Trends Immunol*. 2010;31(6):212-219. doi:10.1016/j.it.2010.04.001

99. Chao MP, Alizadeh AA, Tang C, et al. Anti-CD47 Antibody Synergizes with Rituximab to Promote Phagocytosis and Eradicate Non-Hodgkin Lymphoma. *Cell*. 2010;142(5):699-713. doi:10.1016/j.cell.2010.07.044

100. Zhao XW, van Beek EM, Schornagel K, et al. CD47-signal regulatory protein-α (SIRPα) interactions form a barrier for antibody-mediated tumor cell destruction. *Proc Natl Acad Sci U S A*. 2011;108(45):18342-18347. doi:10.1073/pnas.1106550108

101. Cameron CM, Barrett JW, Mann M, Lucas A, McFadden G. Myxoma virus M128L is expressed as a cell surface CD47-like virulence factor that contributes to the downregulation of macrophage activation in vivo. *Virology*. 2005;337(1):55-67. doi:10.1016/j.virol.2005.03.037

102. Sosale NG, Ivanovska II, Tsai RK, et al. "Marker of Self" CD47 on lentiviral vectors decreases macrophage-mediated clearance and increases delivery to SIRPA-expressing lung carcinoma tumors. *Mol Ther - Methods Clin Dev*. 2016;3:16080. doi:10.1038/mtm.2016.80

103. Milani M, Annoni A, Moalli F, et al. Phagocytosis-shielded lentiviral vectors improve liver gene therapy in nonhuman primates. *Sci Transl Med*. 2019;11(493):7325. doi:10.1126/scitranslmed.aav7325

104. Tarar A, Alyami EM, Peng C-A. Efficient Expression of Soluble Recombinant Protein Fused with Core-Streptavidin in Bacterial Strain with T7 Expression System. *Methods Protoc*. 2020;3(4):82. doi:10.3390/mps3040082

105. Dübel S, Breitling F, Kontermann R, Schmidt T, Skerra A, Little M. Bifunctional and multimeric complexes of streptavidin fused to single chain antibodies (scFv). *J Immunol Methods*. 1995;178(2):201-209. doi:10.1016/0022-1759(94)00257-W

106. Landázuri N, Gupta M, Le Doux JM. Rapid concentration and purification of retrovirus by flocculation with Polybrene. *J Biotechnol*. 2006;125(4):529-539. doi:10.1016/j.jbiotec.2006.03.026

107. Hu W-W, Lang MW, Krebsbach PH. Development of adenovirus immobilization strategies for in situ gene therapy. *J Gene Med*. 2008;10(10):1102-1112. doi:10.1002/jgm.1233

108. Morrissey MA, Vale RD. CD47 suppresses phagocytosis by repositioning SIRPA and preventing integrin activation. *bioRxiv*. Published online August 2019:752311. doi:10.1101/752311

109. Hsu YC, Acuña M, Tahara SM, Peng CA. Reduced Phagocytosis of Colloidal Carriers Using Soluble CD47. *Pharm Res*. 2003;20(10):1539-1542. doi:10.1023/A:1026114713035

110. Salehi N, Peng C-A. Purification of CD47-streptavidin fusion protein from bacterial lysate using biotin-agarose affinity chromatography. *Biotechnol Prog*. 2016;32(4):949-958. doi:10.1002/btpr.2293

111. Stachelek SJ, Finley MJ, Alferiev IS, et al. The effect of CD47 modified polymer surfaces on inflammatory cell attachment and activation. *Biomaterials*. 2011;32(19):4317-4326. doi:10.1016/j.biomaterials.2011.02.053

112. Guido C, Maiorano G, Cortese B, D'Amone S, Palamà IE. Biomimetic Nanocarriers for Cancer Target Therapy. *Bioeng (Basel, Switzerland)*. 2020;7(3):111. doi:10.3390/bioengineering7030111

113. Murata Y, Kotani T, Ohnishi H, Matozaki T. The CD47-SIRP signalling system: its physiological roles and therapeutic application. *J Biochem*. 2014;155(6):335-344. doi:10.1093/jb/mvu017

114. Oronsky B, Carter C, Reid T, Brinkhaus F, Knox SJ. Just eat it: A review of CD47 and SIRP-α antagonism. *Semin Oncol*. 2020;47(2-3):117-124. doi:10.1053/j.seminoncol.2020.05.009

115. Cronin J, Zhang X-Y, Reiser J. Altering the tropism of lentiviral vectors through pseudotyping. *Curr Gene Ther*. 2005;5(4):387-398. doi:10.2174/1566523054546224

116. Murray RZ, Kay JG, Sangermani DG, Stow JL. A Role for the Phagosome in Cytokine Secretion. *Science (80-)*. 2005;310(5753):1492 LP - 1495. doi:10.1126/science.1120225

117. Aderem A. Phagocytosis and the Inflammatory Response. *J Infect Dis*. 2003;187(s2):S340-S345. doi:10.1086/374747

118. Manderson AP, Kay JG, Hammond LA, Brown DL, Stow JL. Subcompartments of the macrophage recycling endosome direct the differential secretion of IL-6 and TNFα . *J Cell Biol*. 2007;178(1):57-69. doi:10.1083/jcb.200612131

119. Sano T, Pandori MW, Chen X, Smith CL, Cantor CR. Recombinant core streptavidins: A minimum-sized core streptavidin has enhanced structural stability and higher accessibility to biotinylated macromolecules. *J Biol Chem*. 1995;270(47):28204-28209. doi:10.1074/jbc.270.47.28204

120. Singh A, Upadhyay V, Upadhyay AK, Singh SM, Panda AK. Protein recovery from inclusion bodies of Escherichia coli using mild solubilization process. *Microb Cell Fact*. 2015;14(1):41. doi:10.1186/s12934-015-0222-8

121. Brown EJ, Frazier WA. Integrin-associated protein (CD47) and its ligands. *Trends Cell Biol*. 2001;11(3):130-135.

122. Hayashida K, Bartlett AH, Chen Y, Park PW. Molecular and cellular mechanisms of ectodomain shedding. *Anat Rec (Hoboken)*. 2010;293(6):925-937. doi:10.1002/ar.20757

123. Burns JC, Friedmann T, Driever W, Burrascano M, Yee JK. Vesicular stomatitis virus G glycoprotein pseudotyped retroviral vectors: concentration to very high titer and efficient gene transfer into mammalian and nonmammalian cells. *Proc Natl Acad Sci U S A*. 1993;90(17):8033-8037. doi:10.1073/pnas.90.17.8033

124. Chan L, Nesbeth D, MacKey T, et al. Conjugation of Lentivirus to Paramagnetic Particles via Nonviral Proteins Allows Efficient Concentration and Infection of Primary Acute Myeloid Leukemia Cells. *J Virol*. 2005;79(20):13190-13194. doi:10.1128/jvi.79.20.13190-13194.2005

125. Smith JS, Keller JR, Lohrey NC, et al. Redirected infection of directly biotinylated recombinant adenovirus vectors through cell surface receptors and antigens. *Proc Natl Acad Sci*. 1999;96(16):8855-8860. doi:10.1073/PNAS.96.16.8855

126. Zhong Q, Kolls JK, Schwarzenberger P. Retrovirus Molecular Conjugates: A NOVEL, HIGH TRANSDUCTION EFFICIENCY, POTENTIALLY SAFETY-IMPROVED, GENE TRANSFER SYSTEM*. *J Biol Chem*. 2001;276(27):24601-24607. doi:https://doi.org/10.1074/jbc.M010318200

127. Selvarangan P, Gandham M, Sanjay K, A. TJ, Castillas M. Conjugate-Based Targeting of Recombinant Adeno-Associated Virus Type 2 Vectors by Using Avidin-Linked Ligands. *J Virol*. 2002;76(24):12900-12907. doi:10.1128/JVI.76.24.12900-12907.2002

128. Purow B, Staveley-O'Carroll K. Targeting of vaccinia virus using biotin-avidin viral coating and biotinylated antibodies. *J Surg Res*. 2005;123(1):49-54. doi:https://doi.org/10.1016/j.jss.2004.04.022

129. Barry MA, Campos SK, Ghosh D, et al. Biotinylated gene therapy vectors. *Expert Opin Biol Ther*. 2003;3(6):925-940. doi:10.1517/14712598.3.6.925

130. Parrott MB, Adams KE, Mercier GT, Mok H, Campos SK, Barry MA. Metabolically biotinylated adenovirus for cell targeting, ligand screening, and vector purification. *Mol Ther*. 2003;8(4):688-700. doi:https://doi.org/10.1016/S1525-0016(03)00213-2

131. Huang BH, Lin Y, Zhang ZL, et al. Surface labeling of enveloped viruses assisted by host cells. *ACS Chem Biol*. 2012;7(4):683-688. doi:10.1021/cb2001878

132. Sung K-J, Miller EA, Sikes HD. Engineering hyperthermostable rcSso7d as reporter molecule for in vitro diagnostic tests. *Mol Syst Des Eng*. 2018;3(6):877-882. doi:10.1039/C8ME00049B

133. Mouro-Chanteloup I, Delaunay J, Gane P, et al. Evidence that the red cell skeleton protein 4.2 interacts with the Rh membrane complex member CD47: Presented in part at the 43rd Annual Meeting of the American Society of Hematology, Orlando, FL, December 7-11, 2001.46. *Blood*. 2003;101(1):338-344. doi:https://doi.org/10.1182/blood-2002-04-1285

134. Ikeda K, Ichikawa T, Wakimoto H, et al. Oncolytic virus therapy of multiple tumors in the brain requires suppression of innate and elicited antiviral responses. *Nat Med*. 1999;5(8):881-887. doi:10.1038/11320

135. Wakimoto H, Ikeda K, Abe T, et al. The complement response against an oncolytic virus is species-specific in its activation pathways. *Mol Ther*. 2002;5(3):275-282. doi:10.1006/mthe.2002.0547

136. Sakurai H, Kawabata K, Sakurai F, Nakagawa S, Mizuguchi H. Innate immune response induced by gene delivery vectors. *Int J Pharm*. 2008;354(1):9-15. doi:https://doi.org/10.1016/j.ijpharm.2007.06.012

137. Tsai V, Johnson DE, Rahman A, et al. Impact of Human Neutralizing Antibodies on Antitumor Efficacy of an Oncolytic Adenovirus in a Murine Model. *Clin Cancer Res*. 2004;10(21):7199 LP - 7206. doi:10.1158/1078-0432.CCR-04-0765

138. Marelli G, Howells A, Lemoine NR, Wang Y. Oncolytic Viral Therapy and the Immune System: A Double-Edged Sword Against Cancer. *Front Immunol*. 2018;9:866. doi:10.3389/fimmu.2018.00866

139. Lemos de Matos A, Franco LS, McFadden G. Oncolytic Viruses and the Immune System: The Dynamic Duo. *Mol Ther Methods Clin Dev*. 2020;17:349-358. doi:10.1016/j.omtm.2020.01.001

140. Mader EK, Maeyama Y, Lin Y, et al. Mesenchymal Stem Cell Carriers Protect Oncolytic Measles Viruses from Antibody Neutralization in an Orthotopic Ovarian Cancer Therapy Model. *Clin Cancer Res*. 2009;15(23):7246 LP - 7255. doi:10.1158/1078-0432.CCR-09-1292

141. Barclay AN, Wright GJ, Brooke G, Brown MH. CD200 and membrane protein interactions in the control of myeloid cells. *Trends Immunol*. 2002;23(6):285-290. doi:https://doi.org/10.1016/S1471-4906(02)02223-8

142. McMaster WR, Williams AF. Monoclonal Antibodies to Ia Antigens from Rat Thymus: Cross Reactions with Mouse and Human and Use in Purification of Rat Ia Glycoproteins. *Immunol Rev*. 1979;47(1):117-137. doi:https://doi.org/10.1111/j.1600-065X.1979.tb00291.x

143. Dick AD, Broderick C, Forrester J V, Wright GJ. Distribution of OX2 Antigen and OX2 Receptor within Retina. *Invest Ophthalmol Vis Sci*. 2001;42(1):170-176.

144. Hatherley D, Lea SM, Johnson S, Barclay AN. Structures of CD200/CD200 Receptor Family and Implications for Topology, Regulation, and Evolution. *Structure*. 2013;21(5):820-832. doi:https://doi.org/10.1016/j.str.2013.03.008

145. Hoek RM, Ruuls SR, Murphy CA, et al. Down-Regulation of the Macrophage Lineage Through Interaction with OX2 (CD200). *Science (80-)*. 2000;290(5497):1768 LP - 1771. doi:10.1126/science.290.5497.1768

146. Wright GJ, Puklavec MJ, Willis AC, et al. Lymphoid/neuronal cell surface OX2 glycoprotein recognizes a novel receptor on macrophages implicated in the control of their function. *Immunity*. 2000;13(2):233-242. doi:10.1016/S1074-7613(00)00023-6

147. Kawasaki BT, Farrar WL. Cancer stem cells, CD200 and immunoevasion. *Trends Immunol*. 2008;29(10):464-468. doi:https://doi.org/10.1016/j.it.2008.07.005

148. Gorczynski RM, Cattral MS, Chen Z, et al. An Immunoadhesin Incorporating the Molecule OX-2 Is a Potent Immunosuppressant That Prolongs Allo- and Xenograft Survival. *J Immunol*. 1999;163(3):1654 LP - 1660. http://www.jimmunol.org/content/163/3/1654.abstract

149. Taylor N, McConachie K, Calder C, et al. Enhanced tolerance to autoimmune uveitis in CD200-deficient mice correlates with a pronounced Th2 switch in response to antigen challenge. *J Immunol*. 2005;174(1):143-154. doi:10.4049/jimmunol.174.1.143

150. Gorczynski RM, Yu K, Clark D. Receptor Engagement on Cells Expressing a Ligand for the Tolerance-Inducing Molecule OX2 Induces an Immunoregulatory Population That Inhibits Alloreactivity In Vitro and In Vivo. *J Immunol*. 2000;165(9):4854 LP - 4860. doi:10.4049/jimmunol.165.9.4854

151. Holmannová D, Kolácková M, Kondelková K, Kunes P, Krejsek J, Ctirad A. CD200/CD200R paired potent inhibitory molecules regulating immune and inflammatory responses; Part II: CD200/CD200R potential clinical applications. *Acta Medica (Hradec Kralove)*. 2012;55(2):59-65. doi:10.14712/18059694.2015.56

152. Ngwa C, Liu F. *CD200-CD200R Signaling and Diseases: A Potential Therapeutic Target?* Vol 11.; 2019. www.ijppp.org

153. Cao X-Z, Ma H, Wang J-K, et al. Postoperative cognitive deficits and neuroinflammation in the hippocampus triggered by surgical trauma are exacerbated in aged rats. *Prog Neuro-Psychopharmacology Biol Psychiatry*. 2010;34(8):1426-1432. doi:https://doi.org/10.1016/j.pnpbp.2010.07.027

154. Hayakawa K, Pham L-DD, Seo JH, et al. CD200 restrains macrophage attack on oligodendrocyte precursors via toll-like receptor 4 downregulation. *J Cereb Blood Flow Metab*. 2016;36(4):781-793. doi:10.1177/0271678X15606148

155. Ocaña-Guzman R, Vázquez-Bolaños L, Sada-Ovalle I. Receptors that inhibit macrophage activation: Mechanisms and signals of regulation and tolerance. *J Immunol Res*. 2018;2018. doi:10.1155/2018/8695157

156. Mukhopadhyay S, Plüddemann A, Hoe JC, et al. Immune Inhibitory Ligand CD200 Induction by TLRs and NLRs Limits Macrophage Activation to Protect the Host from Meningococcal Septicemia. *Cell Host Microbe*. 2010;8(3):236-247. doi:https://doi.org/10.1016/j.chom.2010.08.005

157. Sauter IP, Madrid KG, de Assis JB, et al. TLR9/MyD88/TRIF signaling activates host immune inhibitory CD200 in Leishmania infection. *JCI Insight*. 2019;4(10). doi:10.1172/jci.insight.126207

158. Zhang J, Peng CA. Diminution of Phagocytosed Micro/Nanoparticles by Tethering with Immunoregulatory CD200 Protein. *Sci Rep*. 2020;10(1):1-13. doi:10.1038/s41598-020-65559-z

159. Shiratori I, Yamaguchi M, Suzukawa M, et al. Down-Regulation of Basophil Function by Human CD200 and Human Herpesvirus-8 CD200. *J Immunol*. 2005;175(7):4441 LP - 4449. doi:10.4049/jimmunol.175.7.4441

160. Cameron CM, Barrett JW, Liu L, Lucas AR, McFadden G. Myxoma virus M141R expresses a viral CD200 (vOX-2) that is responsible for down-regulation of macrophage and T-cell activation in vivo. *J Virol*. 2005;79(10):6052-6067. doi:10.1128/JVI.79.10.6052-6067.2005

161. Jenmalm MC, Cherwinski H, Bowman EP, Phillips JH, Sedgwick JD. Regulation of Myeloid Cell Function through the CD200 Receptor. *J Immunol*. 2006;176(1):191-199. doi:10.4049/jimmunol.176.1.191

162. Lyons A, Minogue AM, Jones RS, et al. Analysis of the Impact of CD200 on Phagocytosis. *Mol Neurobiol*. 2017;54(7):5730-5739. doi:10.1007/s12035-016-0223-6

163. Farré D, Martínez-Vicente P, Engel P, Angulo A. Immunoglobulin superfamily members encoded by viruses and their multiple roles in immune evasion. *Eur J Immunol*. 2017;47(5):780-796. doi:https://doi.org/10.1002/eji.201746984

164. Zhang L, Stanford M, Liu J, et al. Inhibition of Macrophage Activation by the Myxoma Virus M141 Protein (vCD200). *J Virol*. 2009;83(18):9602-9607. doi:10.1128/JVI.01078-09

165. Akkaya M, Kwong L-S, Akkaya E, Hatherley D, Barclay AN. Rabbit CD200R binds host CD200 but not CD200-like proteins from poxviruses. *Virology*. 2016;488:1-8. doi:10.1016/j.virol.2015.10.026

166. Foster-Cuevas M, Wright GJ, Puklavec MJ, Brown MH, Barclay AN. Human Herpesvirus 8 K14 Protein Mimics CD200 in Down-Regulating Macrophage Activation through CD200 Receptor. *J Virol*. 2004;78(14):7667 LP - 7676. doi:10.1128/JVI.78.14.7667-7676.2004

167. Karen M, A. CS, Rahim RSA, et al. Suppression of Antigen-Specific T Cell Responses by the Kaposi's Sarcoma-Associated Herpesvirus Viral OX2 Protein and Its Cellular Orthologue, CD200. *J Virol*. 2012;86(11):6246-6257. doi:10.1128/JVI.07168-11

168. Rezaee SAR, Gracie JA, McInnes IB, Blackbourn DJ. Inhibition of neutrophil function by the Kaposi's sarcoma-associated herpesvirus vOX2 protein. *AIDS*. 2005;19(16). https://journals.lww.com/aidsonline/Fulltext/2005/11040/Inhibition_of_neutrophil_function_by_the_Kaposi_s.20.aspx

169. Elhelu MA. The Role of Macrophages in Immunology. *J Natl Med Assoc*. 1983;75(3).

170. Oh N, Park JH. Endocytosis and exocytosis of nanoparticles in mammalian cells. *Int J Nanomedicine*. 2014;9(SUPPL.1):51-63. doi:10.2147/IJN.S26592

171. Rattan R, Bhattacharjee S, Zong H, et al. Nanoparticle-macrophage interactions: A balance between clearance and cell-specific targeting. *Bioorganic Med Chem*. 2017;25(16):4487-4496. doi:10.1016/j.bmc.2017.06.040

172. Yoo J-W, Chambers E, Mitragotri S. Factors that Control the Circulation Time of Nanoparticles in Blood: Challenges, Solutions and Future Prospects. *Curr Pharm Des*. 2010;16(21):2298-2307. doi:10.2174/138161210791920496

173. Bartlett DW, Su H, Hildebrandt IJ, Weber WA, Davis ME. Impact of tumor-specific targeting on the biodistribution and efficacy of siRNA nanoparticles measured by multimodality in vivo imaging. *Proc Natl Acad Sci U S A*. 2007;104(39):15549-15554. doi:10.1073/pnas.0707461104

174. Gabizon AA, Barenholz Y, Bialer M. Prolongation of the circulation time of doxorubicin encapsulated in liposomes containing a polyethylene glycol-derivatized phospholipid: pharmacokinetic studies in rodents and dogs. Published online 1993:307-308.

175. Hatakeyama H, Akita H, Harashima H. The polyethyleneglycol dilemma: Advantage and disadvantage of PEGylation of liposomes for systemic genes and nucleic acids delivery to tumors. *Biol Pharm Bull*. 2013;36(6):892-899. doi:10.1248/bpb.b13-00059

176. Knop K, Hoogenboom R, Fischer D, Schubert US. Poly(ethylene glycol) in drug delivery: Pros and cons as well as potential alternatives. *Angew Chemie - Int Ed*. 2010;49(36):6288-6308. doi:10.1002/anie.200902672

177. Remaut K, Lucas B, Braeckmans K, Demeester J, De Smedt SC. Pegylation of liposomes favours the endosomal degradation of the delivered phosphodiester oligonucleotides. *J Control Release*. 2007;117(2):256-266. doi:10.1016/j.jconrel.2006.10.029

178. Rodriguez PL, Harada T, Christian DA, Pantano DA, Richard K, Discher DE. Minimal "Self" Peptides That Inhibit Phagocytic Clearance and Enhance Delivery of Nanoparticlesic. *Science (80-)*. 2013;339(6122):971-975. doi:10.1126/science.1229568.Minimal

179. Moghimi SM, Hunter AC, Murray JC. Long-Circulating and Target-Specific Nanoparticles : Theory to Practice. *Pharmacol Rev*. 2001;53(2):283-318.

180. Salehi N, Peng CA. Purification of CD47-streptavidin fusion protein from bacterial lysate using biotin-agarose affinity chromatography. *Biotechnol Prog*. 2016;32(4):949-958. doi:10.1002/btpr.2293

181. Rosenblum MD, Olasz EB, Yancey KB, et al. Expression of CD200 on Epithelial Cells of the Murine Hair Follicle: A Role in Tissue-Specific Immune Tolerance? *J Invest Dermatol*. 2004;123(5):880-887. doi:https://doi.org/10.1111/j.0022-202X.2004.23461.x

182. Blazar BR, Lindberg FP, Ingulli E, et al. CD47 (Integrin-associated Protein) engagement of dendritic cell and macrophage counterreceptors is required to prevent the clearance of donor lymphohematopoietic cells. *J Exp Med*. 2001;194(4):541-549. doi:10.1084/jem.194.4.541

183. Hatherley D, Barclay AN. The CD200 and CD200 receptor cell surface proteins interact through their N-terminal immunoglobulin-like domains. *Eur J Immunol*. 2004;34(6):1688-1694. doi:10.1002/eji.200425080

184. Wright GJ, Cherwinski H, Foster-Cuevas M, et al. Characterization of the CD200 Receptor Family in Mice and Humans and Their Interactions with CD200. *J Immunol*. 2003;171(6):3034-3046. doi:10.4049/jimmunol.171.6.3034

185. Tsai RK, Rodriguez PL, Discher DE. Self inhibition of phagocytosis: The affinity of "marker of self" CD47 for SIRPα dictates potency of inhibition but only at low expression levels. *Blood Cells, Mol Dis*. 2010;45(1):67-74. doi:10.1016/j.bcmd.2010.02.016

186. Hatherley D, Cherwinski HM, Moshref M, Barclay AN. Recombinant CD200 Protein Does Not Bind Activating Proteins Closely Related to CD200 Receptor. *J Immunol*. 2005;175(4):2469-2474. doi:10.4049/jimmunol.175.4.2469

187. Ura T, Okuda K, Shimada M. Developments in viral vector-based vaccines. *Vaccines*. 2014;2(3):624-641. doi:10.3390/vaccines2030624

188. Nayerossadat N, Maedeh T, Ali, A P. Viral and nonviral delivery systems for gene delivery. *Adv Biomed Res*. 2012;1(27).

189. Lorson T, Lübtow MM, Wegener E, et al. Poly(2-oxazoline)s based biomaterials: A comprehensive and critical update. *Biomaterials*. 2018;178:204-280. doi:10.1016/j.biomaterials.2018.05.022

190. Xia Q, Zhang Y, Li Z, Hou X, Feng N. Red blood cell membrane-camouflaged nanoparticles: a novel drug delivery system for antitumor application. *Acta Pharm Sin B*. 2019;9(4):675-689. doi:10.1016/j.apsb.2019.01.011

191. Gulati NM, Stewart PL, Steinmetz NF. Bioinspired Shielding Strategies for Nanoparticle Drug Delivery Applications. *Mol Pharm*. 2018;15(8):2900-2909. doi:10.1021/acs.molpharmaceut.8b00292

192. Chen EY, Chu SH, Gov L, et al. CD200 modulates macrophage cytokine secretion and phagocytosis in response to poly(lactic-co-glycolic acid) microparticles and films. *J Mater Chem B*. 2017;5(8):1574-1584. doi:10.1039/c6tb02269c

193. Choueiry F, Torok M, Shakya R, et al. CD200 promotes immunosuppression in the pancreatic tumor microenvironment. *J Immunother cancer*. 2020;8(1):189. doi:10.1136/jitc-2019-000189

194. Lawlor RT, Daprà V, Girolami I, et al. CD200 expression is a feature of solid pseudopapillary neoplasms of the pancreas. *Virchows Arch*. 2019;474(1):105-109. doi:10.1007/s00428-018-2437-7

195. Walker DG, Dalsing-Hernandez JE, Campbell NA, Lue LF. Decreased expression of CD200 and CD200 receptor in Alzheimer's disease: A potential mechanism leading to chronic inflammation. *Exp Neurol*. 2009;215(1):5-19. doi:10.1016/j.expneurol.2008.09.003

196. Zhang L, Xu J, Gao J, Wu Y, Yin M, Zhao W. CD200-, CX3CL1-, and TREM2-mediated neuron-microglia interactions and their involvements in Alzheimer's disease. *Rev Neurosci*. 2018;29(8):837-848. doi:10.1515/revneuro-2017-0084

197. Bolla AC, Valente T, Miguez A, et al. CD200 is up-regulated in R6/1 transgenic mouse model of Huntington's disease. *PLoS One*. 2019;14(12):e0224901. doi:10.1371/journal.pone.0224901

198. Liu R, Wei H, Gao P, et al. CD47 promotes ovarian cancer progression by inhibiting macrophage phagocytosis. *Oncotarget*. 2017;8(24):39021-39032. doi:10.18632/oncotarget.16547

199. Takimoto CH, Chao MP, Gibbs C, et al. The Macrophage "Do not eat me" signal, CD47, is a clinically validated cancer immunotherapy target. *Ann Oncol*. 2019;30(3). doi:doi.org/10.1093/annonc/mdz006

200. Chen Z, Kapus A, Khatri I, KOs O, Gorczynski R. Cell membrane-bound CD200 signals both via an extracellular domain and following nuclear translocation of a cytoplasmic fragment. *Leuk Res*. 2018;69.

201. Wong KK, Zhu F, Khatri I, Huo Q, Spaner DE, Gorczynski RM. Characterization of CD200 ectodomain shedding. *PLoS One*. 2016;11(4). doi:10.1371/journal.pone.0152073

202. Lin Y, Yan XQ, Yang F, et al. Soluble extracellular domains of human SIRPα and CD47 expressed in Escherichia coli enhances the phagocytosis of leukemia cells by macrophages in vitro. *Protein Expr Purif*. 2012;85(1):109-116. doi:10.1016/j.pep.2012.07.002

203. Woeppel KM, Zheng XS, Cui XT. Enhancing surface immobilization of bioactive molecules via a silica nanoparticle based coating. *J Mater Chem B*. 2018;6(19):3058-3067. doi:10.1039/c8tb00408k

204. Zhang L, Liu X, Liu D. A Conditionally Releasable “Do not Eat Me” CD47 Signal Facilitates Microglia-Targeted Drug Delivery for the Treatment of Alzheimer’s Disease. *Adv Funct Mater*. 2020;30(24). doi:10.1002/adfm.201910691

205. Song S, Jin X, Zhang L. PEGegylated and CcD47-conjugated nanoellipsoidal artificial antigen-presenting cells minimize phagocytosis and augment anti-tumor T-cell responses. *Int J Nanomedicine*. 2019;14. doi:10.2147/IJN.S195828

206. Kany S, Vollrath JT, Relja B. Cytokines in inflammatory disease. *Int J Mol Sci*. 2019;20(23). doi:10.3390/ijms20236008

207. Anderson JM, Rodriguez A, Chang DT. Foreign body reaction to biomaterials. *Semin Immunol*. 2008;20(2):86-100. doi:10.1016/j.smim.2007.11.004

208. Zhang J, Peng C-A. Blockade of macrophage adhesion to CD200-treated polystyrene culture surface. *J Biomed Mater Res Part A*. 2020;109(3):365-373. doi:https://doi.org/10.1002/jbm.a.37029

209. Murphy EA, Majeti BK, Barnes LA, et al. Nanoparticle-mediated drug delivery to tumor vasculature suppresses metastasis. *Proc Natl Acad Sci U S A*. 2008;105(27):9343-9348. doi:10.1073/pnas.0803728105